

# **TURBULENCE RESEARCH LABORATORY**

**School of Engineering and Applied Sciences**

**STATE UNIVERSITY OF NEW YORK AT BUFFALO**

(NASA-CR-199075) LES, DNS AND RANS  
FOR THE ANALYSIS OF HIGH-SPEED  
TURBULENT REACTING FLOWS Annual  
Report, 1 Aug. 1994 - 31 Jul. 1995  
(State Univ. of New York) 67 p

N95-32219

Unclas

G3/34 0061019

State University of New York Report

**LES, DNS and RANS for the Analysis of  
High-Speed Turbulent Reacting Flows**

by

**V. Adumitroaie, P.J. Colucci,  
D.B. Taulbee and P. Givi**

**Department of Mechanical and Aerospace Engineering  
State University of New York at Buffalo  
Buffalo, New York 14260-4400**

**Annual Report Submitted to  
NASA Langley Research Center**

**Progress Report on Activities Supported Under Grant NAG 1-1122**

for the Period

**August 1, 1994 - July 31, 1995**

# Contents

<b>1</b>	<b>Introduction</b>	<b>2</b>
<b>2</b>	<b>Algebraic Turbulence Closures for High Speed Turbulent Flows</b>	<b>2</b>
2.1	Introduction . . . . .	2
2.2	Governing Equations . . . . .	4
2.3	Models Development . . . . .	8
2.3.1	ARSM . . . . .	8
2.3.2	ATFM . . . . .	15
2.3.3	ASFM . . . . .	18
2.3.4	Explicit Solution . . . . .	20
2.4	Results and Conclusion . . . . .	22
<b>3</b>	<b>Monte Carlo Large Eddy Simulation of Reacting Turbulent Flows</b>	<b>24</b>
3.1	Introduction . . . . .	24
3.2	Governing Equations . . . . .	26
3.2.1	Modeling of Unresolved Scales . . . . .	27
3.3	PDF Methodology . . . . .	29
3.3.1	The Probability Distribution Function . . . . .	30
3.3.2	The Probability Density Function . . . . .	31
3.3.3	Determination of Mean Values from the PDF . . . . .	31
3.3.4	Functions of More Than One Random Variable . . . . .	32
3.3.5	Large Eddy PDF . . . . .	34
3.3.6	PDF Transport Equation . . . . .	35
3.3.7	Modeling of Unclosed Terms . . . . .	35
3.3.8	Langevin Equation . . . . .	36
3.4	Numerical Solution . . . . .	37
3.4.1	Finite Difference Procedure . . . . .	38
3.4.2	Monte Carlo Particle Method . . . . .	39
3.4.3	Determination of Filtered Quantities . . . . .	40

3.5	Results . . . . .	40
3.6	Conclusion . . . . .	42
<b>4</b>	<b>Work in Progress</b>	<b>43</b>
<b>5</b>	<b>Personnel and Management</b>	<b>44</b>

# LES, DNS and RANS for the Analysis of High-Speed Turbulent Reacting Flows

V. Adumitroaie, P.J. Colucci, D.B. Taulbee and P. Givi  
Department of Mechanical and Aerospace Engineering  
State University of New York at Buffalo  
Buffalo, New York 14260-4400

## Abstract

The purpose of this research is to continue our efforts in advancing the state of knowledge in large eddy simulation (LES), direct numerical simulation (DNS) and Reynolds averaged Navier Stokes (RANS) methods for the computational analysis of high-speed reacting turbulent flows. In the second phase of this work, covering the period: August 1, 1994 - August 1, 1995, we have focused our efforts on two programs: (1) Developments of explicit algebraic moment closures for statistical descriptions of compressible reacting flows, (2) Development of Monte Carlo numerical methods for LES of chemically reacting flows. This report provides a complete description of our efforts during this past year as supported by the NASA Langley Research Center under Grant NAG-1-1122.

## Technical Monitor:

Dr. J. Philip Drummond (Hypersonic Propulsion Branch, NASA LaRC, Mail Stop 197, Tel: 804-864-2298) is the Technical Monitor of this Grant.

# 1 Introduction

We have just completed our Year 2 of the Phase II activities on this NASA LaRC sponsored project. The total time allotted for this phase is three years; this phase was followed at the conclusion of Phase I activities (also for three years). Thus, in total we have completed five years of NASA LaRC supported research and one more year is remaining. Within the past five years, we have considered many issues of interest to the NASA LaRC in improving the state of affairs in DNS, LES and RANS of high speed turbulent reacting flows. Our previous four annual reports provide detail information on our past achievements. This report provides a complete description of our activities in Year 5.

Our efforts within the past year have been primarily concentrated on two main tasks: (1) Development of algebraic moment closures for statistical description of (highly) compressible flows, and (2) Development of an efficient Monte Carlo computational procedure for LES of chemically reactive flows. The efforts in (1) are in continuation of our previous work<sup>1</sup> (discussed in our Year 4 annual report), and the work pertaining to (2) is in continuation of our previous work<sup>2,3</sup> (discussed in our Year 3 annual report). In addition, we have devoted a portion of our efforts to make use of the models in (1) for the purpose of LES. At this point, our achievements are not yet a level suitable for documentation. Our achievements on each of the two constituents of the work in Year 5 are described in the next two sections.

## 2 Algebraic Turbulence Closures for High Speed Turbulent Flows

### 2.1 Introduction

For the incompressible regime the literature on computational prediction of nonreactive turbulent transport is abundant with schemes based on single-point statistical closures for moments up to the “second-order”.<sup>4-8</sup> Referred to as Reynolds stress models (RSM), these schemes are based on transport equations for the second order velocity correlations and lead to determination of “non-isotropic eddy-diffusivities.” This methodology is more advantageous than the more conventional models based on the Boussinesq approximations with isotropic eddy diffusivities (such as the  $k - \epsilon$  type closures<sup>4,9</sup>). However, the need for solving additional transport equations for the higher order moments could potentially make RSM less attractive, especially for practical applications. For example, it has been recently demonstrated<sup>10</sup> that the computational requirement associated with RSM for predictions of three-dimensional engineering flows is more than 80% higher than that required to implement the  $k - \epsilon$  model. The increase is naturally higher for second-order modeling of chemically reacting flows owing to the additional length and time scales which have to be considered.<sup>11-17</sup> A remedy to overcome the high computational cost associated with RSM is to utilize “algebraic” closures.<sup>18-25</sup> Such closures are either derived directly from the RSM transport equations, or other types of representations<sup>26-29</sup> that lead to anisotropic eddy diffusivities. One

of the original contributions in the development of algebraic Reynolds stress models (ARSM) is due to Rodi.<sup>20</sup> In this work, all the stresses are determined from a set of “implicit” equations which must be solved in an iterative manner. Pope<sup>18</sup> offers an improvement of the procedure by providing an “explicit” solution for the Reynolds stresses. This solution is generated via the use of the Cayley-Hamilton theorem, but is only applicable for predictions of two-dimensional (mean) flows. The extension of Pope’s formulation has been recently done by Taulbee<sup>19</sup> and Gatski and Speziale.<sup>24</sup> In these efforts, the Cayley-Hamilton theorem and the “symbolic” matrix manipulation techniques are used to generate explicit algebraic Reynolds stress models which are valid in both two- and three-dimensional flows.

In recent years the fundamental research on compressible turbulent flows has experienced a period of impetus owing to an increasing involvement of the propulsion community in the design high-speed-high-altitude ramjet engines. Although new experimental and numerical information is continuously accumulating over the years (for reviews see Lele,<sup>30</sup> Gutmark *et al.*<sup>31</sup>) the theory of compressible turbulence has not reached maturity yet. Several important aspects have been recognized about the nature of the turbulent state of a compressible medium and progress has been made in advancing the modeling of simple physical flow phenomena, but the inclusion of compressibility effects and of variable inertia effects in the turbulence models is an issue still under investigation, especially for the second-order moment closures. Using dimensional analysis in physical space<sup>32</sup> or in Fourier space,<sup>33</sup> asymptotic analysis,<sup>34</sup> rapid-distortion theory,<sup>35</sup> singular perturbation method<sup>36</sup> inside acoustic theory previous contributions have exploited the decomposition concept of the compressible field to generate models for terms specific to high-speed flows, *i.e.* pressure dilatation and dilatational dissipation which have been perceived to contribute to the reduced growth rate of the compressible mixing layer. These models have been applied in many instances as compressibility corrections in conjunction with the standard  $k - \epsilon$  model<sup>37</sup> or with a generalized form of the  $k - \epsilon$  model<sup>33</sup> or with the actualized incompressible Reynolds stress turbulence model.<sup>38,39</sup> By contrast true compressible second-order modeling attempts<sup>35,40</sup> are very few.

The specific objective is to provide explicit algebraic relations for the Reynolds stress and for the “turbulent flux” of scalar variables in the high-speed regime. Both non-reacting and reacting flows with heat release are considered. In the latter, a second-order irreversible chemical reaction is considered in turbulent flows with initially segregated reactants. The closures explicitly account for the influence of the the turbulent Mach number and Damköhler number (only in the scalar model) and density gradient, pressure gradient and mean dilatation effects are included in the closures. Similar to previous contributions,<sup>18,41,19-25</sup> the starting equations are the differential equations for the second order moments. Linear closures for the pressure-strain and the pressure-scalar gradient correlations are proposed and simple models for the averaged Favré scalar fluctuations are derived and embedded in the final explicit algebraic models.

## 2.2 Governing Equations

In the statistical approach to the turbulence problem the instantaneous equations are used to obtain the governing equations for the mean variables. Denote by overline ensemble average and by brackets density weighted (Favré) ensemble averaging:

$$\langle X \rangle = \frac{\overline{\rho X}}{\bar{\rho}}$$

Accordingly, we have the following decomposition rules:

$$X = \bar{X} + X', \quad \overline{X'} = 0$$

$$X = \langle X \rangle + X'', \quad \langle X'' \rangle = 0, \quad \overline{X''} = \bar{X} - \langle X \rangle$$

The governing equations are written in normalized form (with respect to reference values:  $\delta_\omega$  - vorticity thickness for length,  $\rho_\infty$ ,  $u_\infty$ ,  $T_\infty$ ,  $\mu_\infty$ ) for a compressible, reacting with heat release ( $A + rB \rightarrow (r+1)P + \text{heat}$ ) mean turbulent flow.

Continuity:

$$\frac{\partial \bar{\rho}}{\partial t} + \frac{\partial \bar{\rho} \langle u_j \rangle}{\partial x_j} = 0. \quad (1)$$

Conservation of momentum:

$$\frac{\partial \bar{\rho} \langle u_i \rangle}{\partial t} + \frac{\partial \bar{\rho} \langle u_i \rangle \langle u_j \rangle}{\partial x_j} = - \frac{\partial \bar{\rho} \langle u_i'' u_j'' \rangle}{\partial x_j} - \frac{\partial \bar{\rho}}{\partial x_i} + \frac{\partial \bar{\sigma}_{ji}(u)}{\partial x_j}, \quad i, j = 1, 2, 3 \quad (2)$$

where the stress tensor is  $\sigma_{ji}(u) = 2\mu[S_{ij}(u) - \frac{1}{3}S_{pp}(u)\delta_{ij}]/Re = 2\mu S_{ij}^*(u)/Re$ . The present notation for strain rate  $S_{ij}(u) = (\frac{\partial u_i}{\partial x_j} + \frac{\partial u_j}{\partial x_i})/2$  and for all the other linear differential operator is more suitable for the compressible problem where the two type of averages (which have different properties with respect to the linear differential operators) are naturally encountered. Hereinafter the star exponent will indicate the traceless tensor (deviatoric part) correspondent to the unstarred tensor. The mean viscosity  $\langle \mu \rangle$  follows a Maxwell-Rayleigh variation law with the mean temperature, i.e.  $\langle \mu \rangle / \mu_{ref} = (\langle T \rangle / T_{ref})^n$ ,  $n = 0.76$ . The fluctuations of the viscosity are neglected so that its correlations with other variables in the flow are zero. Within the present notation the averaged stress  $\bar{\sigma}_{ji}(u)$  is equal to  $\sigma_{ji}(\langle u \rangle) + \sigma_{ji}(\overline{u''})$ .

Let  $e_t = (T - \gamma C_e Y_P + u_j u_j / 2) / (\gamma(\gamma - 1)M^2)$ . Then the total energy equation is:

$$\frac{\partial \bar{\rho} \langle e_t \rangle}{\partial t} + \frac{\partial \bar{\rho} \langle e_t \rangle \langle u_j \rangle}{\partial x_j} = - \frac{\partial \bar{q}_j(T, Y_P)}{\partial x_j} - \frac{\partial \bar{\rho} \langle u_j'' e_t'' \rangle}{\partial x_j} - \frac{\partial}{\partial x_j} (\overline{u_i \sigma_{ji}(u)} - \bar{\rho} u_j) \quad (3)$$

where the averaged heat flux is

$$q_j(T, Y_P) = -\frac{\mu}{(\gamma - 1)RePrM^2} \frac{\partial}{\partial x_j} \left( T - \frac{Ce}{Le} Y_P \right)$$

$$\bar{q}_j(T, Y_P) = q_j(\langle T \rangle, \langle Y_P \rangle) + q_j(\bar{T}''', \bar{Y}_P'''),$$

$$\bar{p}u_j = \bar{p}\langle u_j \rangle + \frac{1}{\gamma M^2} \bar{\rho} \langle u_j'' T'' \rangle,$$

$$\bar{u}_i \bar{\sigma}_{ji}(u) = \langle u_i \rangle \sigma_{ji}(\langle u \rangle) + \langle u_i \rangle \sigma_{ji}(\bar{u}''') + \bar{u}'' \sigma_{ji}(\langle u \rangle) + \bar{u}_i \bar{\sigma}_{ji}(u'')$$

and

$$\bar{\rho} \langle u_j'' e_t'' \rangle = \frac{1}{\gamma(\gamma - 1)M^2} \bar{\rho} \langle u_j'' T'' \rangle - \frac{Ce}{(\gamma - 1)M^2} \bar{\rho} \langle u_j'' Y_P'' \rangle + \bar{\rho} \langle u_j'' u_i'' \rangle \langle u_i \rangle + \bar{\rho} \frac{\langle u_j'' u_i'' u_i'' \rangle}{2}.$$

Conservation of species:

$$\frac{\partial \bar{\rho} \langle Y_\alpha \rangle}{\partial t} + \frac{\partial \bar{\rho} \langle Y_\alpha \rangle \langle u_j \rangle}{\partial x_j} = -\frac{\partial \bar{\rho} \langle u_j'' Y_\alpha'' \rangle}{\partial x_j} + \frac{\partial}{\partial x_j} \left( \frac{\mu}{ScRe} \frac{\partial \bar{Y}_\alpha}{\partial x_j} \right) + \bar{\omega}_\alpha, \quad \alpha = A, B, P. \quad (4)$$

where  $\bar{\omega}_\alpha$  represents the rate of chemical reaction ( $\bar{\omega}_A = \frac{1}{r} \bar{\omega}_B = -\frac{1}{r+1} \bar{\omega}_P$ ):

$$\bar{\omega}_\alpha = -Da \exp \left[ -Ze \left( \frac{1}{T} - \frac{1}{T_f} \right) \right] \rho^2 Y_A Y_B, \quad (5)$$

and its mean approximated as:

$$\bar{\omega}_\alpha \simeq -Da \exp \left[ -Ze \left( \frac{1}{\langle T \rangle} - \frac{1}{T_f} \right) \right] \bar{\rho}^2 \langle Y_A Y_B \rangle, \quad (6)$$

And in the assumption of a perfect gas mixture, the equation of state:

$$\bar{p} = \frac{1}{\gamma M^2} \bar{\rho} \langle T \rangle \quad (7)$$

Here  $\rho$ ,  $u_i$ ,  $p$ ,  $e_t$ ,  $T$ ,  $Y_\alpha$ ,  $Re$ ,  $Pr$ ,  $M$ ,  $Ce$ ,  $Le$ ,  $Sc$ ,  $Ze$  and  $Da$  denote the fluid density, the  $i$ -th component of the velocity vector, the pressure, total energy, temperature, mass fraction of species  $\alpha$ , the Reynolds number, the Prandtl number, the Mach number, the heat release parameter, the Lewis number, the Schmidt number, the Zel'dovich number and the Damköhler number, respectively.

The closure problem consists in providing models or closed transport equations for the second order moments that appear in the equations for the mean variables. In general, the models are based on length scales and time scales constructed from second order quantities obtained from the following

transport equations. The equation for the kinetic energy of the turbulence  $\langle k \rangle = \langle u_i'' u_i'' \rangle / 2$  reads:

$$\begin{aligned} \frac{\partial \bar{\rho} \langle k \rangle}{\partial t} + \frac{\partial \bar{\rho} \langle k \rangle \langle u_j \rangle}{\partial x_j} = & - \frac{\partial}{\partial x_j} \left[ \bar{\rho} \langle u_j'' k \rangle + \overline{p' u_j''} - \overline{u_i'' \sigma_{ji}(u'')} \right] \\ & - \bar{\rho} \langle u_i'' u_j'' \rangle \frac{\partial \langle u_i \rangle}{\partial x_j} + \overline{p' \frac{\partial u_i''}{\partial x_i}} - \overline{u_j'' \frac{\partial \bar{p}}{\partial x_j}} + \overline{u_j'' \frac{\partial \sigma_{ji}(u)}{\partial x_j}} - \overline{\sigma_{ji}(u'')} \frac{\partial u_i''}{\partial x_j}, \end{aligned} \quad (8)$$

The turbulent dissipation  $\bar{\rho} \bar{\epsilon} = \overline{\sigma_{ji}(u'') \frac{\partial u_i''}{\partial x_j}} = \bar{\rho}(\bar{\epsilon}_s + \bar{\epsilon}_d) = \overline{2\mu \Omega_{ij}(u'') \Omega_{ij}(u'')} + \frac{4}{3} \overline{\mu S_{pp}^2(u'')}$  is split into solenoidal and dilatational parts,<sup>42,32,34</sup> with  $\Omega_{ij}(u) = \frac{1}{2}(\frac{\partial u_i}{\partial x_j} - \frac{\partial u_j}{\partial x_i})$  as the rotation rate. The solenoidal part is computed from the equation:

$$\frac{\partial \bar{\rho} \bar{\epsilon}_s}{\partial t} + \frac{\partial \bar{\rho} \bar{\epsilon}_s \langle u_j \rangle}{\partial x_j} = - \frac{\partial}{\partial x_j} \left[ \bar{\rho} \langle u_j'' \epsilon_s \rangle - \frac{\mu}{Re} \frac{\partial \bar{\epsilon}_s}{\partial x_j} \right] - C_{\epsilon_1} \bar{\rho} \frac{\bar{\epsilon}_s}{\langle k \rangle} \langle u_i'' u_j'' \rangle \frac{\partial \langle u_i \rangle}{\partial x_j} - C_{\epsilon_2} \bar{\rho} \frac{\bar{\epsilon}_s^2}{\langle k \rangle}, \quad (9)$$

with  $C_{\epsilon_1} = 1.44$  and  $C_{\epsilon_2} = 1.92$ . For the dilatational part there are available several models.<sup>32-34,36</sup> The model of Taulbee and VanOsdol<sup>33</sup> for the dilatational terms combined requires additional transport equations and our intention this work is to keep the number of equations at minimum. Other options are the model proposed by Sarkar *et al.*<sup>34</sup>

$$\bar{\epsilon}_d = \bar{\epsilon}_s M_t^2 \quad (10)$$

and the model of Ristorcelli<sup>36</sup>

$$\begin{aligned} \bar{\epsilon}_d = & \left\{ \frac{16}{3\alpha^2} [I_2^s + 6I_1^s I_3^s] + \left(\frac{2}{5}\right)^5 \tau^2 [3\sigma^2 + 5\omega^2] \cdot \right. \\ & \left. \left[ \frac{3}{5} I_3^r + \left(\frac{1}{15}\right)^2 [13\sigma^2 + 15\omega^2] \tau^2 \alpha^2 I_1^r \right] \right\} \frac{M_t^4}{R_t} \bar{\epsilon}_s \end{aligned} \quad (11)$$

The parameters are  $I_1^s = 0.3$ ,  $I_2^s = 13.768$ ,  $I_3^s = 2.623$ ,  $I_1^r = 1.392$ ,  $I_3^r = 3$ ,  $\alpha = 1 \div 4$ . Also,  $M_t$  denotes the turbulent Mach number, that is  $M_t^2 = \frac{2}{3} \langle k \rangle / c^2$  and  $R_t$  the turbulent Reynolds number  $R_t = \bar{\rho} \langle k \rangle^2 / (9\epsilon_s \mu) Re$ . The local speed of sound is given by  $c^2 = T / M^2$ .

The corresponding second-order quantities necessary for the temperature calculations are the temperature variance  $\langle T''^2 \rangle$  and the thermal turbulent dissipation,  $\bar{\rho} \bar{\epsilon}_\theta = \frac{\gamma \mu}{Pr Re} \frac{\partial T''}{\partial x_j} \frac{\partial T''}{\partial x_j}$ . For the former, starting from the temperature equation with  $c_v$  constant, we have:

$$\begin{aligned} \frac{\partial \bar{\rho} \langle T''^2 \rangle}{\partial t} + \frac{\partial \bar{\rho} \langle T''^2 \rangle \langle u_j \rangle}{\partial x_j} = & - \frac{\partial \bar{\rho} \langle u_j'' T''^2 \rangle}{\partial x_j} + \frac{\partial}{\partial x_j} \left( \frac{\gamma \mu}{Pr Re} \frac{\partial \overline{T''^2}}{\partial x_j} \right) - 2\bar{\rho} \langle u_j'' T'' \rangle \frac{\partial \langle T \rangle}{\partial x_j} - \\ & \frac{2\gamma \mu}{Pr Re} \frac{\partial T''}{\partial x_j} \frac{\partial T''}{\partial x_j} + \frac{\partial}{\partial x_j} \left( \frac{2\gamma \mu}{Pr Re} \overline{T''} \frac{\partial \langle T \rangle}{\partial x_j} \right) - \frac{2\gamma \mu}{Pr Re} \frac{\partial \overline{T''}}{\partial x_j} \frac{\partial \langle T \rangle}{\partial x_j} + 2\gamma C_e \overline{\dot{\omega}_P T''} - \\ & 2(\gamma - 1) \bar{\rho} \left( \langle T \rangle \left\langle T'' \frac{\partial u_j''}{\partial x_j} \right\rangle + \langle T''^2 \rangle \frac{\partial \langle u_j \rangle}{\partial x_j} + \left\langle T''^2 \frac{\partial u_j''}{\partial x_j} \right\rangle \right) + 2\gamma(\gamma - 1) M^2 T'' \sigma_{ij}(u) \frac{\partial u_j}{\partial x_j}. \end{aligned} \quad (12)$$

The transport equation for the thermal turbulent dissipation is given by:

$$\begin{aligned} \frac{\partial \bar{\rho} \bar{\epsilon}_\vartheta}{\partial t} + \frac{\partial \bar{\rho} \bar{\epsilon}_\vartheta \langle u_j \rangle}{\partial x_j} = & -\frac{\partial}{\partial x_j} \left( \bar{\rho} \langle u_j'' \epsilon_\vartheta \rangle + \frac{\mu}{ScRe} \frac{\partial \bar{\epsilon}_\vartheta}{\partial x_j} \right) - C_{y_1} \bar{\rho} \frac{\bar{\epsilon}_s}{\langle k \rangle} \langle u_j'' T'' \rangle \frac{\partial \langle T \rangle}{\partial x_j} - \\ & C_{y_2} \bar{\rho} \frac{\bar{\epsilon}_\vartheta}{\langle k \rangle} \langle u_i'' u_j'' \rangle \frac{\partial \langle u_i \rangle}{\partial x_j} - C_{y_3} \bar{\rho} \frac{\bar{\epsilon}_\vartheta^2}{\langle T''^2 \rangle} - C_{y_4} \bar{\rho} \frac{\bar{\epsilon}_s \bar{\epsilon}_\vartheta}{\langle k \rangle}. \end{aligned} \quad (13)$$

The constants take the values  $C_{y_1} = 2.0$ ,  $C_{y_3} = 2.0$ ,  $C_{y_4} = C_{e2} - 1 = 0.92$ ,  $C_{y_2} = 0.5$ .

Treatment of the scalar variable requires the solution of additional transport equations for the reactants' covariance  $\langle Y_\alpha'' Y_\beta'' \rangle$  and dissipations  $\bar{\rho} \bar{\epsilon}_{\alpha\beta} = \frac{\mu}{ScRe} \frac{\partial Y_\alpha''}{\partial x_j} \frac{\partial Y_\beta''}{\partial x_j}$ . For the covariances we have:

$$\begin{aligned} \frac{\partial \bar{\rho} \langle Y_\alpha'' Y_\beta'' \rangle}{\partial t} + \frac{\partial \bar{\rho} \langle Y_\alpha'' Y_\beta'' \rangle \langle u_j \rangle}{\partial x_j} = & -\frac{\partial \bar{\rho} \langle u_j'' Y_\alpha'' Y_\beta'' \rangle}{\partial x_j} + \frac{\partial}{\partial x_j} \left( \frac{\mu}{ScRe} \frac{\partial \overline{Y_\alpha'' Y_\beta''}}{\partial x_j} \right) \\ & - \bar{\rho} \langle u_j'' Y_\alpha'' \rangle \frac{\partial \langle Y_\beta \rangle}{\partial x_j} - \bar{\rho} \langle u_j'' Y_\beta'' \rangle \frac{\partial \langle Y_\alpha \rangle}{\partial x_j} - \frac{2\mu}{ScRe} \frac{\partial Y_\alpha''}{\partial x_j} \frac{\partial Y_\beta''}{\partial x_j} \\ & + \overline{\dot{\omega}_\alpha Y_\beta''} + \overline{\dot{\omega}_\beta Y_\alpha''}. \end{aligned} \quad (14)$$

Source terms in the expanded form read (no summation on greek indexes in all subsequent equations)

$$\begin{aligned} \overline{\dot{\omega}_\alpha Y_\beta''} + \overline{\dot{\omega}_\beta Y_\alpha''} = & -Da \exp \left[ -Ze \left( \frac{1}{\langle T \rangle} - \frac{1}{T_f} \right) \right] \bar{\rho}^2 [(\langle Y_\alpha'' Y_A'' \rangle + \langle Y_\beta'' Y_A'' \rangle) \langle Y_B \rangle + (\langle Y_\alpha'' Y_B'' \rangle + \\ & \langle Y_\beta'' Y_B'' \rangle) \langle Y_A \rangle + \langle Y_\alpha'' Y_A'' Y_B'' \rangle + \langle Y_\beta'' Y_A'' Y_B'' \rangle]. \end{aligned} \quad (15)$$

Similarly, the scalar dissipations are obtain from (hereinafter  $\epsilon_\alpha \equiv \epsilon_{\alpha\alpha}$ ):

$$\begin{aligned} \frac{\partial \bar{\rho} \bar{\epsilon}_{\alpha\beta}}{\partial t} + \frac{\partial \bar{\rho} \bar{\epsilon}_{\alpha\beta} \langle u_j \rangle}{\partial x_j} = & -\frac{\partial}{\partial x_j} \left( \bar{\rho} \langle u_j'' \epsilon_{\alpha\beta} \rangle + \frac{\mu}{ScRe} \frac{\partial \bar{\epsilon}_{\alpha\beta}}{\partial x_j} \right) \\ & - C_{y_1} \bar{\rho} \frac{\bar{\epsilon}_s}{\langle k \rangle} \frac{1}{2} \left( \langle u_j'' Y_\alpha'' \rangle \frac{\partial \langle Y_\beta \rangle}{\partial x_j} + \langle u_j'' Y_\beta'' \rangle \frac{\partial \langle Y_\alpha \rangle}{\partial x_j} \right) - C_{y_2} \bar{\rho} \frac{\bar{\epsilon}_{\alpha\beta}}{\langle k \rangle} \langle u_i'' u_j'' \rangle \frac{\partial \langle u_i \rangle}{\partial x_j} \\ & - C_{y_3} \bar{\rho} \frac{\bar{\epsilon}_{\alpha\beta}^2}{\langle Y_\alpha'' Y_\beta'' \rangle} - C_{y_4} \bar{\rho} \frac{\bar{\epsilon}_s \bar{\epsilon}_{\alpha\beta}}{\langle k \rangle} + S_{\alpha\beta}. \end{aligned} \quad (16)$$

In this equation, the chemical source term is of the form:

$$S_{\alpha\beta} = -Da \exp \left[ -Ze \left( \frac{1}{\langle T \rangle} - \frac{1}{T_f} \right) \right] \bar{\rho}^2 [(\bar{\epsilon}_{A\alpha} + \bar{\epsilon}_{A\beta}) \langle Y_B \rangle + (\bar{\epsilon}_{B\beta} + \bar{\epsilon}_{\alpha B}) \langle Y_A \rangle]. \quad (17)$$

To close the transport equations for the second order quantities all the third-order transport terms are described by the gradient diffusion hypothesis. Denoting by  $a''b''$  any of the second-order

correlations, we have:

$$\bar{\rho}\langle u_i'' a'' b'' \rangle = -C_s \bar{\rho} \frac{\langle k \rangle}{\langle \epsilon \rangle} \langle u_i'' u_j'' \rangle \frac{\partial \langle a'' b'' \rangle}{\partial x_j}, \quad (18)$$

where  $C_s$  is taken to be equal to 0.22 for all non-gradient correlations ( $a'' b'' = k$  or  $a'' b'' = Y_\alpha''^2$ ), whereas for the turbulent dissipations ( $a'' b'' = \epsilon_s$  or  $a'' b'' = \epsilon_\alpha$ ),  $C_s = 0.18$ . Also, the molecular transport terms are neglected under the assumption of high Reynolds-Peclet numbers flow.

## 2.3 Models Development

### 2.3.1 ARSM

An improved explicit ARSM has been derived by Taulbee<sup>19</sup> from the modeled transport equation for the Reynolds stresses. This model is based on the general linear pressure-strain closure given by Launder *et al.*<sup>43</sup> The improvement is due to an extended range of validity; the model is valid in both small and large mean strain fields and time scales of turbulence. A similar line of reasoning is made to obtain an algebraic closure for the unclosed correlations in compressible regime. The transport equations governing these correlations are transformed into algebraic expressions by making two assumptions: (1) Existence of a “near-asymptotic” state, and (2) the difference in the transport terms is negligible, in other words we look for the fixed point solution in the structural equilibrium limit. The starting equations for the Reynolds stress equation are described by:

$$\begin{aligned} \frac{\partial \bar{\rho}\langle u_i'' u_j'' \rangle}{\partial t} + \frac{\partial \bar{\rho}\langle u_i'' u_j'' \rangle \langle u_k \rangle}{\partial x_k} = & -\frac{\partial}{\partial x_k} \left[ \bar{\rho}\langle u_i'' u_j'' u_k'' \rangle + \overline{p' u_j'' \delta_{ik}} + \overline{p' u_i'' \delta_{jk}} - \overline{u_i'' \sigma_{kj}(u'')} - \overline{u_j'' \sigma_{ki}(u'')} \right] \\ & - \bar{\rho}\langle u_i'' u_k'' \rangle \frac{\partial \langle u_j \rangle}{\partial x_k} - \bar{\rho}\langle u_k'' u_j'' \rangle \frac{\partial \langle u_i \rangle}{\partial x_k} + p' \left( \frac{\partial u_i''}{\partial x_j} + \frac{\partial u_j''}{\partial x_i} \right) - \overline{u_i'' \frac{\partial \bar{p}}{\partial x_j}} - \overline{u_j'' \frac{\partial \bar{p}}{\partial x_i}} \\ & + \overline{u_j'' \frac{\partial \sigma_{ki}(u)}{\partial x_k}} + \overline{u_i'' \frac{\partial \sigma_{kj}(u)}{\partial x_k}} - \left[ \overline{\sigma_{jk}(u'')} \frac{\partial u_i''}{\partial x_k} + \overline{\sigma_{ki}(u'')} \frac{\partial u_j''}{\partial x_k} \right] \end{aligned} \quad (19)$$

Hereafter,  $\mathbf{a}$  designates the anisotropic stress tensor,  $a_{ij} = [\langle u_i'' u_j'' \rangle / \langle k \rangle - 2\delta_{ij}/3]$ , the Kronecker symbol is  $\delta \equiv [\delta_{ij}] = 1$  for  $i = j = 1, 3$  and 0 otherwise,  $\tau = \langle k \rangle / \bar{\epsilon}_s$  is the local turbulence time scale,  $\sigma = (S_{ij}^*(\langle u \rangle) S_{ji}^*(\langle u \rangle))^{1/2}$  and  $\varpi = (\Omega_{ij}(\langle u \rangle) \Omega_{ji}(\langle u \rangle))^{1/2}$  are tensor invariants.

The Reynolds stress equation is rewritten in terms of  $\mathbf{a}/(\tau\sigma)$ :

$$\begin{aligned} \tau \sigma \bar{\rho} \frac{D a_{ij} / (\tau \sigma)}{Dt} = & \frac{1}{\langle k \rangle} \left[ \frac{\partial T_{ijk}}{\partial x_k} - \frac{\langle u_i'' u_j'' \rangle}{\langle k \rangle} \frac{\partial T_k}{\partial x_k} \right] - \\ & \frac{a_{ij}}{\langle k \rangle} \left[ \frac{\partial T_k}{\partial x_k} - \tau \frac{\partial T_{k\epsilon}}{\partial x_k} \right] - \frac{1}{\langle k \rangle} \left[ P_{ij}^* + \Pi_{ij}^* + \mathcal{M}_{ij}^* + \mathcal{V}_{ij}^* - \bar{p} \epsilon_{ij}^* \right] - \\ & \bar{\rho} \frac{a_{ij}}{\tau} \left[ C_{\epsilon_2} - 2 + (2 - C_{\epsilon_1}) \frac{P}{\bar{\rho} \bar{\epsilon}_s} + \frac{\tau}{\sigma} \frac{D\sigma}{Dt} + 2 \frac{\mathcal{M} + \mathcal{V} + \overline{p'd} - \bar{p} \bar{\epsilon}_c}{\bar{\rho} \bar{\epsilon}_s} \right] \end{aligned} \quad (20)$$

where

$$P_{ij}^* = P_{ij} - \frac{2}{3}P\delta_{ij} = -\bar{\rho} \left[ \langle u_i'' u_k'' \rangle \frac{\partial \langle u_j \rangle}{\partial x_k} + \langle u_k'' u_j'' \rangle \frac{\partial \langle u_i \rangle}{\partial x_k} - \frac{2}{3} \langle u_k'' u_l'' \rangle \frac{\partial \langle u_l \rangle}{\partial x_k} \delta_{ij} \right] \quad (21)$$

is the production of Reynolds stress,

$$\Pi_{ij}^* = \Pi_{ij} - \frac{2}{3}\overline{p'd}\delta_{ij} = \overline{p' \left( \frac{\partial u_i''}{\partial x_j} + \frac{\partial u_j''}{\partial x_i} \right)} - \frac{2}{3}\overline{p' \frac{\partial u_k''}{\partial x_k}} \delta_{ij} \quad (22)$$

is the pressure-strain correlation,

$$\mathcal{V}_{ij}^* = \mathcal{V}_{ij} - \frac{2}{3}\mathcal{V}\delta_{ij} = \overline{u_j'' \frac{\partial \sigma_{ki}(\langle u \rangle)}{\partial x_k}} + \overline{u_i'' \frac{\partial \sigma_{kj}(\langle u \rangle)}{\partial x_k}} - \frac{2}{3}\overline{u_l'' \frac{\partial \sigma_{kl}(\langle u \rangle)}{\partial x_k}} \delta_{ij} \quad (23)$$

is the mass flux/viscous diffusion term,

$$\mathcal{M}_{ij}^* = \mathcal{M}_{ij} - \frac{2}{3}\mathcal{M}\delta_{ij} = - \left[ \overline{u_i'' \frac{\partial \bar{p}}{\partial x_j}} + \overline{u_j'' \frac{\partial \bar{p}}{\partial x_i}} - \frac{2}{3}\overline{u_k'' \frac{\partial \bar{p}}{\partial x_k}} \delta_{ij} \right] \quad (24)$$

is the mass flux/pressure gradient term (also called enthalpic production by exchange with enthalpic energy<sup>42</sup>)

$$\bar{\rho} \epsilon_{ij}^* = \bar{\rho} \left( \bar{\epsilon}_{ij} - \frac{2}{3}\bar{\epsilon}\delta_{ij} \right) = \overline{\sigma_{jk}(u'') \frac{\partial u_i''}{\partial x_k}} + \overline{\sigma_{ki}(u'') \frac{\partial u_j''}{\partial x_k}} - \frac{2}{3}\overline{\sigma_{lk}(u'') \frac{\partial u_l''}{\partial x_k}} \delta_{ij} \quad (25)$$

the anisotropy of the dissipation. The dyads involving the mass flux vector can be added to a single tensor. In free shear flows the viscous diffusion part is negligible owing to the high Reynolds numbers characteristic to these flows. Nevertheless, the present analysis can accommodate the discarded term when necessary, such as near-wall flows. Hence, in subsequent equations the tensor  $\mathcal{M}_{ij}$  can be used to include the viscous effects. Using a rationale similar to the incompressible situation,<sup>43,6</sup> the pressure strain-correlation model can be written as (in this attempt the supplementary compressible terms that appear in the Poisson equation have been neglected as being of second order, a rough approximation, but valid in the low Mach number regime):

$$\Pi_{ij} - \bar{\rho} \epsilon_{ij}^* = \mathcal{A}_{ij} + 2\bar{\rho}(\mathcal{I}_{piqj} + \mathcal{I}_{pjqi})(S_{pq}(\langle u \rangle) + \Omega_{pq}(\langle u \rangle)) \quad (26)$$

Our goal being to obtain an explicit algebraic Reynolds stress model, the integrals  $\mathcal{I}_{piqj}$  as well as the tensor  $\mathcal{A}_{ij}$  will have to be expressed as linear functions of the anisotropy of the Reynolds stress tensor so that the final equation is solvable by exact analytic methods. Therefore

$$\begin{aligned} \mathcal{A}_{ij} &= -C_1\bar{\rho} \bar{\epsilon} a_{ij} + \mathcal{A}_{pp} \\ \frac{\mathcal{I}_{piqj}}{\langle k \rangle} &= \alpha_1 \delta_{qi} \delta_{pj} + \alpha_2 (\delta_{pq} \delta_{ij} + \delta_{qj} \delta_{pi}) + a_1 \delta_{pj} a_{qi} + \\ & a_2 (\delta_{pq} a_{ij} + \delta_{pi} a_{qj} + \delta_{ij} a_{pq} + \delta_{jq} a_{pi}) + a_4 \delta_{qi} a_{pj} \end{aligned} \quad (27)$$

This above form for  $\mathcal{I}_{piqj}$  satisfies already symmetry constraints. To determine the coefficients two more constraints are applied: the normalization condition which translates into  $\mathcal{I}_{ppqj} = \langle u_q'' u_j'' \rangle$  and a matching condition such that from the trace of  $\Pi_{ij}$  is obtained an existing model for the pressure dilatation (replacing the customary incompressible constraint which is recovered from the above condition in the limit of zero Mach number). Some of the existing proposals to model this term necessitate transport equations such as density variance<sup>33</sup> or pressure variance.<sup>35</sup> Two recent pressure dilatation models<sup>44,36</sup> do not require separate equations, the model of Sarkar:<sup>44</sup>

$$\frac{1}{2}\Pi_{pp} = -\overline{p'd} = -\chi_1 M_t^2 \left[ \frac{2}{3} \left( \frac{1}{M_t} - \frac{2}{3} \frac{\chi_2}{\chi_1} \right) \overline{p}\langle k \rangle S_{pp} + \frac{P}{M_t} - \frac{\chi_2}{\chi_1} \overline{p} \bar{\epsilon}_s \right] \quad (28)$$

where  $\chi_1 = 0.15$ ,  $\chi_2 = 0.2$ ,  $\chi_3 = 0.2$  and the model of Ristorcelli<sup>36</sup>

$$\overline{p'd} = -\chi M_t^2 \left[ -\frac{1}{2} \overline{p}\langle k \rangle S_{pp} + P - \overline{p} \bar{\epsilon} + T_k - \frac{2}{3} M_t^2 \gamma (\gamma - 1) (P_T + \overline{p} \bar{\epsilon} + T_T) \right] - \overline{p}\langle k \rangle M_t^2 \chi' \frac{D(3\sigma^2 - 5\varpi^2)}{Dt} \quad (29)$$

where

$$\chi = \frac{2I_{pd}}{1 + 2I_{pd}M_t^2 + \frac{2}{3}I_{pd}M_t^4\gamma(\gamma-1)}, \quad \chi' = \frac{I_{pd}^r}{1 + 2I_{pd}M_t^2 + \frac{2}{3}I_{pd}M_t^4\gamma(\gamma-1)}, \quad (30)$$

$$I_{pd} = \frac{2}{3}I_1^s + I_{pd}^r [2\sigma^2 - 5\varpi^2], \quad I_{pd}^r = \frac{1}{30} \left( \frac{2}{3} \right)^3 \alpha^2 I_1^r$$

Using the latter model, the matching constraint on the  $\mathcal{I}_{piqj}$  produces

$$\mathcal{I}_{piqi}/\langle k \rangle = \frac{\chi M_t^2}{2} \left( \frac{7}{6} \delta_{pq} + a_{pq} \right).$$

The same condition enforces also that

$$\mathcal{A}_{pp} = \chi M_t^2 [\overline{p} \bar{\epsilon} + \frac{2}{3} M_t^2 \gamma (\gamma - 1) (P_T + \overline{p} \bar{\epsilon})] - \overline{p}\langle k \rangle M_t^2 \chi' \frac{D(3\sigma^2 - 5\varpi^2)}{Dt}$$

(transport terms have been neglected based on the local homogeneity assumption). In this manner a linear pressure-strain model is obtained. It is known that with linear forms it is impossible to satisfy realizability conditions requiring that the eigenvalues of the Reynolds stress tensor be positive. To overcome this deficiency we employ a method suggested by Schumann<sup>45</sup> and detailed by Shih and Shabbir.<sup>46</sup> If  $F = 1 + 27III/8 + 9II/4$  is a parameter involving the second invariant  $II = -\frac{1}{2}a_{ij}a_{ji}$  and third invariant  $III = -\frac{1}{3}a_{ij}a_{jk}a_{ki}$  of the Reynolds stress anisotropy tensor, then the following asymptotic behavior for the pressure strain-model ensures that realizability is satisfied:

$$\mathcal{A}_{ce} - \frac{2}{3} \overline{p} \bar{\epsilon} = CF^a \quad \text{as } F \rightarrow 0$$

$$\frac{\partial \langle u_p \rangle}{\partial x_q} \mathcal{I}_{peqe} \rightarrow 0 \quad \text{as } F \rightarrow 0 \quad (31)$$

where the index  $e$  indicates that the relations are written in the principal axes of  $\langle u_i'' u_j'' \rangle$ . To enforce this kind of decay additional parameters are introduced in the pressure strain-model which reads in final form:

$$\begin{aligned} \Pi_{ij}^* - \bar{\rho} \epsilon_{ij}^* &= -C_1 \bar{\rho} \bar{\epsilon} a_{ij} A_r F^{\alpha_r} + \bar{\rho} \langle k \rangle \left[ \left[ \frac{4}{5} + \frac{7}{30} \chi M_t^2 \right] S_{ij}^*(\langle u \rangle) + \right. \\ & [1 - C_3 + \chi M_t^2] \left[ a_{ip} S_{pj}^*(\langle u \rangle) + S_{ip}^*(\langle u \rangle) a_{pj} - \frac{2}{3} S_{pq}^*(\langle u \rangle) a_{pq} \delta_{ij} \right] - \\ & \left. [1 - C_4 - \chi M_t^2] [a_{ip} \Omega_{pj}(\langle u \rangle) - \Omega_{ip}(\langle u \rangle) a_{pj}] + \frac{2}{3} \chi M_t^2 S_{pp}(\langle u \rangle) a_{ij} \right] B_r F^{\beta_r} \end{aligned} \quad (32)$$

with  $C_3 = (5 - 9C_2)/11$  and  $C_4 = (1 + 7C_2)/11$ . The value for the constant  $C_2$  will be the same as in the incompressible model to preserve consistency in the zero Mach number limit, that is  $C_2 = 0.45$ . The parameters are  $\alpha_r = 0.1$ ,  $\beta_r = 0.5$ ,  $A_r = \min(F^{-\alpha_r}, 0.1^{-\alpha_r})$  and  $B_r = \min(F^{-\beta_r}, 0.1^{-\beta_r})$ . The mass flux is usually modeled by gradient-transport hypothesis<sup>38</sup> or solving its transport equations.<sup>33</sup> A compromise between economy and accuracy is obtained using a model proposed by Ristorcelli:<sup>47</sup>

$$\bar{\rho} \overline{u_i''} = \tau_u \left[ \nu_0 \delta_{ij} + \nu_1 \tau_u \frac{\partial \langle u_i \rangle}{\partial x_j} + \nu_2 \tau_u^2 \frac{\partial \langle u_i \rangle}{\partial x_k} \frac{\partial \langle u_k \rangle}{\partial x_j} \right] \langle u_j'' u_p'' \rangle \frac{\partial \bar{\rho}}{\partial x_p} \quad (33)$$

where  $\tau_u = M_t \tau / [1 + \frac{M_t \bar{\epsilon}}{2 \bar{\epsilon}_s} (P / (\bar{\rho} \epsilon) - 1)]$ . Here  $\nu_0$ ,  $\nu_1$  and  $\nu_2$  are the coefficients obtained from the inversion of the matrix  $G_{ij} = \delta_{ij} + \tau_u \frac{\partial \langle u_i \rangle}{\partial x_j}$ :  $\nu_0 = -(1 + I_{\mathbf{G}} + II_{\mathbf{G}}) \nu_2$ ,  $\nu_1 = (1 + I_{\mathbf{G}}) \nu_2$ ,  $\nu_2 = (1 + I_{\mathbf{G}} + II_{\mathbf{G}} + III_{\mathbf{G}})^{-1}$ , the Roman numbers representing the invariants of  $\mathbf{G}$ . For simplicity we will use only the lowest order contribution from this model to obtain:

$$\mathcal{M}_{ij}^* = -\frac{1}{\bar{\rho}} \frac{2}{3} \tau_u \nu_0 \langle k \rangle (\mathcal{R}_{ij} + \mathcal{R}_{ji} - \frac{2}{3} \mathcal{R}_{pp} \delta_{ij}) = -\frac{1}{\bar{\rho}} \frac{2}{3} \tau_u \nu_0 \langle k \rangle \mathcal{R}_{ij}^* \quad (34)$$

where

$$\mathcal{R}_{ij} = \frac{\partial \bar{\rho}}{\partial x_i} \frac{\partial \bar{\rho}}{\partial x_j}$$

is the mean density gradient-mean pressure gradient dyad. If the entire model is to be used in the following equations  $\mathbf{R}^*$  should be replaced with  $\mathcal{M}^*$  and set  $b_2 = -1/(\bar{\rho} \langle k \rangle)$ .

The final equation is obtained introducing the above expressions for the pressure-strain correlation model, production and mass flux terms into the equation for  $a_{ij}$ . To get the fixed point solution we set to zero the Lagrangian derivative as well as the difference in the transport terms. This results in the following linear tensorial equation written in matrix form (the braces signify the trace of the matrix inside the braces):

$$\mathbf{a} = -g\tau \left[ b_1 \mathbf{S}^* + b_2 \mathbf{R}^* + b_3 \left( \mathbf{a} \mathbf{S}^* + \mathbf{S}^* \mathbf{a} - \frac{2}{3} \{ \mathbf{a} \mathbf{S}^* \} \delta \right) - b_4 (\mathbf{a} \Omega - \Omega \mathbf{a}) \right] \quad (35)$$

with  $b_1 = \frac{4}{3} - B_r F^{\beta_r} (\frac{4}{5} + \frac{7}{30} \chi M_t^2)$ ,  $b_2 = \frac{1}{\bar{\rho}^2} \frac{2}{3} \tau_u \nu_0$ ,  $b_3 = 1 - B_r F^{\beta_r} (1 - C_3 + \chi M_t^2)$ ,  $b_4 = 1 - B_r F^{\beta_r} (1 - C_4 - \chi M_t^2)$ , and

$$g = \left[ A_r F^{\alpha_r} C_1 \frac{\bar{\epsilon}}{\bar{\epsilon}_s} + C_{\epsilon_2} - 2 + (2 - C_{\epsilon_1}) \frac{P}{\bar{\rho} \bar{\epsilon}_s} + \frac{\tau}{\sigma} \frac{D\sigma}{Dt} + \frac{2\tau}{3} (1 - \chi M_t^2 B_r F^{\beta_r}) S_{pp}(\langle u \rangle) + 2 \frac{\mathcal{M} + \overline{p'd} - \bar{\rho} \bar{\epsilon}_c}{\bar{\rho} \bar{\epsilon}_s} \right]^{-1} \quad (36)$$

The task of solving the equation (35) is formidable. From the above equation we see that the anisotropy of the Reynolds stress tensor is dependent on three primary second order tensors, two symmetric and one skew-symmetric,  $a_{ij} = a_{ij}(\mathbf{S}^*, \mathbf{\Omega}, \mathbf{R}^*)$ . The solution can be expressed as a finite 3-D tensor polynomial,

$$\mathbf{a} = \sum_{\lambda} C^{\lambda} T^{\lambda} \quad (37)$$

that is a linear combination of all the linear independent tensor products formed from the three primary tensors. The coefficients of this polynomial are function of the set of independent invariants which form the integrity basis for this problem. In this case the dimension of the minimal tensor base is  $\lambda = 41$  (cf. Spencer<sup>48</sup>) and although not all of the tensor products will appear in the final result, there is little hope that the model will be of practical use at this time. A way to circumvent this difficulty is to make a simplifying approximation regarding the  $b_3$  term. For most practical free-shear flow applications  $F > 0.1$ , therefore in the low turbulent Mach number domain  $b_3 \simeq C_3$ . It has been argued<sup>19,25</sup> that for the range of values used for the constant  $C_2$  the inequality  $C_3 \ll C_4$  holds and therefore the term multiplied by  $C_3$  will have small effect on the solution. Thus using the superposition principle  $\mathbf{a} = \mathbf{a}^S + \mathbf{a}^R$  where  $\mathbf{a}^S$  stands for the solution dependent on  $\mathbf{S}^*$ ,

$$\mathbf{a}^S = -g\tau \left[ b_1 \mathbf{S}^* - b_4 (\mathbf{a}^S \mathbf{\Omega} - \mathbf{\Omega} \mathbf{a}^S) \right] \quad (38)$$

and  $\mathbf{a}^R$  denoting the solution dependent on  $\mathbf{R}^*$ ,

$$\mathbf{a}^R = -g\tau \left[ b_2 \mathbf{R}^* - b_4 (\mathbf{a}^R \mathbf{\Omega} - \mathbf{\Omega} \mathbf{a}^R) \right]. \quad (39)$$

Applying the results of Taulbee<sup>19</sup> we have

$$\begin{aligned} \mathbf{a}^S = & -2C_{\mu}\tau \mathbf{S}^* - 4\alpha_2 \tau^2 (\mathbf{S}^* \mathbf{\Omega} - \mathbf{\Omega} \mathbf{S}^*) - 8\alpha_3 \tau^3 (\mathbf{\Omega}^2 \mathbf{S}^* + \mathbf{S}^* \mathbf{\Omega}^2 - \frac{2}{3} \{ \mathbf{S}^* \mathbf{\Omega}^2 \} \delta) \\ & - 16\alpha_4 \tau^4 (\mathbf{\Omega} \mathbf{S}^* \mathbf{\Omega}^2 - \mathbf{\Omega}^2 \mathbf{S}^* \mathbf{\Omega}) - 32\alpha_5 \tau^5 \{ \mathbf{S}^* \mathbf{\Omega}^2 \} (\mathbf{\Omega}^2 - \frac{1}{3} \{ \mathbf{\Omega}^2 \} \delta) \end{aligned} \quad (40)$$

where  $C_{\mu} = b_1 g (1 - \frac{7}{2} h_0^2 \varpi^2) h_1$ ,  $\alpha_2 = \frac{1}{2} b_1 b_4 g^2 h_2$ ,  $\alpha_3 = \frac{3}{4} b_1 b_4^2 g^3 h_1$ ,  $\alpha_4 = -\frac{3}{8} b_1 b_4^3 g^4 h_1$ ,  $\alpha_5 = -\frac{3}{8} b_1 b_4^4 g^5 h_1$ ,  $h_0 = b_4 g \tau$ ,  $h_1 = h_2 [(1 - 2h_0^2 \varpi^2)]^{-1}$  and  $h_2 = [2 - h_0^2 \varpi^2]^{-1}$ . Similarly,

$$\mathbf{a}^R = -2C_{\mu}\tau \mathbf{R}^* - 4\alpha_2 \tau^2 (\mathbf{R}^* \mathbf{\Omega} - \mathbf{\Omega} \mathbf{R}^*) - 8\alpha_3 \tau^3 (\mathbf{\Omega}^2 \mathbf{R}^* + \mathbf{R}^* \mathbf{\Omega}^2 - \frac{2}{3} \{ \mathbf{R}^* \mathbf{\Omega}^2 \} \delta)$$

$$-16\alpha_4\tau^4(\mathbf{\Omega}\mathbf{R}^*\mathbf{\Omega}^2 - \mathbf{\Omega}^2\mathbf{R}^*\mathbf{\Omega}) - 32\alpha_5\tau^5\{\mathbf{R}^*\mathbf{\Omega}^2\}(\mathbf{\Omega}^2 - \frac{1}{3}\{\mathbf{\Omega}^2\}\delta) \quad (41)$$

and the coefficients have the same form as those from the  $\mathbf{a}^S$  solution with the parameter  $b_1$  replaced with  $b_2$ .

In two dimensions the problem is less complicated since the number of tensor products necessary to express the solution is vastly reduced. In this case  $\mathbf{S}, \mathbf{\Omega}, \mathbf{R}$  are two dimensional tensors as the mean quantities are 2-D. First it is necessary to recast the tensorial equation in terms of the proper traceless 2-D tensors, that is  $\underline{S}_{ij}^*(\langle u \rangle) = S_{ij}(\langle u \rangle) - \frac{1}{2}S_{pp}(\langle u \rangle)\delta_{ij}^{(2)}$ ,  $\underline{R}_{ij}^*(\bar{\rho}, \bar{p}) = R_{ij}(\bar{\rho}, \bar{p}) - \frac{1}{2}R_{pp}(\bar{\rho}, \bar{p})\delta_{ij}^{(2)}$ . Here, the two dimensional Kronecker symbol is  $\delta^{(2)} \equiv [\delta_{ij}^{(2)}] = 1$  for  $i = j = 1, 2$  and 0 otherwise. The pressure strain model becomes:

$$\begin{aligned} \Pi_{ij}^* - \bar{\rho} \epsilon_{ij}^* &= -C_1 \bar{\rho} \bar{\epsilon} a_{ij} A_r F^{\alpha r} + \bar{\rho} \langle k \rangle \left[ \left[ \frac{4}{5} + \frac{7}{30} \chi M_t^2 \right] \underline{S}_{ij}^*(\langle u \rangle) + \right. \\ & \left[ 1 - C_3 + \chi M_t^2 \right] \left[ a_{ip} \underline{S}_{pj}^*(\langle u \rangle) + \underline{S}_{ip}^*(\langle u \rangle) a_{pj} - \frac{2}{3} \underline{S}_{pq}^*(\langle u \rangle) a_{pq} \delta_{ij} \right] - \\ & \left[ 1 - C_4 - \chi M_t^2 \right] \left[ a_{ip} \underline{\Omega}_{pj}(\langle u \rangle) - \underline{\Omega}_{ip}(\langle u \rangle) a_{pj} \right] + \\ & \frac{2}{3} \chi M_t^2 S_{pp}(\langle u \rangle) a_{ij} - \left[ \frac{4}{5} + \frac{7}{30} \chi M_t^2 \right] S_{pp}(\langle u \rangle) \left[ \frac{\delta_{ij}}{3} - \frac{\delta_{ij}^{(2)}}{2} \right] - \\ & 2 \left[ 1 - C_3 + \chi M_t^2 \right] \left[ a_{ip} \left( \frac{\delta_{pj}}{3} - \frac{\delta_{pj}^{(2)}}{2} \right) - \frac{1}{3} a_{pq} \left( \frac{\delta_{pq}}{3} - \frac{\delta_{pq}^{(2)}}{2} \right) \delta_{ij} \right] S_{pp}(\langle u \rangle) \Big] B_r F^{\beta r}. \end{aligned} \quad (42)$$

It is important to stress the fact the both expressions (2-D and 3-D) of the pressure-strain correlation model give the same result when applied to a two dimensional mean flow. The recasting is necessary to take advantage of the simplifying properties of this particular case. Also,

$$\mathcal{M}_{ij}^* = -\frac{1}{\rho} \frac{2}{3} \tau_u \nu_0 \langle k \rangle \underline{R}_{ij}^* + \frac{1}{\rho} \frac{2}{3} \tau_u \nu_0 \langle k \rangle R_{pp} \left[ \frac{\delta_{ij}}{3} - \frac{\delta_{ij}^{(2)}}{2} \right] \quad (43)$$

Using the previous information the final equation becomes:

$$\begin{aligned} \mathbf{a} &= -g\tau \left[ b_1 \underline{\mathbf{S}}^* + b_2 \underline{\mathbf{R}}^* + b_3 \left( \mathbf{a} \underline{\mathbf{S}}^* + \underline{\mathbf{S}}^* \mathbf{a} - \frac{2}{3} \{ \mathbf{a} \underline{\mathbf{S}}^* \} \delta \right) - b_4 (\mathbf{a} \underline{\mathbf{\Omega}} - \underline{\mathbf{\Omega}} \mathbf{a}) \right. \\ & \left. - b_5 \left( \frac{\delta}{3} - \frac{\delta^{(2)}}{2} \right) - b_6 \left( \mathbf{a} \left( \frac{\delta}{3} - \frac{\delta^{(2)}}{2} \right) - \frac{1}{3} \left\{ \mathbf{a} \left( \frac{\delta}{3} - \frac{\delta^{(2)}}{2} \right) \right\} \delta \right) \right] \end{aligned} \quad (44)$$

with  $b_1 = \frac{4}{3} - B_r F^{\beta r} \left( \frac{4}{5} + \frac{7}{30} \chi M_t^2 \right)$ ,  $b_2 = \frac{1}{\rho^2} \frac{2}{3} \tau_u \nu_0$ ,  $b_3 = 1 - B_r F^{\beta r} (1 - C_3 + \chi M_t^2)$ ,  $b_4 = 1 - B_r F^{\beta r} (1 - C_4 - \chi M_t^2)$ ,  $b_5 = b_1 S_{pp} + b_2 R_{pp}$ ,  $b_6 = b_3 S_{pp}$  and  $g$  having the same expression as in the 3-D algebraic equation. The polynomial solution  $\mathbf{a} = \sum_{\lambda} C^{\lambda} T^{\lambda}$  is based on only five independent tensors

$$\mathbf{T}^0 = \frac{\delta}{3} - \frac{\delta^{(2)}}{2}, \quad \mathbf{T}^1 = \underline{\mathbf{S}}^*, \quad \mathbf{T}^2 = \underline{\mathbf{S}}^* \underline{\mathbf{\Omega}} - \underline{\mathbf{\Omega}} \{ \underline{\mathbf{S}}^* \}, \quad \mathbf{T}^3 = \underline{\mathbf{R}}^*, \quad \mathbf{T}^4 = \underline{\mathbf{R}}^* \underline{\mathbf{\Omega}} - \underline{\mathbf{\Omega}} \underline{\mathbf{R}}^* \quad (45)$$

and five non-zero independent invariants:

$$\sigma^2 = \{\underline{\mathbf{S}}^{*2}\}, \quad \varpi^2 = \{\underline{\boldsymbol{\Omega}}^2\}, \quad \{\underline{\mathbf{R}}^{*2}\}, \quad \{\underline{\mathbf{R}}^* \underline{\mathbf{S}}^*\}, \quad \{\underline{\mathbf{S}}^* \underline{\mathbf{R}}^* \underline{\boldsymbol{\Omega}}\}. \quad (46)$$

The assertion that there are no other independent tensor products or invariants can be verified using the following  $2 \times 2$  matrix identity:

$$2\mathbf{a}\mathbf{b}\mathbf{c} = \mathbf{b}\mathbf{c}\{\mathbf{a}\} + \mathbf{a}\{\mathbf{b}\mathbf{c}\} + \mathbf{a}\mathbf{c}\{\mathbf{b}\} - \mathbf{b}\{\mathbf{a}\mathbf{c}\} + \mathbf{a}\mathbf{b}\{\mathbf{c}\} + \mathbf{c}\{\mathbf{a}\mathbf{b}\} - \mathbf{c}\{\mathbf{a}\}\{\mathbf{b}\} - \mathbf{a}\{\mathbf{b}\}\{\mathbf{c}\} + (\{\mathbf{a}\mathbf{c}\}\{\mathbf{b}\} - \{\mathbf{a}\mathbf{c}\mathbf{b}\})\delta^{(2)}. \quad (47)$$

To obtain the explicit solution to the algebraic equation in the anisotropic Reynolds stress a procedure similar to one devised by Pope.<sup>18</sup> We define the matrices  $5 \times 5$   $\mathcal{H}_\eta^\lambda$ ,  $\mathcal{J}_\eta^\lambda$ ,  $\mathcal{I}_\eta^\lambda$  such that

$$\begin{aligned} \mathbf{T}^\eta \underline{\mathbf{S}}^* + \underline{\mathbf{S}}^* \mathbf{T}^\eta - \frac{2}{3} \{\mathbf{T}^\eta \underline{\mathbf{S}}^*\} \delta &= \sum_\lambda \mathcal{H}_\eta^\lambda \mathbf{T}^\lambda \\ \mathbf{T}^\eta \underline{\boldsymbol{\Omega}}^* - \underline{\boldsymbol{\Omega}}^* \mathbf{T}^\eta &= \sum_\lambda \mathcal{J}_\eta^\lambda \mathbf{T}^\lambda \\ \mathbf{T}^\eta \left( \frac{\delta}{3} - \frac{\delta^{(2)}}{2} \right) - \frac{2}{3} \left\{ \mathbf{T}^\eta \left( \frac{\delta}{3} - \frac{\delta^{(2)}}{2} \right) \right\} \delta &= \sum_\lambda \mathcal{I}_\eta^\lambda \mathbf{T}^\lambda. \end{aligned} \quad (48)$$

The elements of the matrices are determined from the above equations by making use of matrix relations stemming from the Cayley-Hamilton theorem. Next, the coefficients of the tensor polynomial are obtained from

$$C^\lambda = -g\tau \left[ b_1 \delta_{1\lambda} + b_2 \delta_{3\lambda} + b_3 \sum_\eta C^\eta \mathcal{H}_\eta^\lambda - b_4 \sum_\eta C^\eta \mathcal{J}_\eta^\lambda - b_5 \delta_{0\lambda} - b_6 \sum_\eta C^\eta \mathcal{I}_\eta^\lambda \right]. \quad (49)$$

The resulting model for the anisotropy of the Reynolds stress tensor is:

$$\begin{aligned} \mathbf{a} = -2C_\mu \tau \left[ \mathcal{Q}_2 \underline{\mathbf{S}}^* + (\mathcal{Q}_1 + \mathcal{Q}_3) b_3 g f_2 \tau \sigma^2 \left( \frac{2}{3} \delta - \delta^{(2)} \right) + \mathcal{Q}_2 b_4 g f_1 \tau (\underline{\mathbf{S}}^* \underline{\boldsymbol{\Omega}} - \underline{\boldsymbol{\Omega}} \underline{\mathbf{S}}^*) \right] \\ - 2C'_\mu \tau [\underline{\mathbf{R}}^* + b_4 g f_1 \tau (\underline{\mathbf{R}}^* \underline{\boldsymbol{\Omega}} - \underline{\boldsymbol{\Omega}} \underline{\mathbf{R}}^*)] \end{aligned} \quad (50)$$

The parameters  $C_\mu$  and  $C'_\mu$  are given by:

$$C_\mu = \frac{b_1 g f_1 / 2}{1 - \frac{2}{3} (b_3 g \tau \sigma)^2 f_1 f_2 - 2(b_4 g f_1 \tau \varpi)^2} \quad (51)$$

$$C'_\mu = \frac{b_2 g f_1 / 2}{1 - 2(b_4 g f_1 \tau \varpi)^2} \quad (52)$$

and

$$\mathcal{Q}_1 = 1 + \frac{b_2}{b_1} \left[ \frac{\{\underline{\mathbf{S}}^* \underline{\mathbf{R}}^*\}}{\sigma^2} + 2g f_1 \tau b_4 \frac{\{\underline{\mathbf{S}}^* \underline{\mathbf{R}}^* \underline{\boldsymbol{\Omega}}\}}{\sigma^2} \right] \quad (53)$$

$$Q_2 = 1 + \frac{2}{3} \frac{(b_3 g \tau \sigma)^2 f_1 f_2}{1 - 2(b_4 g f_1 \tau \varpi)^2} (Q_1 - 1) - \frac{b_3 b_5}{3 b_1} g f_2 \tau \quad (54)$$

$$Q_3 = -\frac{b_5}{b_1 b_3} \frac{1 - 2(b_4 g f_1 \tau \varpi)^2}{2 g f_1 \tau \sigma^2} \quad (55)$$

with  $f_1 = (1 + b_6 g \tau / 6)^{-1}$  and  $f_2 = (1 - b_6 g \tau / 6)^{-1}$ .

### 2.3.2 ATFM

The temperature flux transport equation reads:

$$\begin{aligned} \frac{\partial \overline{\rho \langle u_i'' T'' \rangle}}{\partial t} + \frac{\partial \overline{\rho \langle u_i'' T'' \rangle \langle u_j \rangle}}{\partial x_j} &= -\frac{\partial (\overline{\rho \langle u_j'' u_i'' T'' \rangle} + \overline{\rho' T''} \delta_{ij} - \overline{T'' \sigma_{ji}(u'')})}{\partial x_j} \\ + \overline{\rho' \frac{\partial T''}{\partial x_i}} - \overline{\rho} \left( \langle u_j'' u_i'' \rangle \frac{\partial \langle T \rangle}{\partial x_j} + \langle u_j'' T'' \rangle \frac{\partial \langle u_i \rangle}{\partial x_j} \right) &- \overline{T''} \frac{\partial \overline{\rho}}{\partial x_i} + \overline{T''} \frac{\partial \sigma_{ji}(u'')}{\partial x_j} + \gamma C e \overline{u_i'' \dot{\omega}_P} \\ + \frac{\partial}{\partial x_j} \left[ \frac{\mu}{Pr Re} \overline{u_i'' \frac{\partial T''}{\partial x_j}} \right] - \frac{\mu}{Pr Re} \frac{\partial \overline{u_i''}}{\partial x_j} \frac{\partial \langle T \rangle}{\partial x_j} - \frac{\mu}{Pr Re} \frac{\partial \overline{u_i''}}{\partial x_j} \frac{\partial T''}{\partial x_j} - \overline{\sigma_{ji}(u'')} \frac{\partial T''}{\partial x_j} \\ - (\gamma - 1) \overline{\rho} \left( \langle u_i'' T'' \rangle \frac{\partial \langle u_j \rangle}{\partial x_j} + \langle T \rangle \left\langle u_i'' \frac{\partial u_j''}{\partial x_j} \right\rangle + \left\langle u_i'' T'' \frac{\partial u_j''}{\partial x_j} \right\rangle \right) &+ \gamma (\gamma - 1) M^2 \overline{u_i'' \sigma_{kj}} \frac{\partial u_k}{\partial x_j}. \end{aligned} \quad (56)$$

Modeling of  $\overline{T''}$  (following the methodology used by Ristorcelli<sup>47</sup> in deriving a model for  $\overline{u_i''}$ ). From the instantaneous the mean is subtracted:

$$\begin{aligned} \frac{\partial}{\partial t} (\rho T - \overline{\rho \langle T \rangle}) + \frac{\partial}{\partial x_j} (\rho T u_j - \overline{\rho \langle T \rangle \langle u_j \rangle}) &= RHS = \frac{\partial}{\partial x_j} \left( \frac{\gamma \mu}{Pr Re} \frac{\partial}{\partial x_j} (T - \overline{T}) \right) \\ - \gamma (\gamma - 1) M^2 \left( p \frac{\partial u_j}{\partial x_j} - \overline{p \frac{\partial u_j}{\partial x_j}} \right) + \gamma (\gamma - 1) M^2 \left( \sigma_{ij}(u) \frac{\partial u_j}{\partial x_j} - \overline{\sigma_{ij}(u) \frac{\partial u_j}{\partial x_j}} \right) &+ \gamma C e (\dot{\omega}_P - \overline{\dot{\omega}_P}). \end{aligned} \quad (57)$$

Obviously  $\overline{RHS} = 0$ . After expanding the differences on the left hand side, the terms are expressed in non-conservative form and the resulting equation is divided by the instantaneous density. After using the approximation  $1/\rho = (1 - \rho'/\overline{\rho} + \dots)/\overline{\rho}$  the equation is averaged and the terms of order  $\geq \sqrt{\rho'^2/\overline{\rho}}$  are eliminated. For example, the difference term  $\langle u_i'' T'' \rangle - \overline{u_i'' T''} = \overline{\rho' u_i'' T''} / \overline{\rho} \sim O(\sqrt{\rho'^2/\overline{\rho}})$  is discarded. This results in:

$$\frac{D \overline{T''}}{Dt} = \overline{T''} \frac{\partial \overline{u_j''}}{\partial x_j} - \overline{u_j''} \frac{\partial \langle T \rangle}{\partial x_j} + \frac{\langle u_j'' T'' \rangle}{\overline{\rho}} \frac{\partial \overline{\rho}}{\partial x_j} \quad (58)$$

Precedent contributors<sup>49,47</sup> have represented the term correlating fluctuating divergence with velocity fluctuation by a linear relaxation model. Because both the divergence-temperature correlation

and  $\overline{T''}$  are scalars the following relation is valid on dimensional grounds:

$$\overline{T'' \frac{\partial u_j''}{\partial x_j}} = -\frac{\overline{T''}}{\tau_d} \quad (59)$$

where  $\tau_d = M_t \tau$  is the acoustic time scale. Next, assuming that the quantity  $\overline{T''}/\sqrt{\langle T''^2 \rangle}$  reaches a near-asymptotic state we have

$$\frac{D\overline{T''}}{Dt} = \overline{T''} \frac{\overline{\epsilon_\vartheta}}{\langle T''^2 \rangle} \left( \frac{P_\vartheta}{\overline{\rho} \overline{\epsilon_\vartheta}} - 1 \right) \quad (60)$$

where  $P_\vartheta$  is the production of temperature variance. Combining the the equations 58, 59, 60 the following expression is obtained:

$$\overline{\rho T''} = \tau_t \left( \langle u_j'' T'' \rangle \frac{\partial \overline{\rho}}{\partial x_j} - \overline{\rho u_j''} \frac{\partial \langle T \rangle}{\partial x_j} \right) \quad (61)$$

where  $\tau_t = M_t \tau / [1 + \frac{\langle k \rangle \overline{\epsilon_\vartheta}}{\langle T''^2 \rangle \overline{\epsilon_s}} M_t (P_\vartheta / (\overline{\rho} \overline{\epsilon_\vartheta}) - 1)]$ . Similar to the treatment of the Reynolds stress, the temperature flux equation is transformed into the equation for the correlation coefficient

$$\vartheta_i = \frac{\langle u_i'' T'' \rangle}{\sqrt{\langle k \rangle \langle T''^2 \rangle}}, \quad (62)$$

and the transport equation reads

$$\begin{aligned} \frac{\overline{\rho} D\vartheta_i}{Dt} = & \frac{1}{\sqrt{\langle k \rangle \langle T''^2 \rangle}} \left( \frac{\partial T_{ij}^\vartheta}{\partial x_j} - \frac{\vartheta_i}{2} \sqrt{\frac{\langle k \rangle}{\langle T''^2 \rangle}} \frac{\partial T_j^\vartheta}{\partial x_j} - \frac{\vartheta_{i\vartheta}}{2} \sqrt{\frac{\langle T''^2 \rangle}{\langle k \rangle}} \frac{\partial T_j}{\partial x_j} \right) \\ & - \overline{\rho} \left[ \frac{\vartheta_i \overline{\epsilon_\vartheta}}{\langle T''^2 \rangle} \left( \frac{P_\vartheta}{\overline{\rho} \overline{\epsilon_\vartheta}} - 1 \right) + \frac{\vartheta_i}{2\tau} \left( \frac{P}{\overline{\rho} \overline{\epsilon_s}} - 1 + \frac{\mathcal{M} + \mathcal{V} + \overline{p'd} - \overline{\rho} \overline{\epsilon_c}}{\overline{\rho} \overline{\epsilon_s}} \right) \right] \\ & + \frac{1}{\sqrt{\langle k \rangle \langle T''^2 \rangle}} [P_{i\vartheta} + \Phi_{i\vartheta} - \overline{\rho} \overline{\epsilon_{i\vartheta}}], \end{aligned} \quad (63)$$

where the notation  $D/Dt$  indicates the convective transport,  $T_{ij}^\vartheta$ ,  $T_j^\vartheta$  and  $T_j$  denote turbulent transports of the temperature flux, the temperature variance and the kinetic energy, respectively. Moreover  $P_\vartheta = -\sqrt{\langle k \rangle \langle T''^2 \rangle} \vartheta_j \partial \langle T \rangle / \partial x_j$  is the production of temperature variance and the remaining quantities are the normalized production, pressure-gradient correlation and flux dissipation:

$$P_{i\vartheta} = -\sqrt{\langle k \rangle \langle T''^2 \rangle} \left[ \langle k \rangle (a_{ij} + \frac{2}{3} \delta_{ij}) \frac{\partial \langle T \rangle}{\partial x_j} + \vartheta_{j\vartheta} (S_{ij}^*(\langle u \rangle)) + \Omega_{ij}(\langle u \rangle) + \frac{1}{3} \vartheta_{i\vartheta} S_{kk}^*(\langle u \rangle) \right] \quad (64)$$

The pressure-temperature gradient model

$$\Phi_i - \overline{\rho} \overline{\epsilon_{i\vartheta}} = \mathcal{A}_i + 2\overline{\rho} \mathcal{L}_{ijk} (S_{jk}(\langle u \rangle)) + \Omega_{jk}(\langle u \rangle) \quad (65)$$

The linear nature of the temperature equations imposes that the integrals  $\mathcal{I}_{ijk}$  as well as the vector  $\mathcal{A}_i$  be linear in the turbulent flux. Therefore

$$\frac{\mathcal{I}_{ijk}}{\sqrt{\langle k \rangle \langle T''^2 \rangle}} = \beta_1 \delta_{ij} \vartheta_k + \beta_2 (\delta_{ik} \vartheta_j + \delta_{jk} \vartheta_i) + f_1 a_{ij} \vartheta_k + f_2 (a_{ik} \vartheta_j + a_{jk} \vartheta_i) + f_3 \delta_{ij} a_{kp} \vartheta_p \quad (66)$$

The symmetry constraints are satisfied for the above form for  $\mathcal{I}_{ijk}$ . To determine the coefficients more constraints are applied: the normalization condition which translates into  $\mathcal{I}_{iij} = \langle u_i'' T'' \rangle$ . The incompressibility condition is replaced with  $\mathcal{I}_{ikk} / \sqrt{\langle k \rangle \langle T''^2 \rangle} = \xi M_t^2 / 2 (\vartheta_i + a_{ik} \vartheta_k)$ , where the constant  $\xi$  has to be calibrated from DNS. These conditions are still insufficient for the determination of the constants  $f_1, f_2, f_3$ . These coefficients were chosen so that  $\mathcal{I}_{ijk}$  proposed by SLC89 is recovered in the incompressible limit. Realizability criteria is based now on the tensor  $d_{jk} = (\langle u_j'' T'' \rangle \langle u_k'' T'' \rangle - \langle u_j'' u_k'' \rangle \langle T''^2 \rangle) / (\langle u_p'' T'' \rangle \langle u_p'' T'' \rangle - 2 \langle k \rangle \langle T''^2 \rangle)$  and the linear function of the invariants of  $d_{jk}$   $F_D = 9/2 - 27d_{jj}^2/2 + 9d_{jj}^3$ ,  $II_d$  is the second invariant of the tensor  $d_{jk}$ ,  $d_{jj}^2 = d_{ji} d_{ij}$  and  $d_{jj}^3 = d_{jil} d_{lm} d_{mj}$ .

$$\begin{aligned} \tau \langle u_e'' T'' \rangle \mathcal{A}_e - \langle T''^2 \rangle (\mathcal{A}_{ee} - \frac{2}{3} \bar{\rho} \bar{\epsilon}) + 2\bar{\rho} \bar{\epsilon}_\vartheta \langle u_e''^2 \rangle &= C F_D^\alpha \quad \text{as } F_D \rightarrow 0 \\ \frac{\partial \langle u_p \rangle}{\partial x_q} (\langle T''^2 \rangle \mathcal{I}_{peqe} - \langle u_e'' T'' \rangle \mathcal{I}_{epq}) &\rightarrow 0 \quad \text{as } F_D \rightarrow 0 \end{aligned} \quad (67)$$

$$\begin{aligned} \frac{\Phi_{i\vartheta}}{\sqrt{\langle k \rangle \langle T''^2 \rangle}} &= -C_{1\vartheta} \bar{\rho} \frac{\epsilon}{\langle k \rangle} \vartheta_{i\vartheta} A_r F_D^{\alpha_r} + \bar{\rho} \left[ (c_1 + c_2) S_{ij}^* (\langle u \rangle) \vartheta_{j\vartheta} + (c_1 - c_2) \Omega_{ij} (\langle u \rangle) \vartheta_{j\vartheta} \right. \\ &\quad \left. + (c_3 + c_4) a_{ij} S_{jk}^* (\langle u \rangle) \vartheta_{k\vartheta} + c_5 a_{jk} S_{ij}^* (\langle u \rangle) \vartheta_{k\vartheta} + (c_3 - c_4) a_{ij} \Omega_{jk} (\langle u \rangle) \vartheta_{k\vartheta} \right. \\ &\quad \left. + c_5 a_{jk} \Omega_{ij} (\langle u \rangle) \vartheta_{k\vartheta} + c_4 a_{jk} S_{jk}^* (\langle u \rangle) \vartheta_{i\vartheta} + \frac{1}{3} \xi M_t^2 (\vartheta_{i\vartheta} + a_{ik} \vartheta_{k\vartheta}) S_{pp}^* (\langle u \rangle) \right] B_r F_D^{\beta_r} \end{aligned} \quad (68)$$

where  $C_{1\vartheta} = 3.2$ ,  $c_1 = 4/5 - \xi M_t^2 / 5$ ,  $c_2 = -1/5 + 3\xi M_t^2 / 10$ ,  $c_3 = 1/10 + \xi M_t^2 / 2$ ,  $c_4 = -3/10 + 3\xi M_t^2 / 2$ ,  $c_5 = 1/5 - \xi M_t^2$ . The parameters are  $\alpha_r = 0.1$ ,  $\beta_r = 0.5$ ,  $A_r = \min(F_D^{-\alpha_r}, 0.1^{-\alpha_r})$  and  $B_r = \min(F_D^{-\beta_r}, 0.1^{-\beta_r})$ . The coupling between the species and temperature reflected in the temperature flux equation for the reacting case with heat release is neglected for simplification purposes. Using all the present information the equation for  $\vartheta$  is:

$$\vartheta + D_\vartheta \mathbf{A} \vartheta + \mathbf{C}_\vartheta = 0 \quad (69)$$

where the coefficient  $D_\vartheta = 2\tau h_\vartheta$ , with

$$\begin{aligned} h_\vartheta &= \left[ 2A_r F_D^{\alpha_r} C_{1\vartheta} \frac{\bar{\epsilon}}{\bar{\epsilon}_s} - 1 + (1 + 2c_4 B_r F_D^{\beta_r}) \frac{P}{\bar{\rho} \bar{\epsilon}_s} + r_\vartheta \left( \frac{P_\vartheta}{\bar{\rho} \bar{\epsilon}_\vartheta} - 1 \right) + \right. \\ &\quad \left. \frac{2\tau}{3} (1 - \lambda M_t^2 B_r F_D^{\beta_r}) S_{pp} (\langle u \rangle) + \frac{\mathcal{M} + \overline{p'd} - \bar{\rho} \bar{\epsilon}_c}{\bar{\rho} \bar{\epsilon}_s} \right]^{-1}, \end{aligned} \quad (70)$$

where  $r_\vartheta = 2\langle k \rangle (\bar{\epsilon}_\vartheta / (\bar{\epsilon}_s \langle T''^2 \rangle))$  is the time scales ratio. The vector term reads:

$$C_{i\vartheta} = D_\vartheta \sqrt{\frac{\langle k \rangle}{\langle T''^2 \rangle}} \left[ a_{ki} + \frac{2}{3} \delta_{ki} - b_2 \tau_t \mathcal{R}_{ik} \right] \frac{\partial \langle T \rangle}{\partial x_k}. \quad (71)$$

Due to the nonsymmetric properties of the second order tensor  $\mathbf{A}$  an anisotropic turbulent diffusivity tensor will be obtained in the final model.

$$\begin{aligned} A_{ik} = A'_{ik} + \frac{\tau_t}{\rho^2} \mathcal{R}_{ik} = & [1 - (c_1 + c_2) B_r F_D^{\beta r}] S_{ik}^*(\langle u \rangle) + [1 - (c_1 - c_2) B_r F_D^{\beta r}] \Omega_{ik}(\langle u \rangle) - \\ & \left[ (c_3 + c_4) a_{ij} S_{jk}^*(\langle u \rangle) + c_5 a_{kj} S_{ji}^*(\langle u \rangle) + (c_3 - c_4) a_{ij} \Omega_{jk}(\langle u \rangle) - c_5 a_{kj} \Omega_{ji}(\langle u \rangle) \right. \\ & \left. + \frac{1}{3} \xi M_t^2 a_{ik} S_{pp}^*(\langle u \rangle) \right] B_r F_D^{\beta r} + \frac{\tau_t}{\rho^2} \mathcal{R}_{ik}. \end{aligned} \quad (72)$$

Now, the solution of the system is conveniently represented in the matrix form:

$$\varphi_\vartheta = -\mathbf{M}^{-1} \mathbf{C}_\vartheta \quad (73)$$

where  $\mathbf{M}$  denotes the matrix  $[\delta + D_\vartheta \mathbf{A}]$ .

To provide a computationally efficient algorithm, the matrix  $\mathbf{M}$  is inverted analytically. This is achieved via the use of the Cayley-Hamilton theorem and yields an expansion on the minimal vectorial basis for this problem:

$$\varphi_\vartheta = \sum_{n=0}^2 a_n \mathbf{A}^n \mathbf{C}_\vartheta \quad (74)$$

### 2.3.3 ASFM

The methodology used for the temperature flux is now applied to the scalar flux which is transported according to the equation:

$$\begin{aligned} \frac{\partial \overline{\rho \langle u_i'' Y_\alpha'' \rangle}}{\partial t} + \frac{\partial \overline{\rho \langle u_i'' Y_\alpha'' \rangle \langle u_j \rangle}}{\partial x_j} = & - \frac{\partial (\overline{\rho \langle u_j'' u_i'' Y_\alpha'' \rangle} + \overline{p' Y_\alpha''} \delta_{ij} - \overline{Y_\alpha''} \sigma_{ji}(u''))}{\partial x_j} \\ + p' \frac{\partial \overline{Y_\alpha''}}{\partial x_i} - \overline{\rho} \left( \langle u_j'' u_i'' \rangle \frac{\partial \langle Y_\alpha \rangle}{\partial x_j} + \langle u_j'' Y_\alpha'' \rangle \frac{\partial \langle u_i \rangle}{\partial x_j} \right) - & \overline{Y_\alpha''} \frac{\partial \overline{\rho}}{\partial x_i} + \overline{Y_\alpha''} \frac{\partial \sigma_{ji}(u)}{\partial x_j} + \overline{u'' \dot{\omega}_\alpha} \\ + \frac{\partial}{\partial x_j} \left[ \frac{\mu}{ScRe} \overline{u_i'' \frac{\partial Y_\alpha''}{\partial x_j}} - \frac{\mu}{ScRe} \frac{\partial \overline{u_i''}}{\partial x_j} \frac{\partial \langle Y_\alpha \rangle}{\partial x_j} - \frac{\mu}{ScRe} \frac{\partial \overline{u_i''}}{\partial x_j} \frac{\partial \overline{Y_\alpha''}}{\partial x_j} - \overline{\sigma_{ji}(u'')} \frac{\partial \overline{Y_\alpha''}}{\partial x_j} \right] \end{aligned} \quad (75)$$

where the reaction source term can be approximated by:

$$\overline{u'' \dot{\omega}_\alpha} = -Da \exp \left[ -Ze \left( \frac{1}{\langle T \rangle} - \frac{1}{T_f} \right) \right] \overline{\rho^2} (\langle u_i'' Y_\alpha'' \rangle \langle Y_\beta \rangle + \langle u_i'' Y_\beta'' \rangle \langle Y_\alpha \rangle + \langle u_i'' Y_\alpha'' Y_\beta'' \rangle). \quad (76)$$

The model derivations leading to expressions for the averaged Favré fluctuations, pressure scalar gradient correlation are identical with the ones presented for the temperature related quantities. For  $\overline{Y_\alpha''}$  we have:

$$\overline{\rho Y_\alpha''} = \tau_s \left( \langle u_j'' Y_\alpha'' \rangle \frac{\partial \overline{\rho}}{\partial x_j} - \overline{\rho} u_j'' \frac{\partial \langle Y_\alpha \rangle}{\partial x_j} \right) \quad (77)$$

where  $\tau_s = M_t \tau / [1 + \frac{\langle k \rangle \bar{\epsilon}_\alpha}{\langle Y_\alpha''^2 \rangle \bar{\epsilon}_s} M_t (P_\alpha / (\overline{\rho} \bar{\epsilon}_\alpha) - 1)]$ . The correlation coefficient

$$\varphi_{i\alpha} = \frac{\langle u_i'' Y_\alpha'' \rangle}{\sqrt{\langle k \rangle \langle Y_\alpha''^2 \rangle}} \quad (78)$$

evolves according to

$$\begin{aligned} \overline{\rho} \frac{D\varphi_{i\alpha}}{Dt} = & \frac{1}{\sqrt{\langle k \rangle \langle Y_\alpha''^2 \rangle}} \left( \frac{\partial T_{ij}^\alpha}{\partial x_j} - \frac{\varphi_{i\alpha}}{2} \sqrt{\frac{\langle k \rangle}{\langle Y_\alpha''^2 \rangle}} \frac{\partial T_j^\alpha}{\partial x_j} - \frac{\varphi_{i\alpha}}{2} \sqrt{\frac{\langle Y_\alpha''^2 \rangle}{\langle k \rangle}} \frac{\partial T_j}{\partial x_j} \right) \\ & - \overline{\rho} \left[ \frac{\varphi_{i\alpha} \bar{\epsilon}_\alpha}{\langle Y_\alpha''^2 \rangle} \left( \frac{P_\alpha}{\overline{\rho} \bar{\epsilon}_\alpha} - 1 + \frac{S_\alpha}{\overline{\rho} \bar{\epsilon}_\alpha} \right) + \frac{\varphi_{i\alpha}}{2\tau} \left( \frac{P}{\overline{\rho} \bar{\epsilon}_s} - 1 + \frac{\mathcal{M} + \mathcal{V} + \overline{p'd} - \overline{\rho} \bar{\epsilon}_c}{\overline{\rho} \bar{\epsilon}_s} \right) \right] + \\ & \frac{1}{\sqrt{\langle k \rangle \langle Y_\alpha''^2 \rangle}} [P_{i\alpha} + \Phi_{i\alpha} - \overline{\rho} \bar{\epsilon}_{i\alpha} + S_{i\alpha}], \end{aligned} \quad (79)$$

where the notation is similar to the temperature flux case, for example

$P_\alpha = -\sqrt{\langle k \rangle \langle Y_\alpha''^2 \rangle} \varphi_{j\alpha} \partial \langle Y_\alpha \rangle / \partial x_j$  is the production of scalar variance. The terms that appear extra with respect with the previous case are due to the reaction source term and they are:  $S_\alpha = \langle \dot{\omega}_\alpha Y_\alpha'' \rangle$  which is the chemical source term in the  $\langle Y_\alpha''^2 \rangle$  equation and similarly for the flux equation,

$$S_{i\alpha} = -Da \frac{1}{\sqrt{\langle k \rangle \langle Y_\alpha''^2 \rangle}} (\varphi_{i\alpha} \langle Y_\beta \rangle + \varphi_{i\beta} \langle Y_\alpha \rangle + \gamma_{i\alpha\beta} \sqrt{\langle Y_\beta''^2 \rangle}). \quad (80)$$

Here  $\gamma_{i\alpha\beta} = \langle u_i'' Y_\alpha'' Y_\beta'' \rangle / \sqrt{\langle k \rangle \langle Y_\alpha''^2 \rangle \langle Y_\beta''^2 \rangle}$  is the normalized covariance flux vector. It is worth mentioning that for the pressure scalar gradient model the realizability is based on the tensor  $d_{jk} = (\langle u_j'' Y_\alpha'' \rangle \langle u_k'' Y_\alpha'' \rangle - \langle u_j'' u_k'' \rangle \langle Y_\alpha''^2 \rangle) / (\langle u_p'' Y_\alpha'' \rangle \langle u_p'' Y_\alpha'' \rangle - 2\langle k \rangle \langle Y_\alpha''^2 \rangle)$ . The final form of the model is the same as for the pressure temperature gradient model, replacing the temperature flux with the scalar flux along with the appropriate normalization. This procedure leads to an algebraic system of equations for the two unknown vectors  $\varphi_{i\alpha}$  and  $\varphi_{i\beta}$ . For the mixing case the two vectors are uncoupled and the solution is matricially the same as the temperature flux. The reacting can be solved exact, but due to chemical coupling the solution will be too complicated to be of practical use. Therefore either the mixing solution can be utilized or a perturbation solution of the reacting case, the small parameter  $\varepsilon = \tau_i / \overline{\rho}^2$ . The fluxes are decomposed as  $\varphi_{i\alpha} = \varphi_{i\alpha}^0 + \varepsilon \varphi_{i\alpha}^1$  and

$\varphi_{i\beta} = \varphi_{i\beta}^0 + \varepsilon\varphi_{i\beta}^1$ . The solution is obtained from the system of equations

$$\begin{cases} \varphi_\alpha + D_\alpha(\mathbf{A}' + \varepsilon\mathcal{R})\varphi_\alpha + B_\alpha\varphi_\beta + \mathbf{C}_\alpha = 0 \\ \varphi_\beta + D_\beta(\mathbf{A}' + \varepsilon\mathcal{R})\varphi_\beta + B_\beta\varphi_\alpha + \mathbf{C}_\beta = 0 \end{cases} \quad (81)$$

where the coefficients are

$$\begin{aligned} D_\alpha &= \frac{2\tau h_\alpha}{1 + 2Da\bar{\rho} \exp\left[-Ze\left(\frac{1}{\langle T \rangle} - \frac{1}{T_f}\right)\right] \tau h_\alpha \langle Y_\beta \rangle}, \\ B_\alpha &= Da\bar{\rho} \exp\left[-Ze\left(\frac{1}{\langle T \rangle} - \frac{1}{T_f}\right)\right] \langle Y_\alpha \rangle D_\alpha, \end{aligned} \quad (82)$$

And the vector terms read:

$$\begin{aligned} C_{i\alpha} &= D_\alpha \left[ \sqrt{\frac{\langle k \rangle}{\langle Y_\alpha'^2 \rangle}} \left( a_{ki} + \frac{2}{3}\delta_{ki} - b_2\tau_i\mathcal{R}_{ik} \right) \frac{\partial \langle Y_\alpha \rangle}{\partial x_k} + \right. \\ &\quad \left. Da\bar{\rho} \exp\left[-Ze\left(\frac{1}{\langle T \rangle} - \frac{1}{T_f}\right)\right] \sqrt{\langle Y_\beta'^2 \rangle} \gamma_{i\alpha\beta} \right] \end{aligned} \quad (83)$$

The terms indexed with  $\beta$  are obtained from the  $\alpha$  indexed terms by the permutations  $\alpha \rightarrow \beta$  and  $\beta \rightarrow \alpha$  where necessary. The parameters  $h_\alpha$  and  $h_\beta$  have the same form as  $h_\beta$  (Eq. (70)) with the respective change of index. The solution of the system (81) given in matrix form:

$$\begin{cases} \varphi_\alpha^0 = -\mathbf{M}^{-1} [(\delta + D_\beta\mathbf{A})\mathbf{C}_\alpha - B_\alpha\mathbf{C}_\beta] \\ \varphi_\beta^0 = -\mathbf{M}^{-1} [(\delta + D_\alpha\mathbf{A})\mathbf{C}_\beta - B_\beta\mathbf{C}_\alpha] \end{cases} \quad (84)$$

$$\begin{cases} \varphi_\alpha^1 = -\mathbf{M}^{-1} \left[ (\delta + D_\beta\mathbf{A})D_\alpha\mathcal{R}\varphi_\alpha^0 - B_\alpha D_\beta\mathcal{R}\varphi_\beta^0 \right] \\ \varphi_\beta^1 = -\mathbf{M}^{-1} \left[ (\delta + D_\alpha\mathbf{A})D_\beta\mathcal{R}\varphi_\beta^0 - B_\beta D_\alpha\mathcal{R}\varphi_\alpha^0 \right] \end{cases} \quad (85)$$

where  $\mathbf{M}$  denotes the matrix  $[(1 - B_\alpha B_\beta)\delta + (D_\alpha + D_\beta)\mathbf{A} + D_\alpha D_\beta \mathbf{A}^2]$ . Using the methods mentioned in the temperature flux section and described below results:

$$\varphi_\alpha = \sum_{n=0}^2 a_n \mathbf{A}^n \mathbf{C}_\alpha + \sum_{n=0}^2 a_n'' \mathbf{A}^n \mathbf{C}_\beta. \quad (86)$$

### 2.3.4 Explicit Solution

The procedure leading to explicit solutions for the turbulent fluxes vector is described. Consider an arbitrary three-dimensional second-order tensor  $\mathbf{Q} \equiv [Q_{ij}]$  and the corresponding Kronecker tensor  $\delta \equiv [\delta_{ij}]$ . According to the Cayley-Hamilton theorem, this matrix satisfies its own characteristic polynomial:

$$\mathbf{Q}^3 - I_Q \mathbf{Q}^2 + II_Q \mathbf{Q} - III_Q \delta = \mathbf{0} \quad (87)$$

where  $I_Q = \{\mathbf{Q}\} = Q_{ii}$ ,  $II_Q = \frac{1}{2}[\{\mathbf{Q}\}^2 - \{\mathbf{Q}^2\}] = \frac{1}{2}[Q_{ii}Q_{jj} - Q_{ij}Q_{ji}]$ ,  $III_Q = \frac{1}{6}[\{\mathbf{Q}\}^3 - 3\{\mathbf{Q}\}\{\mathbf{Q}^2\} + 2\{\mathbf{Q}^3\}] = \frac{1}{6}[Q_{ii}Q_{jj}Q_{kk} - 3Q_{ii}Q_{jk}Q_{kj} + 2Q_{ij}Q_{jk}Q_{ki}]$  are the three tensorial invariants. Multiplying the characteristic polynomial with  $\mathbf{Q}^{-1}$  and solving for the inverse we obtain:

$$\mathbf{Q}^{-1} = \frac{1}{III_Q}(\mathbf{Q}^2 - I_Q\mathbf{Q} + II_Q\delta). \quad (88)$$

This relation can be used now to find explicit solutions to the problem considered here. We can write:

$$\varphi_\alpha = -(\delta + \mathbf{G})^{-1}\mathbf{C}. \quad (89)$$

Hence:

$$(\delta + \mathbf{G})^{-1} = \frac{1}{III_{\delta+\mathbf{G}}}[\mathbf{G}^2 + (2 - I_{\delta+\mathbf{G}})\mathbf{G} + (1 - I_{\delta+\mathbf{G}} + II_{\delta+\mathbf{G}})\delta]. \quad (90)$$

It is easy to show that  $I_{\delta+\mathbf{G}} = I_{\mathbf{G}} + \{\delta\}$ ,  $II_{\delta+\mathbf{G}} = 2I_{\mathbf{G}} + II_{\mathbf{G}} + \{\delta\}$ ,  $III_{\delta+\mathbf{G}} = I_{\mathbf{G}} + II_{\mathbf{G}} + III_{\mathbf{G}} + \frac{\{\delta\}}{3}$ . Therefore the normalized turbulent flux vector takes the form:

$$\varphi_\alpha = a_0\mathbf{C} + a_1\mathbf{G}\mathbf{C} + a_2\mathbf{G}^2\mathbf{C} \quad (91)$$

with the coefficients:

$$a_0 = -\frac{1 + I_{\mathbf{G}} + II_{\mathbf{G}}}{1 + I_{\mathbf{G}} + II_{\mathbf{G}} + III_{\mathbf{G}}} \quad (92)$$

$$a_1 = \frac{1 + I_{\mathbf{G}}}{1 + I_{\mathbf{G}} + II_{\mathbf{G}} + III_{\mathbf{G}}} \quad (93)$$

$$a_2 = -\frac{1}{1 + I_{\mathbf{G}} + II_{\mathbf{G}} + III_{\mathbf{G}}}. \quad (94)$$

The reacting case is somewhat more complex. Nevertheless, by following the same procedure explicit solutions are obtained:

$$\varphi_\alpha = a_0\mathbf{C}_\alpha + a'_0\mathbf{C}_\beta + a_1\mathbf{A}\mathbf{C}_\alpha + a'_1\mathbf{A}\mathbf{C}_\beta + a_2\mathbf{A}^2\mathbf{C}_\alpha + a'_2\mathbf{A}^2\mathbf{C}_\beta \quad (95)$$

$$\varphi_\beta = b_0\mathbf{C}_\alpha + b'_0\mathbf{C}_\beta + b_1\mathbf{A}\mathbf{C}_\alpha + b'_1\mathbf{A}\mathbf{C}_\beta + b_2\mathbf{A}^2\mathbf{C}_\alpha + b'_2\mathbf{A}^2\mathbf{C}_\beta, \quad (96)$$

with the coefficients:

$$a_0 = -\frac{F_\beta(F_\alpha + D_\alpha^2\frac{\{\mathbf{A}^3\}}{3}) + B_\alpha B_\beta \left[ \frac{\{\mathbf{A}^3\}}{3}(D_\beta F_\alpha - ED_\alpha)D_\beta - E(E + \frac{\{\mathbf{A}^3\}}{3})D_\alpha D_\beta \right]}{(1 - B_\alpha B_\beta)(F_\alpha F_\beta - E^2 B_\alpha B_\beta)}, \quad (97)$$

$$a'_0 = B_\alpha \frac{F_\alpha(F_\beta + D_\beta^2\frac{\{\mathbf{A}^3\}}{3}) + D_\alpha \frac{\{\mathbf{A}^3\}}{3}(D_\alpha F_\beta - ED_\beta) - EB_\alpha B_\beta(E + \frac{\{\mathbf{A}^3\}}{3})D_\alpha D_\beta}{(1 - B_\alpha B_\beta)(F_\alpha F_\beta - E^2 B_\alpha B_\beta)}, \quad (98)$$

$$a_1 = \frac{B_\alpha B_\beta [E(D_\beta - D_\alpha) + F_\alpha D_\beta] - D_\alpha F_\beta}{D_\alpha(F_\alpha F_\beta - E^2 B_\alpha B_\beta)} \quad (99)$$

$$a'_1 = \frac{B_\alpha D_\alpha F_\beta - D_\beta F_\alpha - E(D_\beta - D_\alpha B_\alpha B_\beta)}{D_\alpha F_\alpha F_\beta - E^2 B_\alpha B_\beta} \quad (100)$$

$$a_2 = \frac{D_\alpha F_\beta - E D_\beta B_\alpha B_\beta}{F_\alpha F_\beta - E^2 B_\alpha B_\beta} \quad (101)$$

$$a'_2 = -B_\alpha \frac{D_\alpha F_\beta - E D_\beta}{F_\alpha F_\beta - E^2 B_\alpha B_\beta}, \quad (102)$$

with the shorthand notations:

$$F_\alpha = (1 - B_\alpha B_\beta) \left( D_\alpha \frac{\{\mathbf{A}^2\}}{2} - \frac{1}{D_\alpha} - \frac{B_\alpha B_\beta}{D_\beta} \right) - D_\alpha^2 \frac{\{\mathbf{A}^3\}}{3} \quad (103)$$

$$F_\beta = (1 - B_\alpha B_\beta) \left( D_\beta \frac{\{\mathbf{A}^2\}}{2} - \frac{1}{D_\beta} - \frac{B_\alpha B_\beta}{D_\alpha} \right) - D_\beta^2 \frac{\{\mathbf{A}^3\}}{3} \quad (104)$$

$$E = \left( \frac{1}{D_\alpha} + \frac{1}{D_\beta} \right) (1 - B_\alpha B_\beta) - D_\alpha D_\beta \frac{\{\mathbf{A}^3\}}{3}. \quad (105)$$

The coefficients  $b_i$  are obtained from the  $a_i$ 's through the permutations  $\alpha \rightarrow \beta$ ,  $\beta \rightarrow \alpha$ ,  $a_0 \rightarrow b'_0$ ,  $a'_0 \rightarrow b_0$ ,  $a_1 \rightarrow b'_1$ ,  $a'_1 \rightarrow b_1$ ,  $a_2 \rightarrow b'_2$  and  $a'_2 \rightarrow b_2$ .

## 2.4 Results and Conclusion

The theory built in previous chapters will be used to simulate numerically a non-premixed, turbulent reacting with heat release, spatially developing mixing layer over a wide range of Mach numbers. The simulations are performed on a uniform grid in the computational space. By means of a coordinate transformation the mesh is transversally compressed in the physical space in the region corresponding to the actual mixing layer and the equations are solved in vector form. The numerical solution procedure for the integration of the governing equations is based on a Gottlieb-Turkel predictor-corrector finite difference scheme.<sup>50</sup> The method has dissipative properties and it is second-order accurate in time and fourth-order accurate in space. The interest at the present time lies in the steady-state solution and therefore, to accelerate the convergence towards steadiness, a local time stepping technique is used. The convergence criteria is imposed to be that the reduction of the steady-state residual in average sense attains a minimum acceptable level. More specifically, the simulation is considered at steady-state when is observed at least a 1.5 order of

magnitude reduction of a global quantity, such as the absolute value of the residual averaged over the whole domain. Figure 2.1 shows a typical evolution for the the previously mentioned quantity obtained with the Gottlieb-Turkel scheme. Although the criteria is quite stringent it is known<sup>51</sup> that predictor-corrector type of schemes are not able to achieve better rates of residual reduction. The set of initial conditions is obtained by propagating the inflow conditions throughout the entire domain, hence, in this procedure, the flow has to sweep at least one time the domain to obtain a meaningful result. The boundary conditions are set according to the elliptic nature of the problem on all four boundaries. The inflow BC specifies smoothed step or smoothed hat profiles for the primary variables. At the outflow and outer boundaries zero gradient boundary conditions are applied for their nonreflective properties in relation with the outgoing waves. The grid overlaying the computational domain of  $120\delta_\omega \times 60\delta_\omega$  had  $128 \times 64$  points, where the vorticity thickness  $\delta_\omega = (u_1 - u_2)/(\partial u/\partial y)_{max}$ . In the first stage of this work we have concentrated mainly on hydrodynamics. Test simulations were performed with simplified versions of the algebraic model for the Reynolds stresses. The particular set of conditions for the two streams of air were a prescribed velocity ratio  $r_v = 1/4$  and equal thermodynamic properties. The issue of reduced spreading rate of the shear layers with increasing free stream Mach number is well established experimentally. The compressibility effects parameter called convective Mach number correlates with the growth rate normalized by its incompressible value at the same ratios for velocity and density<sup>52</sup> and had the expression in this case  $M_c = M (1 - r_v)/2$ . The fully developed shear layer at high Reynolds numbers grows linearly and the spreading rate can be expressed as  $d\delta_u/dx = C_\delta(1 - r_v)/(1 + r_v)$  where  $\delta = \delta(x)$  is the thickness of the shear layer based on the normalized velocity profile and  $C_\delta$  is constant (approximatively). Figure 2.2 represents the downstream-evolution of the shear-layer width. The linear growth is attained after a phase of development near the inlet. The confirmation that a fully developed regime with linear growth has been installed in the flow, stems from the self-similar property of the velocity profiles and normalized Reynolds stresses. As it can be seen from figures 2.3, 2.4, 2.5 the profiles, plotted in similarity coordinates, collapse for each axial coordinate considered in the outflow region of the domain. The temperature profile shows the same self-similar behavior as the other mentioned quantities and as a result of the velocity gradients displays an increase in the middle of the layer. The correlation profile of the normalized  $C_\delta$  versus  $M_c$  has yet to be completed. The simulations will be continued with the full set of algebraic models and tests will be made for the entire range of interest of convective Mach number.

The purpose of the efforts in this part of our activities was to develop closures for the “second order moments” in the contexts of both RANS and LES of high speed turbulent flows. In particular, we have obtained a complete set of explicit algebraic models derived from a hierarchy of second-order moment closures that are valid for compressible turbulent flows. The primary methodology based on the Cayley-Hamilton theorem and its corrolaries was developed during the past twenty years<sup>18,19,1</sup> and the present work extends it further. The models are based on new compressible closures for the pressure-strain and pressure-scalar gradient correlations. Explicit algebraic relations are provided for the Reynolds stresses, velocity-temperature and velocity-scalar correlations in both

non-reacting and reacting flows with heat release. As theoretical novelty we mention that density gradient, pressure gradient and mean dilatation effects are included in the models. Also, the role of the turbulent Mach number and Damköhler number is exhibited as well as compressibility and variable inertia effects for application of the models to turbulent flows with nonpremixed reactants.

## 3 Monte Carlo Large Eddy Simulation of Reacting Turbulent Flows

### 3.1 Introduction

The purpose of the efforts in this part of our activities is to develop and implement a robust computational procedure for LES of turbulent reactive flows. The procedure is based on a Monte Carlo solver for the Probability Density Function (PDF) of Subgrid Scale (SGS) of reactive species.

The purpose of the efforts described in this report is to develop and implement a robust computational procedure for Large Eddy Simulations (LES) capable of capturing the intricate physics associated with turbulent reactive flowfields. LES is considered somewhere between Direct Numerical Simulation (DNS) and Reynolds Averaged Navier-Stokes (RANS) computation.<sup>53-58, 11, 59</sup> Over the past thirty years since the early work of Smagorinsky<sup>60</sup> there has been relatively little effort, compared to that in RANS calculations, to make full use of LES for engineering applications. The most prominent model has been the Smagorinsky eddy viscosity based closure which relates the unknown subgrid scale (SGS) Reynolds stresses to the local large scale rate of flow strain. This viscosity is aimed to provide the role of mimicking the dissipative behavior of the unresolved small scales. The extensions to ‘dynamic’ models<sup>61-64</sup> has shown some improvements. This is particularly the case in transitional flow simulations where the dynamic evolutions of the empirical model ‘constant’ result in (somewhat) better predictions of the large scale flow features.

A survey of combustion literature reveals relatively little work in LES of chemically reacting turbulent flows.<sup>55, 65</sup> It appears that Schumann<sup>66</sup> was one of the first to conduct LES of a reacting flow. However, the assumption made in his work simply to “neglect” the contribution of the SGS scalar fluctuations to the filtered reaction rate is debatable. The importance of such fluctuations is well recognized in RANS of reacting flows in both combustion<sup>12, 15, 11, 17</sup> and chemical engineering<sup>67-70</sup> problems. Therefore, it is natural to expect that these fluctuations will also have a significant influence in LES.

Modeling of scalar fluctuations in RANS has been the study of intense investigations since the pioneering work of Toor.<sup>71</sup> The aim of statistical moment methods is to provide a closure for these correlations in terms of mean flow variables. Because of the lack of models with universal applicability to accurately predict the scalar correlations in turbulent reactive flows, simulations involving turbulent combustion are often met with a degree of skepticism. Another approach which

has proven particularly useful is based on the Probability Density Function (PDF) or joint PDF of scalar quantities.<sup>72,55,73</sup> This approach offers the advantage that all the statistical information pertaining to the scalar field is embedded within the PDF. Because of their capabilities, PDF methods have been widely used in RANS for a variety of reacting systems (see Dopazo<sup>73</sup> for a recent review). A systematic approach for determining the PDF is by means of solving the transport equation governing its evolution.<sup>74</sup> In this equation the effects of chemical reaction appear in a closed form. However, modeling is needed to account for transport of the PDF in the domain of the random variables. In addition, there is an extra dimensionality associated with the composition domain which must be treated. An alternative approach is based on *assumed* methods. In these methods the shape of the PDF is assumed *a priori* usually in terms of low order moments of the random variable(s). Obviously, this method is *ad hoc* but it offers more flexibility than the first approach. Presently the use of assumed methods in RANS is justified in cases where there is strong evidence that the PDF assumes a particular distribution.<sup>75-77</sup>

Despite the demonstrated capabilities of PDF methods in RANS, their use in LES is limited.<sup>55,78,59</sup> The first application of PDF-LES is due to Madnia and Givi<sup>78</sup> in which the assumed *Pearson* family of PDF's are used for modeling of the SGS reactant conversion rate in homogenous flows under chemical equilibrium conditions. This very same procedure was also used by CR<sup>79</sup> in the LES of a similar flow. The extension of the model for LES of nonequilibrium reacting flows is reported by Frankel *et al.*<sup>3</sup> for LES of reacting shear flows. While the generated results are encouraging, they do point out the drawbacks of assumed PDF methods. These can be overcome only by considering the PDF transport directly.

The approach advocated here is to solve the transport equation for the PDF. Because of the added dimensionality due to the compositional variables, solution of the PDF transport equation by conventional numerical methods is possible in only the simplest of cases.<sup>80</sup> An analysis performed by Pope<sup>81</sup> suggests that the solution of the joint velocity-scalar PDF by finite difference methods is impractical for more than three scalars.

The numerical solution of the subgrid PDF may be accomplished by means of a "Monte Carlo" scheme. The use of such schemes in RANS has proven very effective,<sup>72</sup> however no attempt has ever been made to utilize Monte Carlo schemes in the context of LES. Two classes of Monte Carlo schemes exist. In the Eulerian type scheme, the PDF within the subgrid is represented by an ensemble of  $M$  computational elements at fixed grid points. These elements are "transported" in physical space by the combined actions of large scale convection and diffusion (molecular and sub-grid eddy). In addition, transport in compositional space occurs due to the processes of chemical reaction and molecular mixing. Preliminary implementation of an Eulerian Monte Carlo method for LES of a non-reacting mixing layer has been performed in unpublished work. The Smagorinsky closure was used for the modeling of the subgrid eddy diffusion and the stochastic model of Curl<sup>82</sup> was utilized for modeling of the molecular mixing. Unfortunately, the results were quite discouraging. The major difficulty with this formulation lies in the numerical implementation of the large

scale convection. Due to the nature of the grid based scheme, excessive artificial diffusion is created which greatly degrades the solution of the large scale structures. It is important to realize that the errors induced by this scheme are not at all due to the PDF formulation itself but rather to the numerical implementation of the closed mean convection term. A remedy for the problem is to divorce from the Eulerian discretization and to invoke the Monte Carlo solver for the LES-PDF in a “grid free” Lagrangian manner.

In this work we provide a computational methodology for solution of the PDF of SGS scalar variables in LES of reacting flows under nonequilibrium chemical conditions. The solution procedure involves the transport of  $N$  Lagrangian elements within the “whole” computational domain of interest. The advantages of Lagrangian numerical procedures in reducing numerical diffusion in DNS are well-recognized.<sup>83-86</sup> In this Lagrangian framework, the elements are free to move *anywhere* within the domain. The particles carry information pertaining to the scalar field only; the LES of hydrodynamic variables is conducted by conventional Eulerian finite difference procedures. The effects of convection and diffusion are to move the elements in physical space, while the effects of mixing and reaction are to modify the compositional makeup of the elements.

### 3.2 Governing Equations

The primary independent transport variables in a compressible, two-dimensional flow undergoing chemical reaction are the density  $\rho$ , the velocity vector  $u_i$ , the total specific energy  $E$ , the pressure  $p$ , the temperature  $T$ , and the species mass fractions  $f_\alpha$  ( $\alpha = 1, 2, \dots, N_s$ ). The conservation equations governing these variables are the continuity, momentum and species mass fraction equations, along with an equation of state relating thermodynamic variables. They are expressed as:

Continuity :

$$\frac{\partial \rho}{\partial t} + \frac{\partial \rho u_i}{\partial x_i} = 0 \quad (106)$$

Conservation of momentum :

$$\frac{\partial \rho u_j}{\partial t} + \frac{\partial \rho u_i u_j}{\partial x_i} = \frac{\partial \tau_{ij}}{\partial x_i} \quad (107)$$

Conservation of total energy :

$$\frac{\partial \rho E}{\partial t} + \frac{\partial \rho u_i E}{\partial x_i} = \frac{\partial \tau_{ij} u_j}{\partial x_i} - \frac{\partial q_i}{\partial x_i} \quad (108)$$

Conservation of chemical species :

$$\frac{\partial \rho f_\alpha}{\partial t} + \frac{\partial \rho u_i f_\alpha}{\partial x_i} = -\frac{\partial J_i^\alpha}{\partial x_i} + \dot{\omega}_\alpha \quad (109)$$

Equation of state :

$$p = \rho R^0 T \sum_{i=1}^{N_s} f_i / \mathcal{M}_i \quad (110)$$

The total specific energy is given by :

$$E = \sum_{i=1}^{N_s} h_i f_i - \frac{p}{\rho} + \frac{u^2 + v^2}{2} \quad (111)$$

and the enthalpy of species  $i$  is defined as

$$h_i = h_i^0 + \int_{T_r}^T c_{p_i}(T') dT' \quad (112)$$

Additionally, the viscous stress tensor  $\tau_{ij}$ , heat flux  $q_i$  and mass flux  $J_i^\alpha$  of chemical species  $\alpha$  are given as:

$$\tau_{ij} = \delta_{ij} p + \mu \left( \frac{\partial u_i}{\partial x_j} + \frac{\partial u_j}{\partial x_i} \right) + \delta_{ij} \lambda \frac{\partial u_k}{\partial x_k} \quad (113)$$

$$q_i = -k \frac{\partial T}{\partial x_i} \quad (114)$$

$$J_i^\alpha = -\rho D \frac{\partial f_\alpha}{\partial x_i} \quad (115)$$

### 3.2.1 Modeling of Unresolved Scales

The aero-thermodynamic equations of the previous section constitute a complete set of governing equations. Unfortunately, due to the limited power of today's computers, it is impossible to accurately solve these equations for typical engineering problems. The great variation in length scales would require grid resolutions that would be too prohibitive for even the fastest of today's supercomputers. RANS provides the engineer with an alternative; instead of obtaining a fully resolved solution which can be afforded in only limited cases, time averaged solutions which do not attempt to resolve the the fine structure of the turbulence could be attempted. Due to the non-linear nature of the equations, the time averaging procedure yields unclosed terms which have been the focus of much attention in the past. On the other hand it may be desirable to resolve some of the lower frequency turbulent structures. Instead of averaging over all time (and implicitly length) scales, LES attempts to resolve the larger, energy containing eddies. Because only the finer turbulent structure is modeled, it is expected that LES models would be more universal in application. This is accomplished by use of a local spatial filter:

$$\bar{\phi}(\mathbf{x}, t) = \int_{-\infty}^{+\infty} \phi(\mathbf{x}, t) G(\mathbf{x}' - \mathbf{x}) d\mathbf{x}' \quad (116)$$

The fluctuation about the filtered value is given by

$$\phi' = \phi - \bar{\phi}. \quad (117)$$

The filter  $G(\mathbf{x})$  can take many forms. In this work we have elected to work with a local volume average box filter. For compressible flows, it is desirable to work with Favré averages:

$$\tilde{\phi} = \frac{\overline{\rho\phi}}{\bar{\rho}} \quad (118)$$

and the fluctuation about this mean is denoted by

$$\phi'' = \phi - \tilde{\phi}. \quad (119)$$

For compressible flows with reaction it is convenient to work with the density weighted mass fraction

$$\mathcal{F}_\alpha = \rho f_\alpha / \bar{\rho} \quad (120)$$

so that  $\overline{\mathcal{F}_\alpha} = \tilde{f}_\alpha$ . Note that while

$$\sum_{k=1}^{N_s} f_\alpha = 1, \quad (121)$$

$$\sum_{k=1}^{N_s} \mathcal{F}_\alpha = \rho / \bar{\rho} \neq 1. \quad (122)$$

When the LES Favré averaging procedure is applied to the governing transport equations, the result is:

$$\frac{\partial \bar{\rho}}{\partial t} + \frac{\partial \bar{\rho} \tilde{u}_i}{\partial x_i} = 0 \quad (123)$$

$$\frac{\partial \bar{\rho} \tilde{u}_j}{\partial t} + \frac{\partial \bar{\rho} \tilde{u}_i \tilde{u}_j}{\partial x_i} = \frac{\partial \bar{\tau}_{ij}}{\partial x_i} - \frac{\partial T_{ij}}{\partial x_i} \quad (124)$$

$$\frac{\partial \bar{\rho} \tilde{E}}{\partial t} + \frac{\partial \bar{\rho} \tilde{u}_i \tilde{E}}{\partial x_i} = \frac{\partial \bar{\tau}_{ij} u_j}{\partial x_i} - \frac{\partial \bar{q}_i}{\partial x_i} - \frac{\partial Q_i}{\partial x_i} \quad (125)$$

$$\frac{\partial \bar{\rho} \tilde{f}_\alpha}{\partial t} + \frac{\partial \bar{\rho} \tilde{u}_i \tilde{f}_\alpha}{\partial x_i} = - \frac{\partial \bar{J}_i^\alpha}{\partial x_i} - \frac{\partial M_i^\alpha}{\partial x_i} + \dot{\omega}_\alpha \quad (126)$$

where

$$T_{ij} = \bar{\rho}(\widetilde{u_i u_j} - \tilde{u}_i \tilde{u}_j) \quad (127)$$

$$Q_i = \bar{\rho}(\widetilde{u_i E} - \tilde{u}_i \tilde{E}) \quad (128)$$

$$M_i^\alpha = \bar{\rho}(\widetilde{u_i f_\alpha} - \tilde{u}_i \tilde{f}_\alpha) \quad (129)$$

are unclosed terms and therefore a model must be provided to account for their effects.

In this preliminary work, which is restricted to no heat release and low compressibility, the in-

compressible Smagorinsky eddy viscosity subgrid model is employed. The use of an incompressible model is justified in lieu of the fact that the density variations are expected to be quite small. Using this formulation, the SGS stresses are given by:

$$T_{ij} - (\delta_{ij}/3)T_{kk} = -2\mu_t\tilde{S}_{ij}. \quad (130)$$

where  $\tilde{S}_{ij}$  is the large scale strain rate tensor. A similar eddy viscosity formulation is used to close the SGS heat and mass fluxes:

$$Q_i = -\frac{\mu_t c_v}{Pr_t} \frac{\partial \tilde{T}}{\partial x_i}, \quad (131)$$

$$M_i^\alpha = -\frac{\mu_t}{Sc_t} \frac{\partial \tilde{f}_\alpha}{\partial x_i}. \quad (132)$$

The Smagorinsky eddy viscosity is given by:

$$\mu_t = \rho C_S \Delta^2 |\tilde{S}|. \quad (133)$$

where  $|\tilde{S}| = \sqrt{2\tilde{S}_{ij}\tilde{S}_{ij}}$  and  $\Delta$  is the filter width. In this work, the constants  $C_S$ ,  $Pr_t$  and  $Sc_t$  are set to the values 0.010, 0.7 and 0.7, respectively.

Thus far we have not yet addressed the issue of how to deal with SGS scalar correlations in the filtered chemical source terms. While the SGS terms discussed in this section are of a *convective* nature and they can be reasonably well modeled by a *diffusive* process, the same cannot be said for the unclosed terms in the species production rates. Because the physical mechanism of the SGS stresses and fluxes is inherently different from the scalar correlations in the source terms, it is expected that the models will differ. In fact, when eddy viscosity concepts are extended to treat chemical source terms, the resulting models (“eddy break up models”) perform mediocre at best. The focus of the following sections is to discuss how the methodology of LES via PDF (hereinafter referred to as LES-PDF) is used to overcome the closure problem of the chemical source terms and to develop robust numerical methods for the simulation of turbulent reactive flows.

### 3.3 PDF Methodology

The most common approach to turbulent reactive flow problems in the past has been to solve the governing transport equations for the Favré averaged flow variables. As a consequence of the averaging process, unclosed terms appear and must be modeled. This type of methodology is referred to as moment closure methods as closures must be provided for the unknown correlations. An alternate approach is consider the joint PDF of scalar quantities rather than to directly solve the scalar transport equations directly. Once the joint PDF is known, all statistical quantities

involving the scalar variables can be determined. The average species production rate  $\bar{\dot{\omega}}_\alpha$  can then be determined since it is dependent on such scalar correlations. The natural starting point for the consideration of PDF methods is to examine the transport equation governing its evolution. First, however, it is convenient to discuss some preliminaries. The following is intended only as a brief review and is by no means complete. For further information the reader is encouraged to consult one of the many fine texts on stochastic analysis such as those by Schuss<sup>87</sup> and Papoulis<sup>88</sup> and Billingsly.<sup>89</sup> An excellent reference of PDF methods in the application to turbulent reactive flows is provided by Pope.<sup>72</sup>

### 3.3.1 The Probability Distribution Function

Let  $\phi(x, t)$  be a random variable. The possible values that can be assumed by  $\phi$  constitute the *sample space*. In general the sample space may consist of all of the real numbers, but further physical restrictions may restrict allowable values to a subset of the real numbers. For example, the thermodynamic temperature  $T$  can only take on non-negative values. If we regard  $T$  as a random variable, the sample space of  $T$  consists of all the non-negative real numbers. In a similar manner the sample space for the mass fraction of any species consists of all the real numbers from 0 to 1.

The probability distribution function (also commonly referred to as the Cumulative Distribution Function or CDF) is defined for a continuous random variable  $\phi$  by:

$$F_\phi(\psi) = P\{\phi \leq \psi\}, \quad (134)$$

where  $P\{A\}$  is the probability that the event  $A$  occurs. The probability of an impossible event is zero, while the probability of a certain event is unity. Some fundamental properties of CDF's are

$$F_\phi(-\infty) = P\{\phi \leq -\infty\} = 0, \quad (135)$$

$$F_\phi(+\infty) = P\{\phi \leq +\infty\} = 1, \quad (136)$$

$$\frac{\partial F_\phi}{\partial \psi} \geq 0. \quad (137)$$

The last requirement merely states that the CDF is a non-decreasing function.

The probability distribution function is useful because we can use it to determine the likelihood that a random variable will fall between two values. For example, the probability that the random variable  $\phi$  will fall between the values  $\psi_a$  and  $\psi_b$  is given by

$$P\{\psi_a < \phi \leq \psi_b\} = F_\phi(\psi_b) - F_\phi(\psi_a). \quad (138)$$

### 3.3.2 The Probability Density Function

The PDF is defined to be the derivative of the CDF:

$$f_{\phi}(\psi) = \frac{dF_{\phi}(\psi)}{d\psi}. \quad (139)$$

The PDF, like the CDF, is useful for determining the probability that a random variable falls between two values. Upon integrating Eq. (139) between  $\psi_a$  and  $\psi_b$  the following is obtained:

$$P\{\psi_a < \phi \leq \psi_b\} = F_{\phi}(\psi_b) - F_{\phi}(\psi_a) = \int_{\psi_a}^{\psi_b} f_{\phi}(\psi) d\psi \quad (140)$$

Over a small interval  $f_{\phi} \Delta\psi$  is an approximation to  $P\{\psi < \phi \leq \psi + \Delta\psi\} = \Delta F_{\phi}$  and in the limit  $f_{\phi}(\psi)d\psi$  represents the differential probability  $dF_{\phi}$  that the random variable  $\phi$  lies in the infinitesimal interval of width  $d\psi$  in the vicinity of  $\psi$ .

Some fundamental properties of the PDF are

$$f_{\phi}(\psi) \geq 0, \quad (141)$$

$$f_{\phi}(-\infty) = 0, \quad (142)$$

$$f_{\phi}(+\infty) = 0, \quad (143)$$

$$\int_{-\infty}^{+\infty} f_{\phi}(\psi) d\psi = 1. \quad (144)$$

### 3.3.3 Determination of Mean Values from the PDF

Let  $A(\phi)$  be a function of the random variable  $\phi$ . In general, the *expected* or *mean* value of  $A(\phi)$ , denoted by  $\bar{A}(\phi)$  or  $\langle A(\phi) \rangle$  is given by the expression:

$$\bar{A}(\phi) = \langle A(\phi) \rangle = \int_{-\infty}^{+\infty} A(\psi) f_{\phi}(\psi) d\psi. \quad (145)$$

From this equation the PDF can be regarded as a normalized weighing function that assigns various weights to each possible outcome in the sample space. The integration serves to sum over each of these weighted possibilities to yield the expected value. The term *ensemble average* is also used to denote the mean.

In particular, the mean value of the random variable  $\phi$  is simply

$$\bar{\phi} = \int_{-\infty}^{+\infty} \psi f_{\phi}(\psi) d\psi, \quad (146)$$

and the  $n^{\text{th}}$  central moment is given by

$$\mu_n = \langle (\phi - \bar{\phi})^n \rangle = \int_{-\infty}^{+\infty} (\psi - \bar{\phi})^n f_\phi(\psi) d\psi. \quad (147)$$

For example, the second central moment, or variance is given by

$$\mu_2 = \sigma^2 = \langle (\phi - \bar{\phi})^2 \rangle = \int_{-\infty}^{+\infty} (\psi - \bar{\phi})^2 f_\phi(\psi) d\psi. \quad (148)$$

The variance represents the mean value of the square of the fluctuation and is useful in determining how a random variable fluctuates about the mean. A random variable with a large variance deviates more about the mean compared to a random variable with a smaller variance. The square root of the variance is called the standard deviation and is denoted by the greek letter  $\sigma$ .

In PDF methods, it is often useful to express the PDF as the mean value of the delta function:

$$f_\phi(\psi) = \langle \delta(\psi - \phi) \rangle. \quad (149)$$

The delta function  $\delta(\psi - \phi)$  is commonly referred to as the *fine grained PDF*. Each fine grained PDF  $\delta(\psi - \phi)$  corresponds to a realization from the sample space with the fine grain value  $\phi = \psi$ . This utilization of the delta function is important when we extend the concept of PDF's to spatially filtered quantities.

### 3.3.4 Functions of More Than One Random Variable

Up to the present point functions of only one random variable have been addressed. The corresponding PDF's are referred to as *univariate* since they only depend on one random variable. Many situations, however, require the use of functions that depend on more than one random variable. The distributions associated with such random variables are referred to as *joint* or *multivariate*. For example, the reaction rate of a chemical species generally depends upon multiple scalar quantities such as several species mass fractions  $\mathcal{F}_\alpha$  ( $\alpha = 1, 2, \dots, N_s$ ) and the temperature  $T$ . Denote  $\phi_n = \mathcal{F}_n$  for  $n = 1, 2, \dots, N_s$  and  $\phi_{N_\phi} = T$  where  $N_\phi = N_s + 1$  so that  $\phi$  is a random vector of dimension  $N_\phi$ . The reaction rate of species  $\alpha$ ,  $\dot{\omega}_\alpha$  is

$$\dot{\omega}_\alpha = \dot{\omega}_\alpha(\phi) = \dot{\omega}_\alpha(\phi_1, \phi_2, \dots, \phi_{N_\phi}). \quad (150)$$

Notice that the sample space is a  $N_\phi$  dimensional hypervolume. Each point within this hypervolume represents a possible composition. Some of these outcomes are more likely than others while others may not be possible at all. A multivariate PDF is useful for characterizing the entire statistical behavior of the random field. To introduce the concept of a multivariate distribution, we begin with a *bivariate* distribution which involves two random variables. Extension to higher dimension PDF's is inductive.

Let  $\phi_1$  and  $\phi_2$  be two independent random variables. The distribution function  $F_{\phi_1\phi_2}(\psi_1, \psi_2)$  is given by

$$F_{\phi_1\phi_2}(\psi_1, \psi_2) = P\{\phi_1 < \psi_1, \phi_2 < \psi_2\}, \quad (151)$$

and the bivariate PDF is given by

$$f_{\phi_1\phi_2}(\psi_1, \psi_2) = \frac{\partial^2}{\partial\psi_1\partial\psi_2} F_{\phi_1\phi_2}(\psi_1, \psi_2). \quad (152)$$

The univariate PDF of  $\phi_1$  may be obtained by integrating the multivariate PDF once:

$$f_{\phi_1}(\psi_1) = \int_{-\infty}^{+\infty} f_{\phi_1\phi_2}(\psi_1, \psi_2) d\psi_2. \quad (153)$$

Similarly,

$$f_{\phi_2}(\psi_2) = \int_{-\infty}^{+\infty} f_{\phi_1\phi_2}(\psi_1, \psi_2) d\psi_1. \quad (154)$$

Some additional properties of bivariate CDF's and PDF's are:

$$F_{\phi_1}(\psi_1) = F_{\phi_1\phi_2}(\psi_1, +\infty), \quad (155)$$

$$F_{\phi_2}(\psi_2) = F_{\phi_1\phi_2}(+\infty, \psi_2), \quad (156)$$

$$F_{\phi_1\phi_2}(-\infty, \psi_2) = F_{\phi_1\phi_2}(\psi_1, -\infty) = 0, \quad (157)$$

$$F_{\phi_1\phi_2}(+\infty, +\infty) = 1, \quad (158)$$

$$\int_{-\infty}^{+\infty} \int_{-\infty}^{+\infty} f_{\phi_1\phi_2}(\psi_1, \psi_2) d\psi_1 d\psi_2 = 1, \quad (159)$$

$$f_{\phi_1\phi_2}(\psi_1, \psi_2) \geq 0. \quad (160)$$

Consider a function of two random variables  $A(\phi_1, \phi_2)$ . The mean value of this function is obtained by integrating over the two dimensional region:

$$\bar{A} = \int_{-\infty}^{+\infty} \int_{-\infty}^{+\infty} A(\psi_1, \psi_2) f_{\phi_1\phi_2}(\psi_1, \psi_2) d\psi_1 d\psi_2. \quad (161)$$

The covariance  $C_{\phi_1\phi_2}$  of two random variables is defined as

$$C_{\phi_1\phi_2} = \langle (\phi_1 - \bar{\phi}_1)(\phi_2 - \bar{\phi}_2) \rangle. \quad (162)$$

Higher order joint moments of the product  $\phi_1^j \phi_2^k$  are given by

$$m_{jk} = \langle \phi_1^j \phi_2^k \rangle. \quad (163)$$

and higher order joint central moments are given by

$$\mu_{jk} = \langle (\phi_1 - \bar{\phi}_1)^j (\phi_2 - \bar{\phi}_2)^k \rangle. \quad (164)$$

Conditional statistics are important in situations where one random variable takes on a prescribed value. For example, the conditional density  $f_{\phi_1|\phi_2}(\psi_1|\psi_2)$  given by

$$f_{\phi_1|\phi_2}(\psi_1|\psi_2) = \frac{f(\psi_1, \psi_2)}{f(\psi_2)} \quad (165)$$

is the probability density function of the random variable  $\phi_1$  for a given value of the random variable  $\phi_2$ . Conditional mean values are given by the expression

$$\bar{A}(\phi_1|\phi_2) = \int_{-\infty}^{+\infty} A(\psi_1) f_{\phi_1|\phi_2}(\psi_1|\phi_2) d\psi_1 \quad (166)$$

and is essentially the average of the function  $A$  at a fixed value of  $\phi_2$ .

Extensions to more than 2 random variables is inductive. For example, the mean of the reaction rate  $\dot{\omega}_\alpha(\phi_1, \phi_2, \dots, \phi_{N_\phi})$  requires knowledge of the joint PDF  $f(\phi_1, \phi_2, \dots, \phi_{N_\phi})$ :

$$\dot{\omega}_\alpha = \int_{-\infty}^{+\infty} \dots \int_{-\infty}^{+\infty} \int_{-\infty}^{+\infty} \dot{\omega}_\alpha(\psi_1, \psi_2, \dots, \psi_{N_\phi}) f(\psi_1, \psi_2, \dots, \psi_{N_\phi}) d\psi_1 d\psi_2 \dots d\psi_{N_\phi}. \quad (167)$$

(When there is no fear of ambiguity as to what random variables are involved, the subscripts for PDF's and CDF's may be dropped).

The extension of Eq. (149) to more than one random variable is:

$$f_\phi(\psi) = \langle \delta(\psi - \phi) \rangle = \langle \delta(\psi_1 - \phi_1) \delta(\psi_2 - \phi_2) \dots \delta(\psi_{N_\phi} - \phi_{N_\phi}) \rangle. \quad (168)$$

### 3.3.5 Large Eddy PDF

The PDF's considered so far are not fully suitable for LES since they do not contain any information about the filter  $G(\mathbf{x})$ . A "Large Eddy PDF" that is consistent with *spatially filtered* quantities may be defined as follows:<sup>90</sup>

$$f_L(\phi; \mathbf{x}, t) = \int_{-\infty}^{+\infty} \delta[\phi - \psi(\mathbf{x}, t)] G(\mathbf{x}' - \mathbf{x}) d\mathbf{x}'. \quad (169)$$

The Large Eddy PDF is therefore seen to be the *spatially filtered* value of a delta function in contrast to the "conventional" PDF which can be defined as the ensemble average of a delta function. In either case the delta function is the fine grained PDF introduced in section 3.3.3

Evaluation of spatial averages and moments is achieved by integrating with the Large Eddy PDF

just as ensemble averages and moments are evaluated using “conventional” PDF’s. Consider the function  $A(\phi)$  of the random vector  $\phi(\mathbf{x}, t)$ . The filtered variable  $\bar{A}(\mathbf{x}, t)$  is then given by the expression:

$$\bar{A}(\mathbf{x}, t) = \int_{-\infty}^{+\infty} A(\mathbf{x}', t) G(\mathbf{x}' - \mathbf{x}) d\mathbf{x}' = \int_{-\infty}^{+\infty} A(\psi) f_L(\psi, \mathbf{x}, t) d\psi. \quad (170)$$

For compressible LES, it is useful to define the Favré PDF  $\tilde{f}_L = \rho f_L / \langle \rho \rangle$ . The Favré filtered variable  $\tilde{A}(\mathbf{x}, t)$  is then given by the expression:

$$\tilde{A}(\mathbf{x}, t) = \int_{-\infty}^{+\infty} A(\phi) \tilde{f}_L(\psi, \mathbf{x}, t) d\psi. \quad (171)$$

### 3.3.6 PDF Transport Equation

The transport equation for the joint compositional PDF in a turbulent reactive flow is given by:<sup>72</sup>

$$\begin{aligned} \frac{\partial[\bar{\rho}(\psi)\tilde{f}_L]}{\partial t} + \frac{\partial[\bar{\rho}(\psi)\tilde{u}_i\tilde{f}_L]}{\partial x_i} + \frac{\partial[\bar{\rho}(\psi)\dot{\omega}_\alpha(\psi)\tilde{f}_L]}{\partial \psi_\alpha} = \\ \frac{\partial}{\partial \psi_\alpha} \left[ \left\langle \frac{1}{\rho} \frac{\partial J_i^\alpha}{\partial x_i} | \psi \right\rangle \bar{\rho}(\psi)\tilde{f}_L \right] - \frac{\partial[\bar{\rho}(\psi)\langle u_i'' | \psi \rangle \tilde{f}_L]}{\partial x_i}. \end{aligned} \quad (172)$$

Summation over  $\alpha = 1, 2, \dots, N_\phi$  is implied. In the context of Large Eddy Simulation, the PDF  $\tilde{f}_L$  has a slightly different meaning than that intended by Pope; the PDF here is the Favré filtered Large Eddy PDF as described in section 3.3.5. The first two terms on the left hand side of the equation represent convection of the PDF by the mean flow in physical space. The last term on the left hand side is due to chemical reaction. Note that this term is closed and requires no modeling. This is the major advantage PDF methods have over other approaches. Also note that the derivative is in compositional space rather than physical space. This is reflected by the fact that the chemical reaction serves to change the compositional makeup of the mixture rather than to provide a mechanism for motion in physical space. The first term on the right hand side is due to molecular mixing. Molecular mixing, like reaction, provides transport in compositional rather than physical space. In general, the mixing term tends to homogenize the fluid and hence lowers the scalar variance. The remaining term represents turbulent transport of the PDF by the small scales.

### 3.3.7 Modeling of Unclosed Terms

The two terms on the right side of Eq. (172) are unclosed and therefore a model must be provided to properly account for the effects they have on the larger scales. In the present work, a simple

gradient-diffusion model has been employed for the turbulent transport term:

$$\bar{\rho} \langle u_i'' | \psi \rangle \tilde{f}_L = -\Gamma_t \frac{\partial \tilde{f}_L}{\partial x_i} \quad (173)$$

where  $\Gamma_t = \mu_t / Sc_t$ .

The modeling of the molecular mixing term has been the focus of intense investigation in the past.<sup>82,91,80,92</sup> Many mixing closures fall under the general category of Coalescence/Dispersion (C/D) models as characterized by Pope.<sup>93</sup> Curl's model and the modified Curl model of Janicka *et al.*<sup>80</sup> fall in this category. In the present work, Dopazo's deterministic relax to mean model has been utilized. Kosaly<sup>94</sup> has shown that Dopazo's model belongs to the general class of C/D closures under certain limiting conditions. This model has been selected due to its ease of implementation into the numerical solution and its efficiency. Although the use of different mixing models results in different behavior of moments of the third order and higher in 0 D turbulent mixing simulations, it is expected that the difference under more realistic conditions will have little effect on mean flow quantities.

### 3.3.8 Langevin Equation

The basis of the numerical scheme used for the solution of the PDF transport equation relies upon the principle of *equivalent systems*.<sup>72</sup> Two systems that display dissimilar behavior may actually have identical statistics. In the Lagrangian solution technique used to solve the compositional PDF equation, Monte Carlo particles are distributed throughout the flowfield. Each of these particles carries information about the scalar field. Additionally each of these particles obey certain equations which govern its motion in three dimensional space. It is important to recognize that the Monte Carlo particles are not fluid elements. In fact, while fluid particles follow smooth trajectories, the Monte Carlo particles follow trajectories which are continuous but not differentiable. The importance, however, of the Monte Carlo particles is that they are developed in such a way such that they evolve with the same PDF associated with genuine fluid particles.

The Monte Carlo particles undergo motion in three dimensional space by convection due to the mean flow velocity and diffusion due to molecular and turbulent viscosities. This type of general diffusion process is represented by a Langevin equation:<sup>72</sup>

$$dX_i(t) = \left[ \tilde{u}_i + \frac{1}{\bar{\rho}} \frac{\partial \Gamma_t}{\partial x_i} \right] dt + \left[ \frac{2\Gamma_t}{\bar{\rho}} \right]^{1/2} dW_i, \quad (174)$$

where  $X_i$  is the Lagrangian position of the Monte Carlo particle. The stochastic term  $W_i$  is the stochastic Wiener process. The Wiener process is best understood by considering the function

$W_d(t_n)$  which changes value at discrete time intervals:<sup>72</sup>

$$W_d(t_n) = (\Delta t)^{1/2} \sum_{i=1}^N \xi_i, \quad (175)$$

where  $\xi_n$  ( $n = 1, 2, \dots, N$ ) are  $N$  independent normalized gaussian random variables and the time interval from  $t = 0$  to  $t = T$  is divided into  $N$  equal subintervals of duration  $\Delta t = T/N$ . Consider the increment

$$\Delta W_d(t_{n-1}) = \xi_n (\Delta t)^{1/2}. \quad (176)$$

The Weiner process can be defined as Eqs. (175)-(176) in the limit  $\Delta t \rightarrow 0$ . Note that although the process is continuous, it is not differentiable since  $\Delta W_d/\Delta t$  is undefined as  $\Delta t$  vanishes.

It must be emphasized that although the Langevin equation given by Eq. (174) is stochastic, Eq. (172) which governs the transport of the joint scalar PDF is deterministic.

### 3.4 Numerical Solution

Because of the added dimensionality the compositional variables present in the PDF Transport equation its solution by conventional finite difference or finite volume methods is intractable for engineering problems. Instead, a Lagrangian Monte Carlo solution algorithm is utilized. It is an established fact that while the work required by finite difference schemes increases exponentially with added dimensionality, the work associated with Monte Carlo schemes only increases linearly.<sup>93</sup> Thus Monte Carlo methods provide an attractive technique to solve problems with a large number of independent variables. The essentials of Lagrangian Monte Carlo schemes in relevance to turbulent flows are due to.<sup>72</sup>

In the solution procedure numerous particles are distributed throughout the domain. Each of these particles carries information about the compositional makeup of the fluid. Although Monte Carlo particles and fluid particles are fundamentally different their PDF's are identical. Thus a solution to the PDF transport equation can be attained *indirectly* by solving for the spatial location and compositional makeup of the Monte Carlo particles. The equation governing the spatial location of the particles is the Langevin equation (Eq. (174)) and the processes of mixing and reaction govern the compositional evolution. Since the compositional PDF provides no information about the density or velocity fields, this information must be determined by alternative means. Conventional finite difference schemes are used to solve the governing transport equations for these variables; the Monte Carlo procedure is used only to determine the species mass fractions. Additionally, in the case of temperature dependent chemical kinetics, the energy (or enthalpy) is solved using the Monte Carlo procedure. In the present research temperature independent kinetics are used and the total energy equation is solved using finite differences in the usual manner.

### 3.4.1 Finite Difference Procedure

The methodology used to solve the large scale continuity, momentum and energy equations is the fourth order spatially accurate finite difference scheme as developed by Gottlieb and Turkell.<sup>50</sup> The generalized transport equation may be written in the vector form:

$$\frac{\partial \mathbf{U}}{\partial t} + \frac{\partial \mathbf{F}}{\partial x} + \frac{\partial \mathbf{G}}{\partial y} = \mathbf{H} \quad (177)$$

where  $\mathbf{U}$  is the vector of dependent conserved variables:

$$\mathbf{U} = \begin{pmatrix} \bar{\rho} \\ \bar{\rho}\tilde{u} \\ \bar{\rho}\tilde{v} \\ \bar{\rho}\tilde{E} \end{pmatrix} \quad (178)$$

The vectors  $\mathbf{F}$  and  $\mathbf{G}$  are the flux vectors in the  $x$  and  $y$  directions respectively:

$$\mathbf{F} = \begin{pmatrix} \bar{\rho}\tilde{u} \\ \bar{\rho}\tilde{u}\tilde{u} - \tilde{\tau}_{xx} + T_{xx} \\ \bar{\rho}\tilde{u}\tilde{v} - \tilde{\tau}_{xy} + T_{xy} \\ (\bar{\rho}\tilde{E} - \tilde{\tau}_{xx})\tilde{u} - \tilde{\tau}_{xy}\tilde{v} + \tilde{q}_x - Q_x \end{pmatrix} \quad (179)$$

$$\mathbf{G} = \begin{pmatrix} \bar{\rho}\tilde{v} \\ \bar{\rho}\tilde{v}\tilde{u} - \tilde{\tau}_{yx} + T_{yx} \\ \bar{\rho}\tilde{v}\tilde{v} - \tilde{\tau}_{yy} + T_{yy} \\ (\bar{\rho}\tilde{E} - \tilde{\tau}_{yy})\tilde{v} - \tilde{\tau}_{yx}\tilde{u} + \tilde{q}_y - Q_y \end{pmatrix} \quad (180)$$

The source vector  $\mathbf{H} = \mathbf{0}$  since the species equations are not solved by the finite difference method and the body force vector is neglected.

The Gottlieb-Turkel scheme is a higher order accurate variant of the well known<sup>95</sup> predictor-corrector method. For Eq. (177) it is implemented in unsplit form as:

$$\mathbf{U}_{i,j}^* = \mathbf{U}_{i,j}^n - \frac{\Delta t}{6\Delta x} [-\mathbf{F}_{i+2,j}^n + 8\mathbf{F}_{i+1,j}^n - 7\mathbf{F}_{i,j}^n] - \frac{\Delta t}{6\Delta y} [-\mathbf{G}_{i,j+2}^n + 8\mathbf{G}_{i,j+1}^n - 7\mathbf{G}_{i,j}^n] + \Delta t \mathbf{H}_{i,j}^n \quad (181)$$

$$\mathbf{U}_{i,j}^{**} = \mathbf{U}_{i,j}^* - \frac{\Delta t}{6\Delta x} [\mathbf{F}_{i-2,j}^* - 8\mathbf{F}_{i-1,j}^* + 7\mathbf{F}_{i,j}^*] - \frac{\Delta t}{6\Delta y} [\mathbf{G}_{i,j-2}^* - 8\mathbf{G}_{i,j-1}^* + 7\mathbf{G}_{i,j}^*] + \Delta t \mathbf{H}_{i,j}^* \quad (182)$$

$$\mathbf{U}_{i,j}^{n+1} = \frac{1}{2} [\mathbf{U}_{i,j}^n + \mathbf{U}_{i,j}^{**}] \quad (183)$$

The CFL condition for this scheme requires that the CFL number should be less than 2/3 for numerical stability.

### 3.4.2 Monte Carlo Particle Method

The species mass fractions are determined using the Monte Carlo particle method. A two stage Runge-Kutta scheme is used to solve the Langevin equation to determine the particle positions. For the general diffusion process governed by:

$$dX_i(t) = D_i(\mathbf{X}(t), t)dt + B(\mathbf{X}(t), t)dW_i(t) \quad (184)$$

a Runge-Kutta scheme can be written as:

$$X_i^* = X_i^n + D_i^n \Delta t + B^n(\Delta t)^{1/2} \xi_i^n \quad (185)$$

$$X_i^{**} = X_i^* + D_i^* \Delta t + B^*(\Delta t)^{1/2} \xi_i^n \quad (186)$$

$$X_i^{n+1} = \frac{1}{2}[X_i^n + X_i^{**}] \quad (187)$$

Note that the standardized gaussian random vector  $\xi_i$  is the same at the predictor and corrector levels. This is to ensure that the numerical approximation given by Eqs. (185)-(187) reflects the Markovian behavior of the general diffusion process.<sup>96</sup> Markovian or “memoryless” processes are stochastic processes in which future states are not influenced by past behavior.<sup>87,97,89</sup>

The drift coefficients  $D_i$  and  $B$  require knowledge of the mean field velocity and viscosity. Interpolation is required for these quantities since the Lagrangian particles are not restricted to the finite difference grid points. Fourth order Lagrange polynomials are used to interpolate the desired quantities from the grid to the particle location.

Each particle contains information regarding the composition of the scalar field. This includes the density weighted species mass fractions (and temperature if the chemistry model requires it). Let  $\phi_\alpha^k$  denote the value of the  $\alpha^{th}$  scalar ( $\alpha = 1, 2, \dots, N_\phi$ ) for the  $k^{th}$  particle ( $k = 1, 2, \dots, N$ ) located at the Lagrangian coordinate  $\mathbf{X}^k$  as described in section 3.3.4. At each time step these compositional values are subject to change due to the effects of molecular mixing and chemical reaction. Using Dopazo’s relax to mean model for molecular mixing the composition of each particle changes according to

$$(\phi_\alpha^k)^{mix} = (\phi_\alpha^k)^n - ((\phi_\alpha^k)^n - \langle \phi_\alpha^k \rangle) \exp[-\frac{1}{2} C_\phi \omega_t \Delta t] + \langle \phi_\alpha^k \rangle \quad (188)$$

at each timestep. The turbulent mixing frequency  $\omega_t$  is backed out from the turbulent viscosity and length scale using the relation  $\omega_t = 3\nu_t/\Delta^2$ . After the mixing step has been completed the particles undergo reaction. This is performed by sweeping over all the particles and determining the fine grain reaction rates  $\dot{\omega}_\alpha^k$ . For example, for the simple reaction  $\mathcal{A} + \mathcal{B} \rightarrow \mathcal{P}$  with reaction rate  $\dot{\omega}_A = -k_f(\rho f_A)(\rho f_B)$ , the fine grain reaction rates are given by

$$\dot{\omega}_A^k = -k_f(\rho f_A^k)(\rho f_B^k) = -k_f(\bar{\rho} \mathcal{F}_A^k)(\bar{\rho} \mathcal{F}_B^k). \quad (189)$$

The new particle composition is then determined from:

$$(\phi_\alpha^k)^{n+1} = (\phi_\alpha^k)^{mix} + \dot{\omega}_\alpha^k \Delta t. \quad (190)$$

### 3.4.3 Determination of Filtered Quantities

For homogeneous flows averages are determined by simply summing over all the particles:

$$\langle A(\phi) \rangle = \sum_{k=1}^N A(\phi^k) = \sum_{k=1}^N A^k. \quad (191)$$

For inhomogeneous flows the situation is complicated by the fact that the PDF varies spatially. A discrete summation consistent with the Large Eddy PDF is:

$$\bar{A}(\mathbf{x}, t) = \frac{\sum_{k=1}^N A(\mathbf{X}^k(t), t) G(\mathbf{X}^k(t) - \mathbf{x})}{\sum_{k=1}^N G(\mathbf{X}^k(t) - \mathbf{x})} = \frac{\sum_{k=1}^N A^k G^k(\mathbf{x})}{\sum_{k=1}^N G^k(\mathbf{x})} \quad (192)$$

Averages and higher order moments can be calculated in this manner. In the present work where a uniform filter of width  $\Delta = 2\Delta x = 2\Delta y$  has been used, calculation of averages at the grid point with coordinates  $(i, j)$  reduces to summing over all particles in the square region of dimension  $2\Delta x$  by  $2\Delta y$  centered at the grid point.

For Reynolds averaged solutions, similar procedures must be taken to generate meaningful ensembles. However it should be noted that in the case of LES the spatial dependency of the ensemble is reflected by the filter  $G(\mathbf{x})$  in the definition of the large eddy PDF (see Eq. (3.3.5)); for the case of RANS there is no such spatial dependency in the “conventional PDF”. Rather, the practice of constructing an ensemble out of particles within some volume of a point is out of *necessity* since in general the Lagrangian particles will not coincide with the Eulerian grid points. In this sense LES is more in tune with the Lagrangian solution procedure.

## 3.5 Results

To demonstrate the feasibility of LES-PDF, one non-reacting and one reacting simulation were performed. For comparison, two additional runs were performed in which the Favré averaged species equations were solved by the finite difference method described in section 3.4.1 rather than the LES-PDF methodology. For the reacting finite difference simulation the mean reaction rate was modeled as  $\dot{\bar{\omega}}_\alpha = \dot{\omega}_\alpha(\bar{\phi})$ . It is well recognized that such an assumption may be off by orders of magnitude and gross errors can be incurred. This simulation was performed to compare to the LES-PDF reacting simulation in which the effects of reaction are accounted for exactly. In order to provide meaningful results, an additional control simulation was run using the LES-PDF using  $\dot{\bar{\omega}}_\alpha = \dot{\omega}_\alpha(\bar{\phi})$  to elucidate any discrepancies with the finite difference procedure.

All simulations were performed at a Reynolds number of 800 based on initial vorticity thickness  $\delta_{\omega_0}$ . The physical domain in all cases is  $60\delta_{\omega_0}$  by  $30\delta_{\omega_0}$  which was discretized into a  $256$  by  $128$  computational domain. The velocity profile at the inlet consists of a 4 to 1 velocity ratio with a hyperbolic tangent distribution. Forcing of the cross stream velocity at the frequency corresponding to the most unstable mode for the hyperbolic tangent velocity profile was used to perturb the layer and induce coherent large scale structures.<sup>98</sup> Zero first derivative conditions are assumed at the freestreams. The chemistry model utilized is an irreversible second order isothermal reaction of the form  $\mathcal{A} + \mathcal{B} \rightarrow \mathcal{P}$ . In each of the reacting simulations the Damköhler number  $Da = k_f/[U_{ref}/\delta_{\omega_0}]$  was set to 2.

In order to save time during the computation, only the region surrounding the reaction zone from  $y = -3.75 \delta_{\omega_0}$  to  $y = 3.75 \delta_{\omega_0}$  is initialized with the Monte Carlo particles (one quarter the computational domain). In each cell in this region 30 particles were randomly placed. Thus on average roughly 120 particles fall within the filter width  $2\Delta x$  by  $2\Delta y$  to constitute an ensemble, although this number may vary somewhat as particles convect and diffuse from cell to cell. Additionally as particles exit the domain, new particles are introduced at  $x = 0$  with a randomly chosen  $y$  coordinate in the vicinity of the reaction zone.

Figure 3.1 is a contour plot displaying the particle density. Note how the Monte Carlo particles are only distributed in the region surrounding the reaction zone. There is some variation locally, however overall the particle density is roughly uniform at a value of 120 particles per ensemble. The oscillatory behavior of the particle zone in the last third of the domain is suggestive of some organized large scale structure. Indeed such coherent structures are evident in Fig./ 3.2 which compares contours of species  $\mathcal{A}$  Favre averaged mass fraction for LES-PDF (3.2(a)) to those of standard finite difference LES (2 – b) for the non-reacting case. The solution provided by the PDF methodology compares favorably with the standard procedure. Such comparison is important in that it demonstrates that the particle method is capable of resolving the convective and diffusive transport mechanisms.

Figure 3.3 displays the contours of species  $\mathcal{A}$  mass fraction for the reacting case. Although at first glance the plots appear similar, it is soon apparent that the gradients in Fig. 3.3(b) (finite difference with  $\tilde{\omega}_\alpha = \tilde{\omega}_\alpha(\bar{\phi})$ ) are steeper suggesting the reactants are separated by a relatively thin reaction zone. This is indicative that the reaction is more vigorous and has progressed further compared to the LES-PDF solution depicted in Fig. 3.3(a). This is more clearly seen in the product mass fraction contours in Fig. 4. Substantial less product formation is predicted by the LES-PDF simulation and the solution is significantly more diffuse. Clearly this is a result of the LES-PDF solution resolving the SGS subgrid fluctuations while these terms are neglected in the finite difference solution.

To assist in further appreciation of the effects due to the SGS scalar fluctuations the covariance  $\overline{(\rho f_A)'(\rho f_B)'}$  is plotted in Fig. 3.5(a) for the non-reacting case and Fig. 3.5(b) for the reacting case as determined by the solution to the large eddy PDF. The negative values of this quantity as predicted by the LES-PDF procedure indicate that neglect of this subgrid term would result in

unphysically high reaction rates and product conversion. Further evidence is given by reaction rate contours predicted by LES-PDF in Fig. 3.6(a) and that predicted by the finite difference solution in Fig. 3.6(b). Clearly the reaction rates in the LES-PDF solution are an order of magnitude lower than that predicted by the solution neglecting the SGS scalar fluctuations. This indicates the approximation  $\dot{\bar{\omega}}_\alpha = \dot{\omega}_\alpha(\bar{\phi})$  cannot be justified. While the scalar covariance is very difficult to model, LES-PDF avoids this obstacle altogether as it has the distinction of being able to *resolve* this term.

To be confident that the LES-PDF calculations are representative of the true physics, an additional simulation was performed with the particle method in which the reaction rate was improperly “modeled” by  $\dot{\bar{\omega}}_\alpha = \dot{\omega}_\alpha(\bar{\phi})$ . Figure 3.7 is a contour plot of the product  $\mathcal{P}$  mass fraction. Notice that the product distribution exhibits a remarkable likeness to the finite difference solution to the species transport equations with the scalar SGS terms neglected. Whether the PDF method or the finite difference procedure is used the product formation is grossly overpredicted if the subgrid correlations are neglected. Figure 3.8 displays the reaction rate contours for this simulation. As expected the predicted reaction rate is an order of magnitude higher due to the neglect of the subgrid terms. This agreement between the finite difference and the PDF procedures is important since it elucidates that the neglect of the SGS terms rather than the difference in numerical procedure is responsible for the discrepancy of the previous runs.

### 3.6 Conclusion

A PDF method suitable for chemically reactive flows is developed in the context of large eddy simulation. The clear advantage of PDF methods is their inherent ability to resolve SGS correlations that otherwise have to be modeled. Because of the lack of robust models to accurately predict these correlations in turbulent reactive flows, simulations involving turbulent combustion are often met with a degree of skepticism. The PDF methodology avoids the closure problem associated with these terms but rather treats the reaction exactly.

The first LES-PDF simulations of a chemically reactive flow have demonstrated the feasibility of utilizing Monte Carlo methods in the context of LES. Comparison with a finite difference solution which does not attempt to model the SGS scalar covariance indicates that neglect of this term leads to unphysically high product conversion rates.

While the present work indicates there is much promise in the LES-PDF methodology, much work needs to be done. Utilization of compressible dynamic SGS models is a natural starting point. Furthermore, the development of LES with variable grid and filter spacing as addressed by<sup>99</sup> is an important step towards the ability of such models to predict engineering flows with complex geometries. PDF transport methods require the closure of molecular mixing; in the present research this has been addressed with a simple deterministic model. Mixing models require a turbulent mixing frequency. Proper determination of this mixing frequency is desirable. Additionally, inclusion of

the energy in the compositional domain is a necessary step in order to simulate reactive flows with temperature dependent kinetics. Furthermore, since the reaction is represented without approximation realistic chemical kinetics present no difficulty to the particle method and hence should be investigated. Much of this work is already underway.

Additional extension of the LES-PDF methodology to solve the joint velocity-composition PDF is also an area to be explored. This area has seen considerable development in the area of RANS by Pope.<sup>100</sup> The velocity-composition PDF has the added advantage that velocity correlations appear in closed form and eddy viscosity models are not required to model their effects.<sup>72</sup> In the case of LES, however, it is expected that the subgrid models are more universal in their applicability and hence the dependency on SGS closures for the scalar PDF method does not pose too much concern. Furthermore, particle methods as described in this report can be incorporated into the large stockpile of existing finite difference and finite volume CFD codes.

## 4 Work in Progress

We are currently in the process of *combining* the techniques discussed in the last two sections for LES of high speed reacting turbulent flows. The primary tool in this part of our activities is the Monte Carlo LES-PDF solver as discussed in the last section. However, our aim is to replace the Smagorinsky hydrodynamic subgrid model with an algebraic closure. For this purpose, the same computer code used for LES-PDF is being modified. presently, we are only considering LES of incompressible reacting flows. Therefore, only the models developed previously<sup>19,1</sup> are being utilized (of course with proper modifications to make them suitable for LES). At this point, there are some computational problems that need to be resolved. We hope to have some results before our next report is due.

In the upcoming year (Year 3 of phase II), our efforts will be concentrated on the following tasks:

- (1) Completion of the mathematical formulation and computational implementation of LES via algebraic closures.
- (2) Generation of extensive computational results via RANS of high speed flows with and without chemical reactions and comparisons with experimental data.
- (3) Fine tuning of the LES-PDF code. Application of this code for simulations of several reacting flow configurations. Comparisons with experimental data.
- (4) Extension of LES with consideration of the joint PDFs of subgrid velocity and scalars. Our efforts will be concentrated primarily on the mathematical formulations and related issues.

## 5 Personnel and Management

Dr. Peyman Givi is the PI of this project. Drs. Dale B. Taulbee and Cyrus K. Madnia serve as the Co-PIs. As before, Dr. Givi is responsible for a timely and successful completion of all the tasks.

There are presently two Ph.D. candidates who are being supported full-time by this grant: Mr. Virgil Adumitroaie and Mr. Paul J. Colucci. Mr. Adumitroaie has been supported under this program since the initiation of Phase II (and departure of Dr. Steven H. Frankel). Mr. Colucci is replacing a former RA, Mr. Craig Steinberger. The reason for this replacement is that the work of Mr. Colucci is more closely related to this program. Mr. Steinberger is continuing his work in DNS of reacting flows the results of which will be utilized for this work. However, he is no longer being financially supported under this grant.

## References

- [1] Adumitroaie, V., Taulbee, D. B., and Givi, P., Algebraic Scalar Flux Models for Turbulent Reacting Flows, *Phys. Fluids*, (1995), submitted.
- [2] Frankel, S. H., Probabilistic and Deterministic Description of Turbulent Flows with Non-premixed Reactants, Ph.D. Thesis, Department of Mechanical and Aerospace Engineering, State University of New York at Buffalo, Buffalo, NY, 1993.
- [3] Frankel, S. H., Adumitroaie, V., Madnia, C. K., and Givi, P., Large Eddy Simulations of Turbulent Reacting Flows by Assumed PDF Methods, in Ragab, S. A. and Piomelli, U., editors, *Engineering Applications of Large Eddy Simulations*, pp. 81-101, ASME, FED-Vol. 162, New York, NY, 1993.
- [4] Launder, B. E. and Spalding, D. B., The Numerical Computation of Turbulent Flows, *Comput. Methods Appl. Mech. Engng.* **3**:269-289 (1974).
- [5] Reynolds, W. C., Computation of Turbulent Flows, *Annu. Rev. Fluid Mech.*, **8**:183-208 (1976).
- [6] Lumley, J. L., Computational Modeling of Turbulent Flows, *Adv. Appl. Mech.*, **18**:123-176 (1978).
- [7] Taulbee, D. B., Engineering Turbulence Models, in George, W. K. and Arndt, R., editors, *Advances in Turbulence*, pp. 75-125, Hemisphere Publishing Co., New York, NY., 1989.
- [8] Launder, B. E., Current Capabilities for Modelling Turbulence in Industrial Flows, *Applied Scientific Research*, **48**:247-269 (1991).
- [9] Wilcox, D. C., *Turbulence Modeling for CFD*, DCW Industries, Inc., La Cañada, CA, 1993.
- [10] Höfler, T., Reynolds Stress Model (RSM) in FIRE, *FIRE Newsletter*, **5**:1 (1993), Fluid Dynamics Research Newsletter of AVL Inc., Graz, Austria.

- [11] Libby, P. A. and Williams, F. A., editors, *Turbulent Reacting Flows*, Academic Press, London, UK, 1994.
- [12] Libby, P. A. and Williams, F. A., editors, *Turbulent Reacting Flows, Topics in Applied Physics*, Vol. 44, Springer-Verlag, Heidelberg, 1980.
- [13] Jones, W. P., Models for Turbulent Flows with Variable Density and Combustion, In Kollmann,<sup>41</sup> pp. 380–421.
- [14] Jones, W. P. and Whitelaw, J. H., Calculation Methods for Reacting Turbulent Flows: A Review, *Combust. Flame*, **48**:1–26 (1982).
- [15] Jones, W. P. and Whitelaw, J. H., Modelling and Measurements in Turbulent Combustion, in *20th Symp. (Int.) on Combustion*, pp. 233–249, The Combustion Institute, Pittsburgh, PA, 1984.
- [16] Borghi, R. and Murthy, S. N. B., editors, *Turbulent Reacting Flows, Lecture Notes in Engineering*, Vol. 40, Springer-Verlag, New York, NY, 1989.
- [17] Jones, W. P., Turbulence Modelling and Numerical Solution Methods for Variable Density and Combusting Flows, In Libby and Williams,<sup>11</sup> chapter 6, pp. 309–374.
- [18] Pope, S. B., A More General Effective-Viscosity Hypothesis, *J. Fluid Mech.*, **72**:331–340 (1975).
- [19] Taulbee, D. B., An Improved Algebraic Reynolds Stress Model and Corresponding Nonlinear Stress Model, *Phys. Fluids A*, **4**(11):2555–2561 (1992).
- [20] Rodi, W., A New Algebraic Relation for Calculating the Reynolds Stresses, *ZAMM*, **56**:T219–T221 (1976).
- [21] Launder, B. E., On the Effects of a Gravitational Field on the Turbulent Transport of Heat and Momentum, *J. Fluid Mech.*, **67**:569–581 (1975).
- [22] Rodi, W., Turbulence Models for Environmental Problems, In Kollmann,<sup>41</sup> pp. 260–349.
- [23] Speziale, C. G., Analytical Methods for the Development of Reynolds Stress Closures in Turbulence, *Ann. Rev. Fluid Mech.*, **23**:107–157 (1991).
- [24] Gatski, T. B. and Speziale, C. G., On Explicit Algebraic Stress Models for Complex Turbulent Flows, *J. Fluid Mech.*, **254**:59–78 (1993).
- [25] Taulbee, D. B., Sonnenmeier, J. R., and Wall, K. W., Stress Relation for Three-Dimensional Turbulent Flows, *Phys. Fluids*, **6**(3):1399–1401 (1993).
- [26] Yakhot, V. and Orszag, S. A., Renormalization Group Analysis of Turbulence. I. Basic Theory, *J. Sci. Comput.*, **1**(1):3–52 (1986).
- [27] Horiuti, K., Higher Order Terms in the Anisotropic Representation of Reynolds Stresses, *Phys. Fluids*, **2**(10):1708–1711 (1969).
- [28] Yoshizawa, A., Statistical Analysis of the Deviation of the Reynolds Stress from its Eddy-Viscosity Representation, *Phys. Fluids*, **27**:1377–1387 (1984).

- [29] Yoshizawa, A., Statistical Modelling of Passive-Scalar Diffusion in Turbulent Shear Flows, *J. Fluid Mech.*, **195**:541–555 (1988).
- [30] Lele, S. K., Compressibility Effects on Turbulence, *Annu. Rev. Fluid Mech.*, **26**:211–254 (1994).
- [31] Gutmark, E. J., Schadow, K. C., and Yu, K. H., Mixing Enhancement in Supersonic Free Shear Flows, *Annu. Rev. Fluid Mech.*, **27**:375–417 (1995).
- [32] O., Z., Dilatation Dissipation: the Concept and Application in Modelling Compressible Mixing Layers, *Phys. Fluids A*, **2**(2):178–188 (1990).
- [33] Taulbee, D. B. and VanOsdol, J., Modeling Turbulent Compressible Flows: the Mass Fluctuating Velocity and Squared Density, AIAA Paper 91-0524, 1991.
- [34] Sarkar, S., Erlebacher, G., Hussain, M. Y., and Kreiss, H. O., The Analysis and Modelling of Dilatational Terms in Compressible Turbulence, *J. Fluid Mech.*, **227**:473–493 (1991).
- [35] Durbin, P. A. and Zeman, O., Rapid Distorsion Theory for Homogeneous Compressed Turbulence with Application to Modeling, *J. Fluid Mech.*, **242**:349–370 (1992).
- [36] Ristorcelli, J. R., A Pseudo-Sound Constitutive Relationship for the Dilatational Covariances in Compressible Turbulence: An Analytical Theory, ICASE Report 95-22, NASA Langley Research Center, Hampton, VA, 1995, Also available as *NASA CR 195064*.
- [37] Viegas, J. R. and Rubesin, M. W., A Comparative Study of Several Compressibility Corrections to Turbulence Models Applied to High-Speed Shear Layers, AIAA Paper 91-1783, 1991.
- [38] Sarkar, S. and Lakshmanan, B., Application of a Reynolds Stress Turbulence Model to the Compressible Shear Layer, *AIAA J.*, **29**(5):743–749 (1991).
- [39] Speziale, C. G. and Sarkar, S., Second Order Closure Models for Supersonic Turbulent Flows, ICASE Report 91-9, NASA Langley Research Center, Hampton, VA, 1991, Also available as *NASA CR 187508*.
- [40] El Baz, A. M. and Launder, B. E., Second-Moment Modelling of Compressible Mixing Layers, *Engineering Turbulence Modelling and Experiments*, Vol. 2, pp. 63–72, Elsevier Publishing Co., North Holland, 1993.
- [41] Kollmann, W., editor, *Prediction Methods for Turbulent Flows*, Hemisphere Publishing Co., New York, NY, 1980.
- [42] Favre, A., Statistical Equations of Turbulent Gases, in *Problems of Hydrodynamics and Continuum Mechanics*, pp. 37–44, SIAM, Philadelphia, 1969.
- [43] Launder, B. E., Reece, G. J., and Rodi, W., Progress in the Development of a Reynolds-Stress Turbulence Closure, *J. Fluid Mech.*, **68**:537–566 (1975).
- [44] Sarkar, S., The Pressure-Dilatation Correlation in Compressible Flows, *Phys. Fluids A*, **4**(12):2674–2682 (1992).
- [45] Schumann, U., Realizability of Reynolds Stress Turbulence Models, *Phys. Fluids*, **20**:721–725 (1977).

- [46] Shih, T.-H. and Shabbir, A., Methods of Ensuring Realizability for Non-Realizable Second Order Closures, ICOMP 94-14, NASA Lewis Research Center, Cleveland, OH, 1994, Also available as *NASA TM 106681*.
- [47] Ristorcelli, J. R., A Representation for the Turbulent Mass Flux Contribution to Reynolds-Stress and Two-Equation Closure for Compressible Turbulence, ICASE Report 93-88, NASA Langley Research Center, Hampton, VA, 1993, Also available as *NASA CR 191569*.
- [48] Spencer, A. J. M., Theory of Invariants, *Continuum Physics*, Vol. 1, pp. 240-352, Academic Press, 1971.
- [49] O., Z. and Coleman, G., Compressible Turbulence Subjected to Shear and Rapid Compression, in *Turbulent Shear Flows 8*, pp. 445-454, Springer-Verlag, 1991.
- [50] Gottlieb, D. and Turkel, E., Dissipative Two-Four Methods for Time Dependent Problems, *Math. Comp.*, **30**(136):703-723 (1976).
- [51] Drummond, J. P., Two-Dimensional Numerical Simulation of a Supersonic, Chemically Reacting Mixing Layer, NASA TM 4055, 1988.
- [52] Papamoschou, D. and Roshko, A., The Compressible Turbulent Shear Layer: An Experimental Study, *J. Fluid Mech.*, **197**:453-477 (1988).
- [53] Voke, P. R. and Collins, M. W., Large Eddy Simulation: Retrospect and Prospects, *PhysicoChemical Hydrodynamics*, **4**(2):119-161 (1983).
- [54] Rogallo, R. S. and Moin, P., Numerical Simulation of Turbulent Flow, *Ann. Rev. Fluid Mech.*, **16**:99-137 (1984).
- [55] Givi, P., Model Free Simulations of Turbulent Reactive Flows, *Prog. Energy Combust. Sci.*, **15**:1-107 (1989).
- [56] Lumley, J. L., editor, *Whither Turbulence? Turbulence at the Crossroads, Lecture Notes in Physics*, Vol. 357, Springer-Verlag, New York, NY, 1990.
- [57] Reynolds, W. C., The Potential and Limitations of Direct and Large Eddy Simulations, In Lumley,<sup>56</sup> pp. 313-343.
- [58] Galperin, B. and Orszag, S. A., editors, *Large Eddy Simulations of Complex Engineering and Geophysical Flows*, Cambridge University Press, Cambridge, U.K., 1993.
- [59] Givi, P., Spectral and Random Vortex Methods in Turbulent Reacting Flows, In Libby and Williams,<sup>11</sup> chapter 8, pp. 475-572.
- [60] Smagorinsky, J., General Circulation Experiments With the Primitive Equations. I. The Basic Experiment, *Monthly Weather Review*, **91**(3):99-164 (1963).
- [61] Germano, M., Turbulence: The Filtering Approach, *J. Fluid Mech.*, **238**:325-336 (1992).
- [62] Germano, M., Piomelli, U., Moin, P., and Cabot, W. H., A Dynamic Subgrid-Scale Eddy Viscosity Model, *Phys. Fluids A*, **3**(7):1760-1765 (1991).
- [63] Moin, P., Squires, W., H., C. W., and Lee, S., A Dynamic Subgrid-Scale Model for Compressible Turbulence and Scalar Transport, *Phys. Fluids A*, **3**:2746-2757 (1991).

- [64] Lilly, D. K., A Proposed Modification Of The Germano Subgrid-Scale Closure Method, *Phys. Fluids A*, **4**(3):633-634 (1992).
- [65] Pope, S. B., Computations of Turbulent Combustion: Progress and Challenges, in *Proceedings of 23rd Symp. (Int.) on Combustion*, pp. 591-612, The Combustion Institute, Pittsburgh, PA, 1990.
- [66] Schumman, U., Subgrid Scale Model for Finite Difference Simulations of Turbulent Flows in Plane Channels and Annuli, *J. Comp. Phys.*, **18**:376-404 (1975).
- [67] Brodkey, R. S., editor, *Turbulence in Mixing Operation*, Academic Press, New York, NY, 1975.
- [68] Toor, H. L., The Non-Premixed Reaction:  $A + B \rightarrow \text{Products}$ , In Brodkey,<sup>67</sup> pp. 123-166.
- [69] Hill, J. C., Homogeneous Turbulent Mixing with Chemical Reaction, *Ann. Rev. Fluid Mech.*, **8**:135-161 (1976).
- [70] Brodkey, R. S., Fundamental of Turbulent Motion, *Chem. Eng. Comm.*, **8**:1-23 (1981).
- [71] Toor, H. L., Mass Transfer in Dilute Turbulent and Nonturbulent Systems with Rapid Irreversible Reactions and Equal Diffusivities, *AIChE J.*, **8**:70-78 (1962).
- [72] Pope, S. B., PDF Methods for Turbulent Reactive Flows, *Prog. Energy Combust. Sci.*, **11**:119-192 (1985).
- [73] Dopazo, C., Recent Developments in PDF Methods, In Libby and Williams,<sup>11</sup> chapter 7, pp. 375-474.
- [74] Lundgren, T. S., Distribution Functions in the Statistical Theory of Turbulence, *Phys. Fluids*, **10**(5):969-975 (1967).
- [75] Madnia, C. K., Frankel, S. H., and Givi, P., Reactant Conversion in Homogeneous Turbulence: Mathematical Modeling, Computational Validations and Practical Applications, *Theoret. Comput. Fluid Dynamics*, **4**:79-93 (1992).
- [76] Frankel, S. H., Madnia, C. K., and Givi, P., Comparative Assessment of Closures for Turbulent Reacting Flows, *AIChE J.*, **39**(5):899-903 (1993).
- [77] Miller, R. S., Frankel, S. H., Madnia, C. K., and Givi, P., Johnson-Edgeworth Translation for Probability Modeling of Binary Scalar Mixing in Turbulent Flows, *Combust. Sci. and Tech.*, **91**(1-3):21-52 (1993).
- [78] Madnia, C. K. and Givi, P., Direct Numerical Simulation and Large Eddy Simulation of Reacting Homogeneous Turbulence, In Galperin and Orszag,<sup>58</sup> chapter 15, pp. 315-346.
- [79] Cook, A. W. and Riley, J. J., A Subgrid Model for Equilibrium Chemistry in Turbulent Flows, *Phys. Fluids*, **6**(8):2868-2870 (1994).
- [80] Janicka, J., Kolbe, W., and Kollmann, W., Closure of the Transport Equation for the Probability Density Function of Turbulent Scalar Field, *J. Nonequil. Thermodyn.*, **4**:47-66 (1979).

- [81] Pope, S. B., A Monte Carlo Method for the PDF Equations of Turbulent Reactive Flow, *Combust. Sci. and Tech.*, **25**:159–174 (1981).
- [82] Curl, R. L., Dispersed Phase Mixing: I. Theory and Effects in Simple Reactors, *AIChE J.*, **9**(2):175–181 (1963).
- [83] Chorin, A. J., Numerical Solution of the Navier-Stokes Equations, *Math. Comp.*, **22**:745–763 (1968).
- [84] Ghoniem, A. F., Vortex Simulation of Reacting Shear Flow, in Oran, E. S. and Boris, J. P., editors, *Numerical Approaches to Combustion Modeling, Progress in Astronautics and Aeronautics*, Vol. 135, chapter 10, pp. 305–348, AIAA Publishing Co., Washington, D.C., 1991.
- [85] Ghoniem, A. F. and Givi, P., Lagrangian Simulation of a Reacting Mixing Layer at Low Heat Release, *AIAA J.*, **26**:690–697 (1988).
- [86] Battaglia, F. and Givi, P., Direct Lagrangian Simulations of a Mixing Layer by the Transport-Element Method, *J. Nonequil. Thermodyn.*, **18**:173–194 (1993).
- [87] Schuss, Z., *Theory and Applications of Stochastic Differential Equations*, John Wiley and Sons, Inc., New York, 1980.
- [88] Papoulis, A., *Probability, Random Variables, and Stochastic Processes*, McGraw-Hill, Inc., New York, 1991.
- [89] Billingsly, P., *Probability and Measure*, John Wiley and Sons, Inc., New York, 1979.
- [90] Gao, F. and O'Brien, E., A Large-Eddy Simulation Scheme for Turbulent Reacting Flows, *Phys. Fluids A*, **5**(6):1282–1284 (1993).
- [91] Dopazo, C. and O'Brien, E. E., Statistical Treatment of Non-Isothermal Chemical Reactions in Turbulence, *Combust. Sci. and Tech.*, **13**:99–112 (1976).
- [92] Kosály, G. and Givi, P., Modeling of Turbulent Molecular Mixing, *Combust. Flame*, **70**:101–118 (1987).
- [93] Pope, S. B., An Improved Turbulent Mixing Model, *Combust. Sci. and Tech.*, **28**:131–145 (1982).
- [94] Kosály, G., Theoretical Remarks on a Phenomenological Model of Turbulent Mixing, *Combust. Sci. and Tech.*, **49**:227–234 (1986).
- [95] MacCormack, R. W., The Effect of Viscosity in Hypervelocity Impact Catering, AIAA Paper 69-354, 1969.
- [96] Helfand, E., Numerical Integration of Stochastic Differential Equations, *Bell System Technical Journal*, **58**(10):2289 – 2299 (1979).
- [97] Papoulis, A., *Probability, Random Variables, and Stochastic Processes*, McGraw-Hill Book Company, New York, NY, 1965.
- [98] Michalke, A., On Spatially Growing Disturbances in an Inviscid Shear Layer, *J. Fluid Mech.*, **23**:521–544 (1965).

- [99] Ghosal, S. and Moin, P., The Basic Equations for the Large Eddy Simulation of Turbulent Flows in Complex Geometry, *J. Comp. Phys.*, **118**:24–37 (1995).
- [100] Pope, S. B., Lagrangian PDF Methods for Turbulent Flows, *Ann. Rev. Fluid Mech.*, **26**:23–63 (1994).

## Figure Captions

Figure 2.1: The reduction of the averaged residual for the Gottlieb-Turkel scheme.

Figure 2.2: Downstream evolution of the shear-layer width at steady-state.

Figure 2.3: Cross-stream variation of  $(U - U_1)/(U_1 - U_2)^2$  for the mixing layer.

Figure 2.4: Cross-stream variation of  $\langle u''^2 \rangle / (U_1 - U_2)^2$  for the mixing layer.

Figure 2.5: Cross-stream variation of  $\langle u'v' \rangle / (U_1 - U_2)^2$  for the mixing layer.

Figure 3.1: Particle number density (per ensemble) contours .

Figure 3.2: Contour plots of species  $\mathcal{A}$  mass fraction ( $Da=0$ ): (a) Monte-Carlo LES-PDF, (b) finite difference.

Figure 3.3: Contour plots of species  $\mathcal{A}$  mass fraction ( $Da=2$ ): (a) Monte-Carlo LES-PDF, (b) finite difference.

Figure 3.4: Contour plots of product  $\mathcal{P}$  mass fraction ( $Da=2$ ): (a) Monte-Carlo LES-PDF, (b) finite difference.

Figure 3.5: Contour plots of SGS species covariance : (a)  $Da=0$ , (b)  $Da=2$ .

Figure 3.6: Reaction rate contours: (a) Monte-Carlo LES-PDF, (b) finite difference.

Figure 3.7: Product  $\mathcal{P}$  mass fraction contours. Results generated by Monte Carlo LES-PDF assuming  $\dot{\bar{\omega}}(\phi) = \dot{\omega}(\bar{\phi})$ .

Figure 3.8: Reaction rate contours. Results generated by Monte Carlo LES-PDF assuming  $\dot{\bar{\omega}}(\phi) = \dot{\omega}(\bar{\phi})$ .

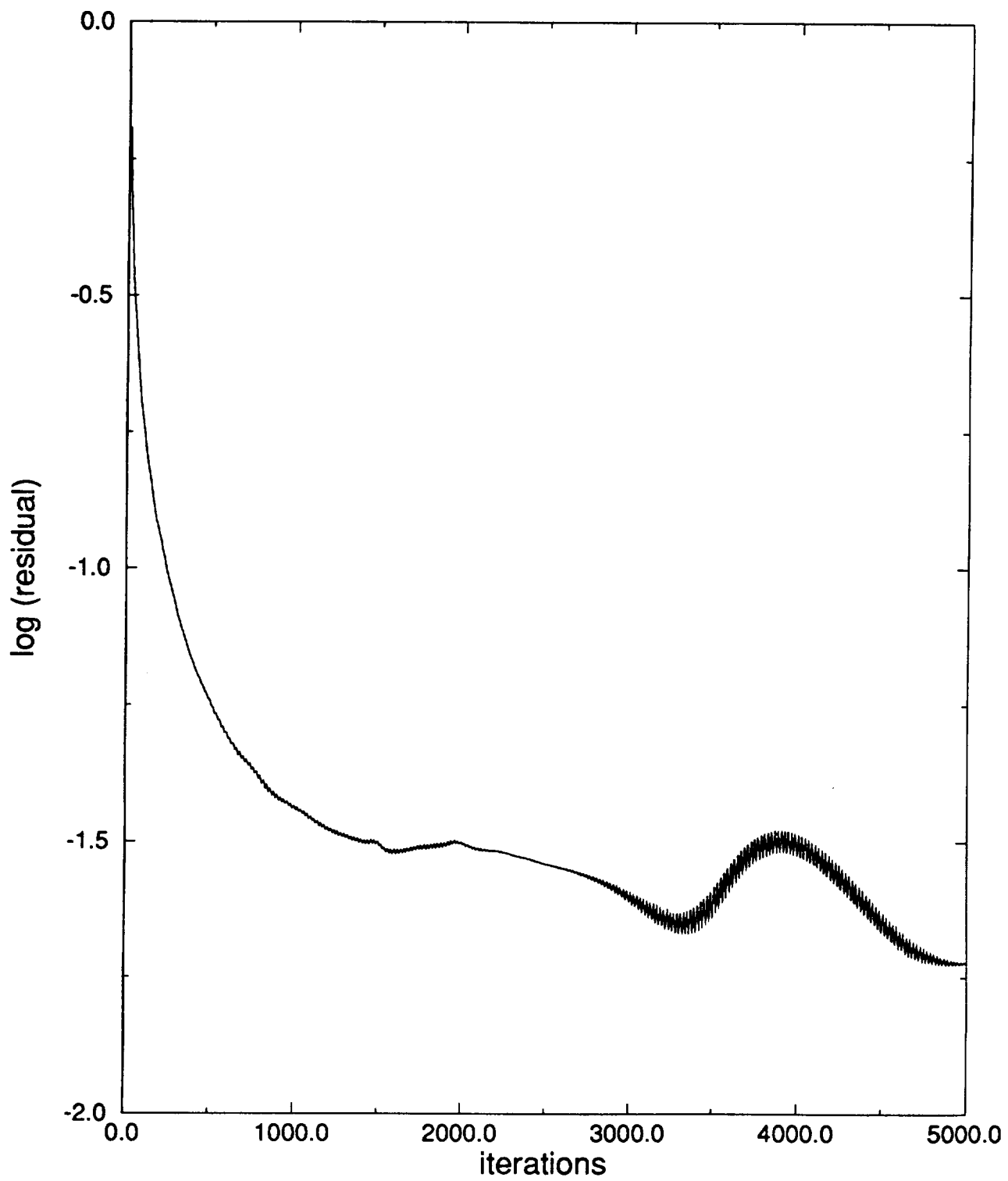


Figure 2.1

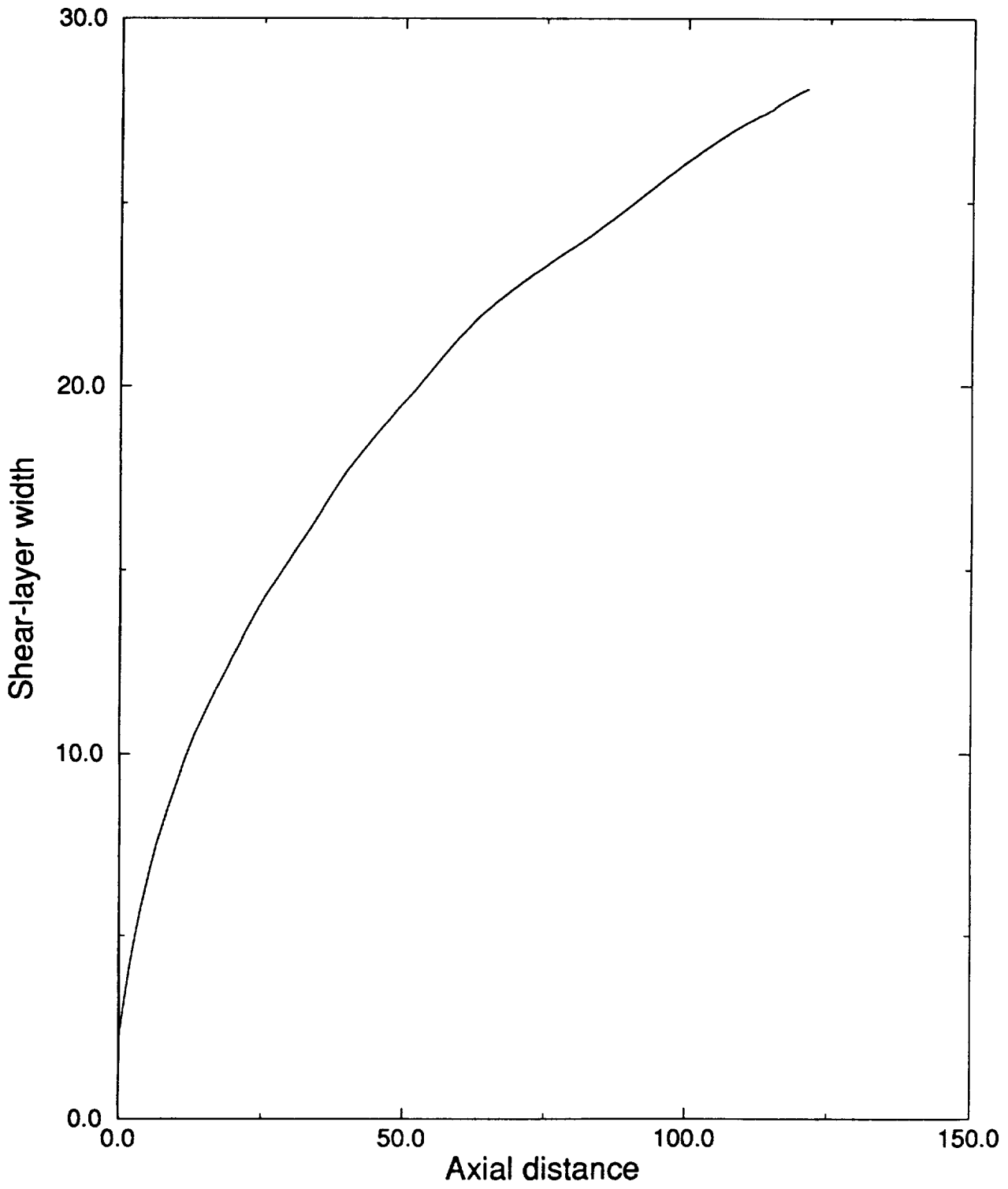


Figure 2.2

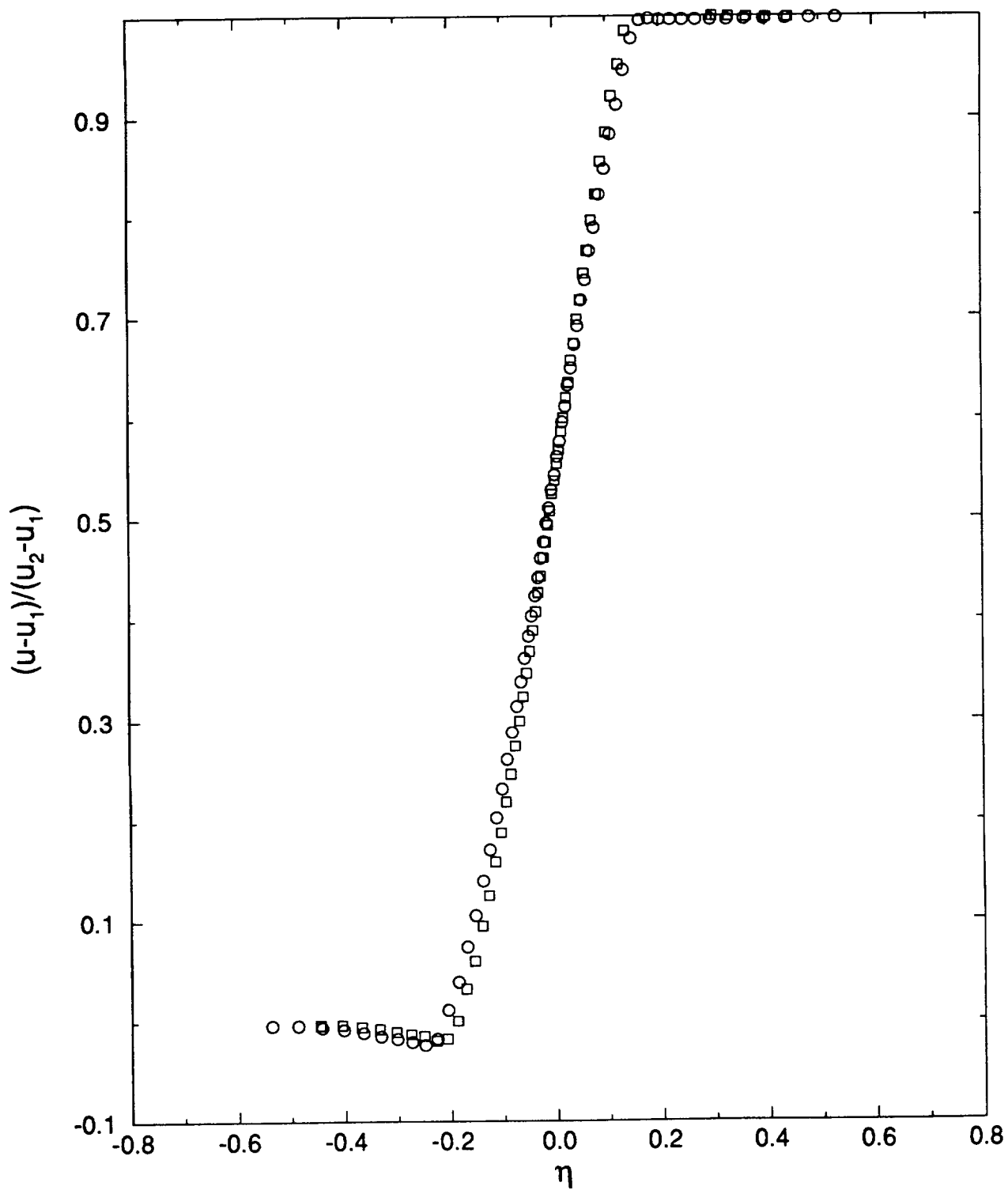


Figure 2.3

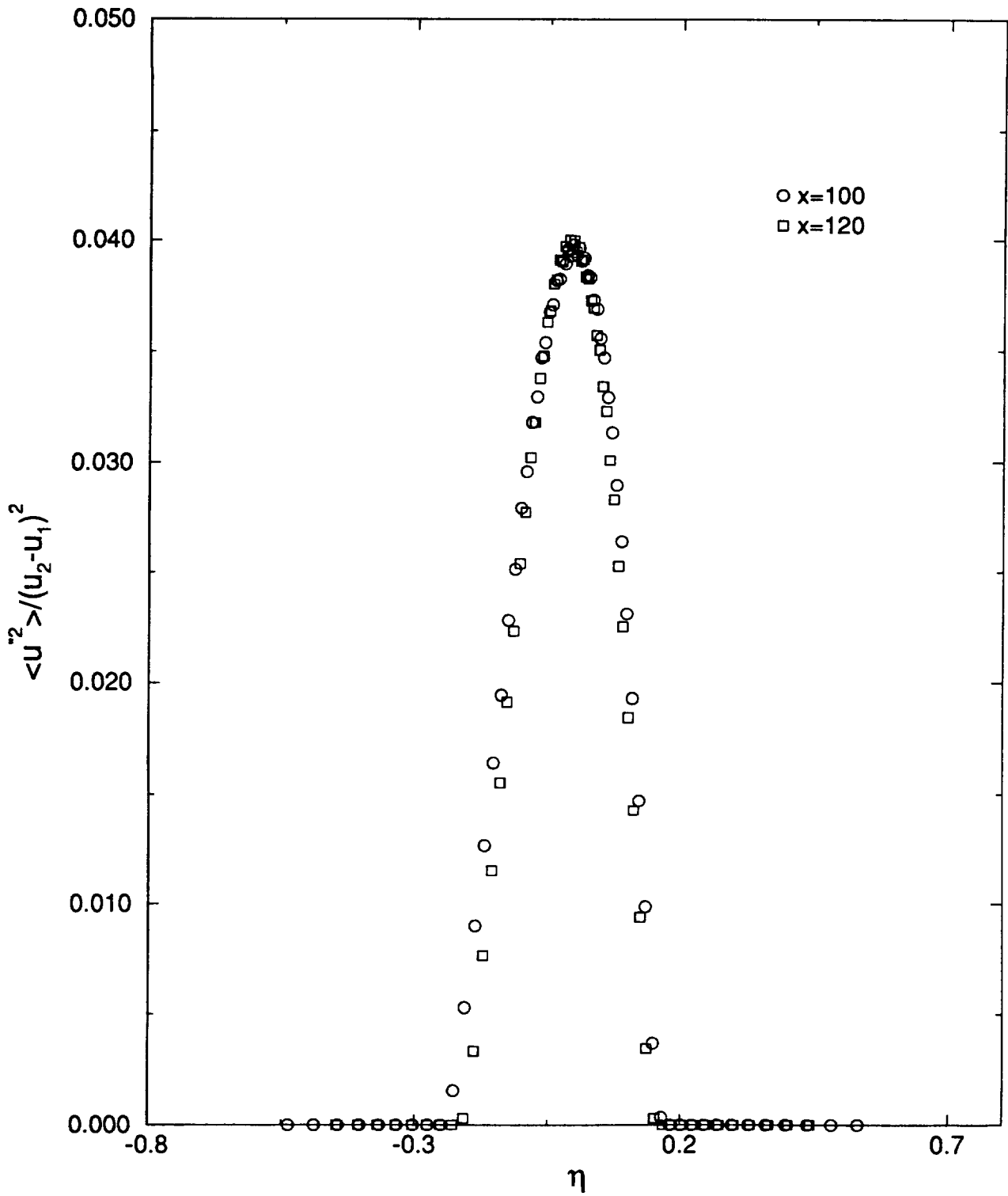


Figure 2.4

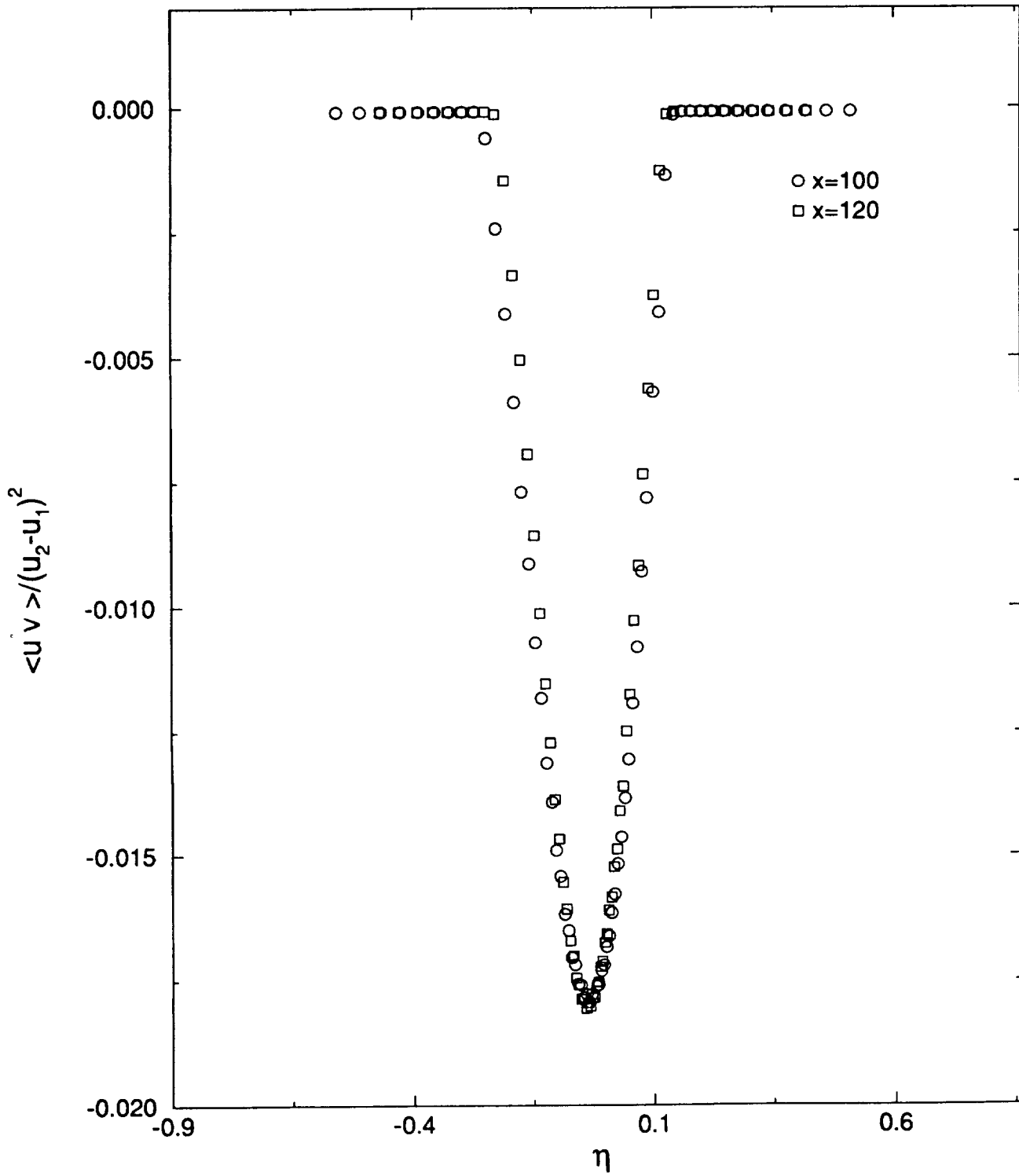


Figure 2.5

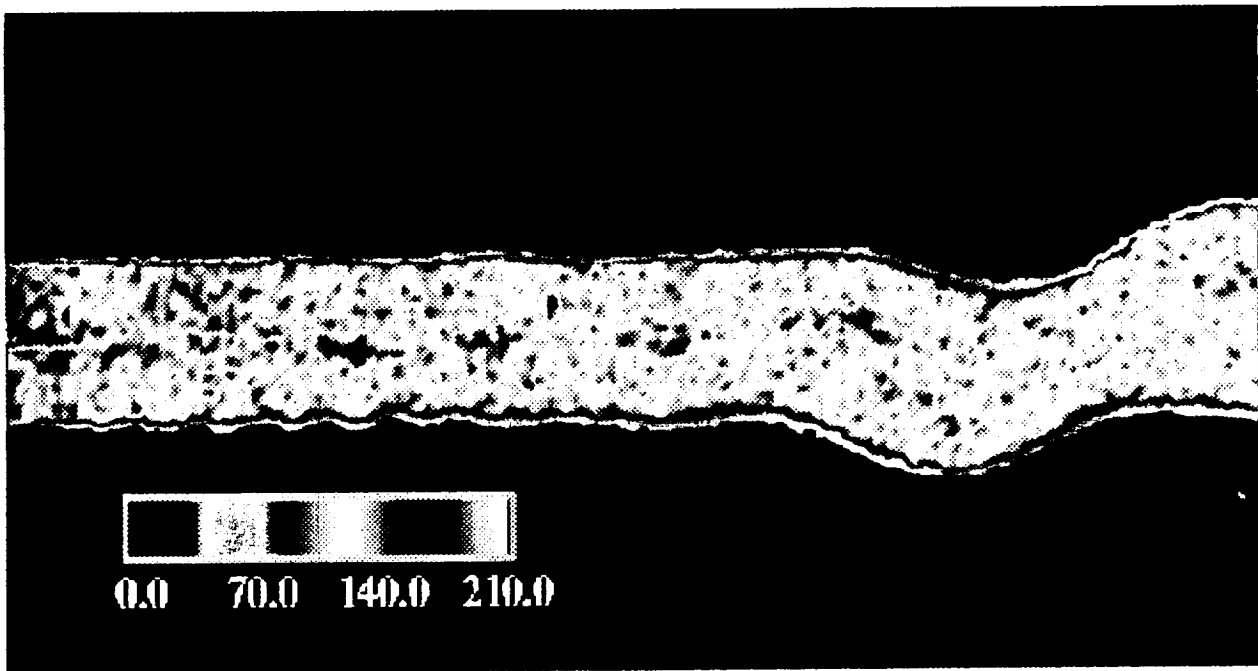
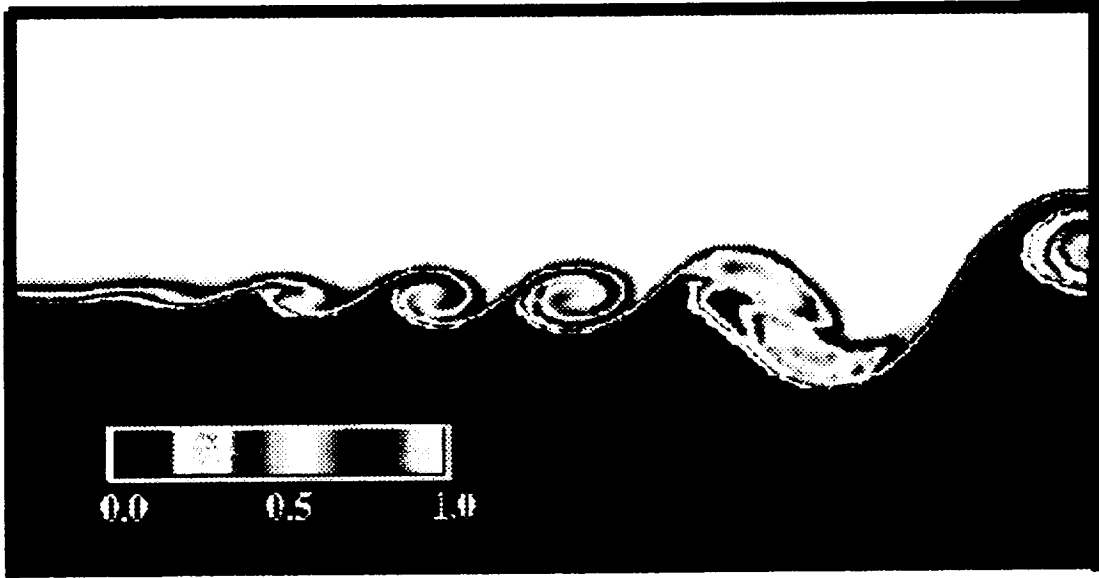
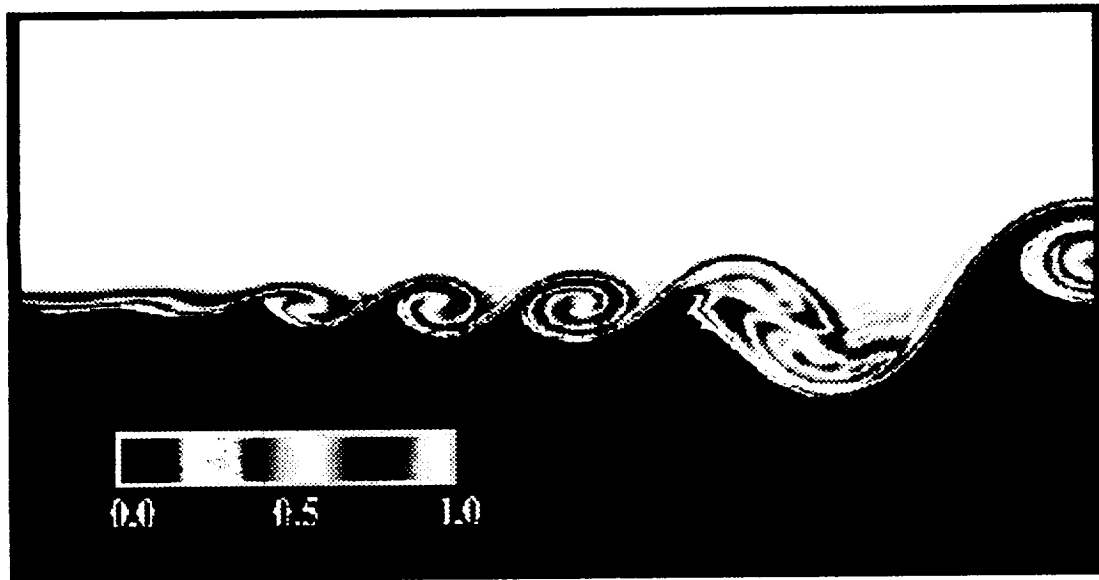


Figure 1: Particle number density (per ensemble) contours

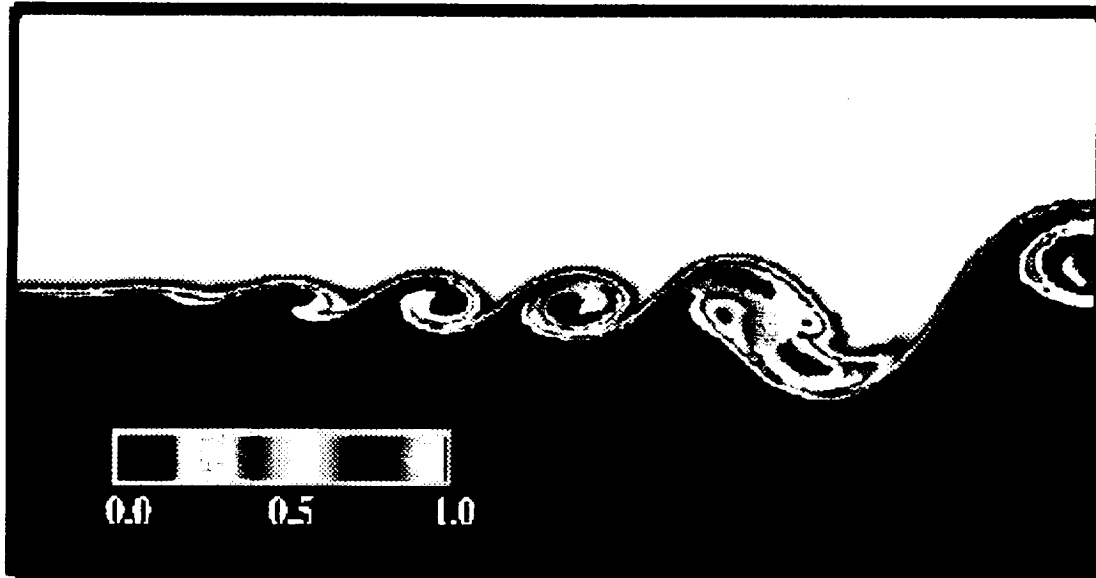


(a)

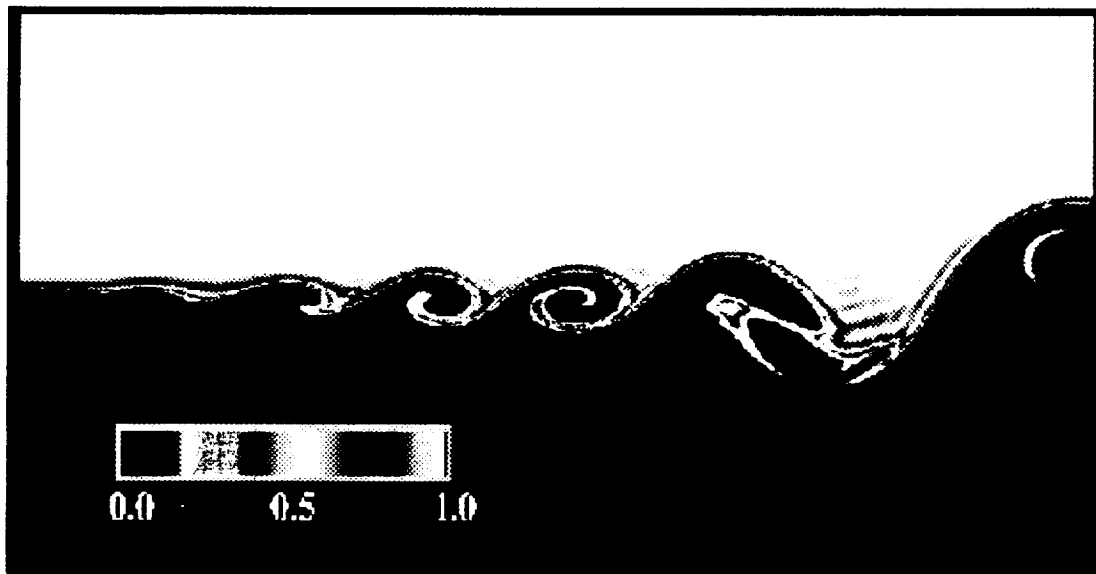


(b)

**Figure 3.2:** Contour plots of species A mass fraction ( $Da=0$ ) (a) Monte-Carlo LES-PDF, (b) finite difference

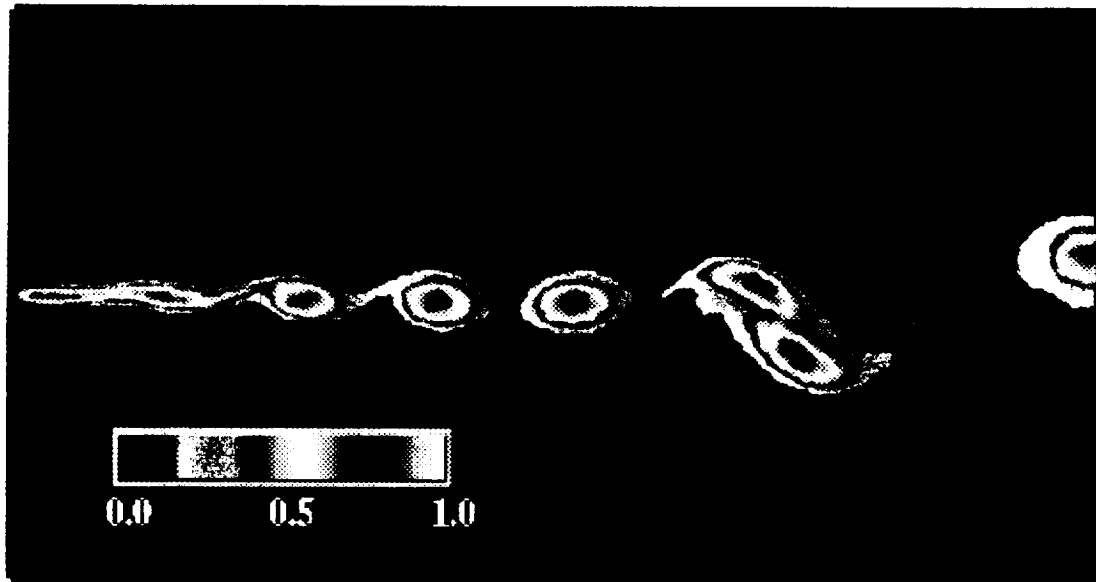


(a)

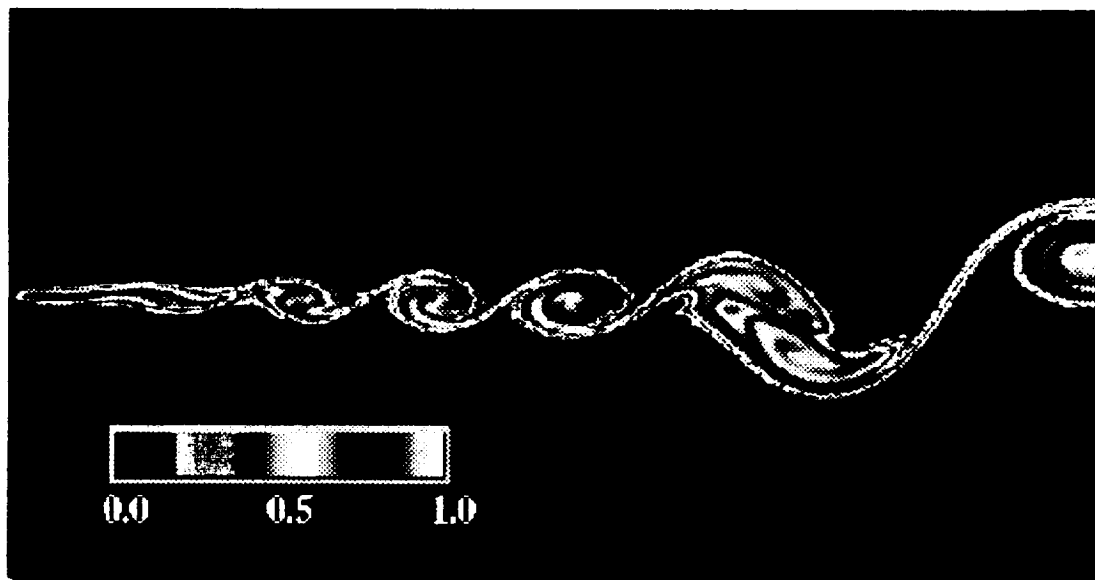


(b)

**Figure 3.3:** Contour plots of species A mass fraction ( $Da=2$ ) (a) Monte-Carlo LES-PDF, (b) finite difference

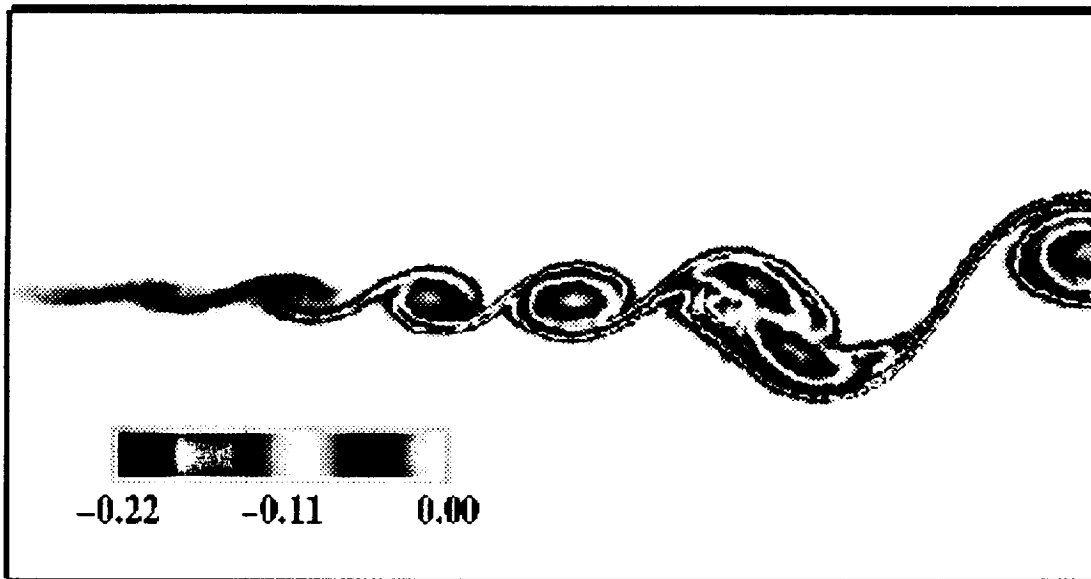


(a)

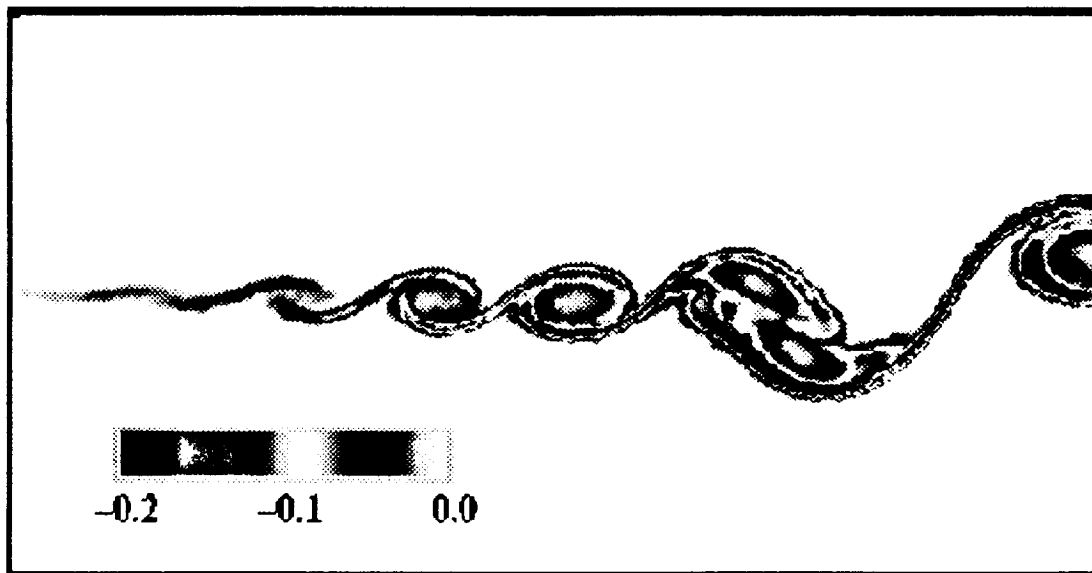


(b)

**Figure 3.4:** Contour plots of product P mass fraction ( $Da=2$ ) (a) Monte-Carlo LES-PDF, (b) finite difference



(a)

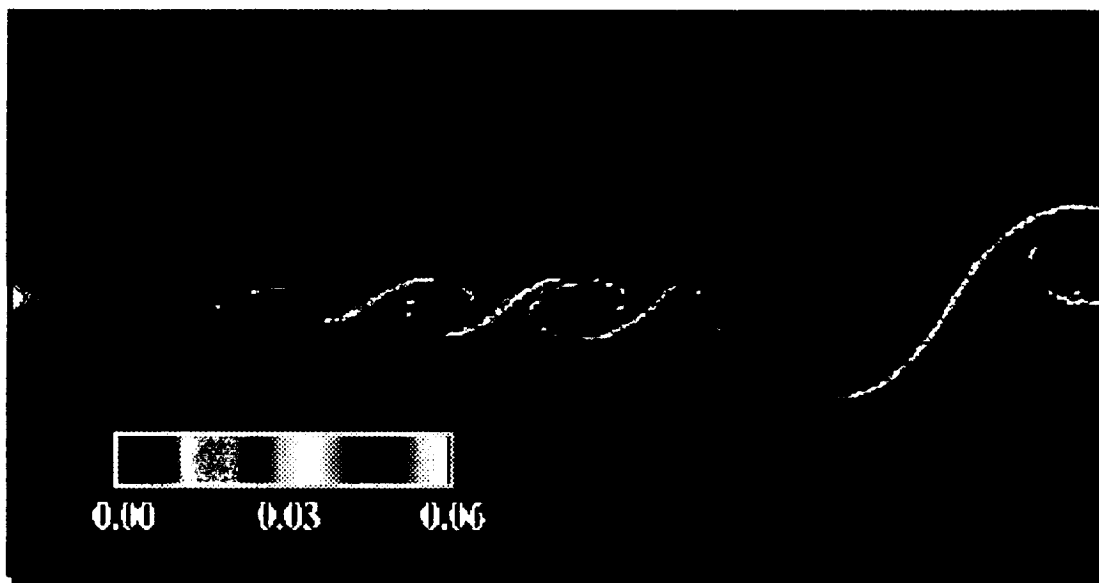


(b)

**Figure 3.5:** Contour plots of SGS species covariance  
(a)  $Da=0$ , (b)  $Da=2$



(a)



(b)

**Figure 3.6:** Reaction rate contours: (a) Monte-Carlo LES-PDF, (b) finite difference

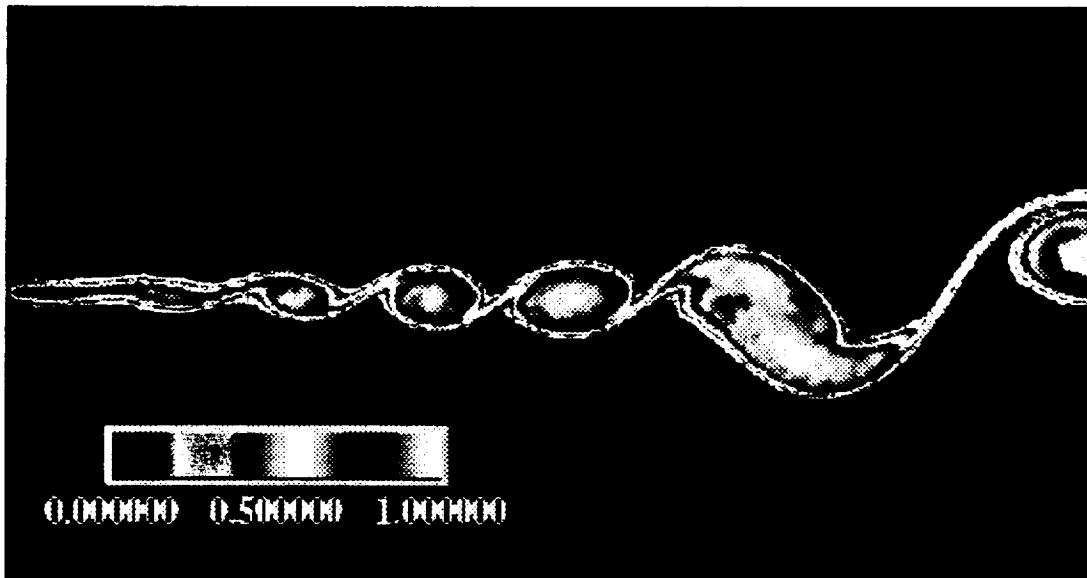


**Figure 3.7:** Product P mass fraction contours. Results generated by Monte-Carlo LES-PDF assuming  $\langle AB \rangle = \langle A \rangle \langle B \rangle$

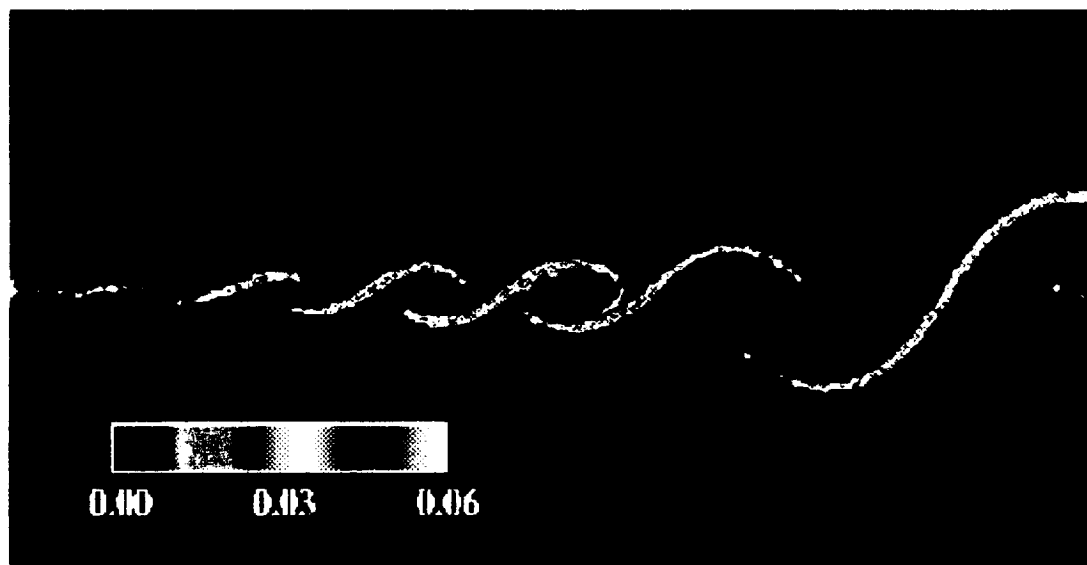


**Figure 3.8:** Reaction rate contours. Results generated by Monte-Carlo LES-PDF assuming  $\langle AB \rangle = \langle A \rangle \langle B \rangle$

